

# GEOLOGY OF THE MCDUFFIE COUNTY GOLD BELT

by  
Jerry M. German



DEPARTMENT OF NATURAL RESOURCES  
ENVIRONMENTAL PROTECTION DIVISION  
GEORGIA GEOLOGIC SURVEY

**BULLETIN 125**

# **GEOLOGY OF THE MCDUFFIE COUNTY GOLD BELT**

by  
**Jerry M. German**

**DEPARTMENT OF NATURAL RESOURCES**  
Joe D. Tanner, Commissioner  
**ENVIRONMENTAL PROTECTION DIVISION**  
Harold F. Reheis, Director  
**GEORGIA GEOLOGIC SURVEY**  
William H. McLemore, State Geologist

Atlanta  
1993

**BULLETIN 125**



## TABLE OF CONTENTS

Abstract .....	1
Acknowledgements .....	1
Introduction .....	1
Methods .....	3
Previous Investigations .....	3
Geology .....	3
Introduction .....	3
Stratigraphy .....	4
Persimmon Fork Formation .....	4
Richtex Formation .....	4
Rocks of the Northern Part of the Modoc Zone .....	9
Intrusive Rocks .....	9
Pre- to Syn-metamorphic Intrusions .....	9
Metagranodiorite .....	9
Metaquartz Monzonite .....	12
Mafic Sheets and Stocks .....	12
Post-metamorphic Intrusive Rocks .....	12
Diabase Dikes .....	12
Lamprophyre Dikes .....	17
Veins and Silicified Breccia Zones .....	21
Metamorphism and Deformation .....	27
Early Paleozoic Deformation .....	27
Late Paleozoic Deformation .....	27
Shear Zones .....	28
Faulting .....	28
Tectonic Environment .....	28
Gold Deposits .....	31
Introduction .....	31
Mining History and Production .....	31
Gold Ore .....	31
Vein Mineralogy and Geometry .....	31
Vein Orientation .....	35
Alteration .....	35
Fluid Inclusions .....	39
Oxygen Isotopes .....	43
Time of Emplacement .....	43
Genesis of the Gold Deposits .....	43
Future Production Outlook .....	46
Summary .....	48
References .....	48
Appendix A .....	53
Appendix B .....	55
Appendix C .....	58

## LIST OF ILLUSTRATIONS

Fig. 1 - Location of the study area in relation to regional geologic features. ....	2
Fig. 2 - Sawed hand sample and outcrop of lapilli metatuffs of intermediate composition. ....	5
Fig. 3 - Embayed quartz crystals in a matrix of quartz, plagioclase, epidote, sericite and chlorite. ....	6

LIST OF ILLUSTRATIONS (Continued)

Fig. 4 - Saprolite exposure along the shoreline of Clark Hill Reservoir of felsic metavolcanic rocks. ....	6
Fig. 5 - Well-preserved original sedimentary structures in metasediments. ....	7
Fig. 6 - Meta-argillite exhibiting a distinct bedding/cleavage relationship. ....	8
Fig. 7 - Scour features in metagraywacke. ....	10
Fig. 8 - "Muscovite fish" along shears in weathered phyllite. ....	10
Fig. 9 - Sawed hand sample containing a contact between metagranodiorite and the phyllite country rock. ....	11
Fig. 10 - Dark-colored xenoliths within the large metagranodiorite body. ....	11
Fig. 11 - Domal features within the large metagranodiorite body. ....	13
Fig. 12 - Saprolite exposure of a leucocratic felsic dike cross-cutting the largest metagranodiorite body. ....	13
Fig. 13 - Chemical classification of metagranodiorites and metaquartz monzonites from the study area. ....	16
Fig. 14 - Sericitization and feldspar zoning in metaquartz monzonite. ....	16
Fig. 15 - Cuneiform intergrowth of quartz and potassium feldspar in metaquartz monzonite. ....	18
Fig. 16 - Chemical classification of mafic meta-intrusive bodies from the study area. ....	18
Fig. 17 - Chemical classification of lamprophyres from the study area. ....	22
Fig. 18 - Quartz and feldspar xenocrysts in a kersantite lamprophyre dike. ....	23
Fig. 19 - Hand sample of the kersantite from Figure 18. ....	22
Fig. 20 - Comparison of major and trace element chemistry of the lamprophyre and diabase dikes. ....	24
Fig. 21 - Hand sample of the silicified breccia zone near Fountain Campground, McDuffie and Warren Counties. ....	26
Fig. 22 - Quartz vein in largest metagranodiorite body offset by a northwest-striking fault. ....	30
Fig. 23 - Chemical classification of felsic and mafic metavolcanic rocks from the study area. ....	30
Fig. 24 - Discrimination of mafic phyllites using major and trace element chemistry. ....	33
Fig. 25 - Plot of trace element chemistry of mafic phyllites on a standard discrimination diagram. ....	34
Fig. 26 - Sawed brecciated auriferous vein from the Phillips Mine. ....	36
Fig. 27 - Sawed brecciated auriferous vein from the Tatham Mine showing ankerite zoning along its borders. ....	36
Fig. 28 - Vein quartz from the Landers Mine showing successive euhedral overgrowths. ....	37
Fig. 29 - Polished thin section from the Landers Mine showing gold grains and sphalerite in quartz. ....	37

## LIST OF ILLUSTRATIONS (Continued)

Fig. 30 - Sawed (phyllite?) host rock and ore from the Tatham Mine, McDuffie County showing euhedral pyrite crystals. ....	38
Fig. 31 - Vein mineral paragenesis of ore bodies in the McDuffie County gold belt. ....	39
Fig. 32 - Polished thin section from the Tatham Mine showing zoned pyrite overgrowth on an aggregate of sphalerite and pyrite. ....	40
Fig. 33 - Polished thin section from the Landers Mine showing interpenetration boundaries between sphalerite and galena and between galena and chalcopyrite. ....	41
Fig. 34 - Polished thin section from the Landers Mine showing aligned inclusions of chalcopyrite in sphalerite. ....	40
Fig. 35 - Polished thin section from the Landers Mine showing galena embaying chalcopyrite. ....	42
Fig. 36 - Polished thin section from the Landers Mine showing chalcopyrite altered to covellite. ....	42
Fig. 37 - Oxygen isotope values for host rocks, veins and silicified zones within the study area. ....	45
Fig. 38 - Sawed sample of phyllite host rock from the Parks Mine. ....	46
Fig. 39 - Gold content of representative rock types within the study area. ....	47

## LIST OF TABLES

Table 1. Modal analysis of representative rock types. ....	8
Table 2. Major oxide, trace element and normative analyses of metagranodiorites. ....	14
Table 3. Major oxide, trace element and normative analyses of metaquartz monzonites. ....	17
Table 4. Major oxide, trace element and normative analyses of mafic intrusives. ....	19
Table 5. Major oxide, trace element and normative analyses of mafic dikes. ....	20
Table 6. Assays of the silicified breccia - Fountain Campground vicinity. ....	26
Table 7. Comparison of structural fabric elements. ....	29
Table 8. Major oxide, trace element and normative analyses of felsic and mafic metavolcanic rocks. ....	32
Table 9. Ore sample assays. ....	34
Table 10. $\delta^{18}\text{O}$ values for rock types within the study area. ....	44

## LIST OF PLATES

Plate 1. Geologic map of the McDuffie County Gold Belt. ....	cover envelope
Plate 2. Geologic map and locations of abandoned mine workings of a part of the McDuffie County Gold Belt. ....	cover envelope

LIST OF PLATES (Continued)

Plate 3. Sample locations.....cover envelope

Cover photo: William Fluker at quartz vein between 50' and 60' levels - Hamilton mine (circa 1934).  
*Photo courtesy of Georgia Department of Archives and History.*

# GEOLOGY OF THE MCDUFFIE COUNTY GOLD BELT

by  
Jerry M. German

## ABSTRACT

The McDuffie County gold belt is located within the Carolina slate belt geologic province just northwest of the Modoc zone, which is the boundary between the Carolina slate belt and the Kiokee belt. Rocks within the gold belt consist of argillite to wacke metasediments and minor felsic metavolcanic rocks of the Richtex Formation and felsic to intermediate metavolcanic rocks and minor mafic metavolcanic rocks of the Persimmon Fork Formation. Available data strongly suggest that these rocks were deposited peripheral to a back-arc basin over crust transitional between oceanic and continental environments. The Richtex and Persimmon Fork Formations were intruded by pre- to syn-kinematic granodiorites, quartz monzonites and gabbros/diorites and by post-kinematic diabase and lamprophyre dikes. The rocks within the study area have been assigned a Cambrian age based on the ages of intrusive rocks and the presence of Cambrian fossils in correlative metasediments.

Rocks within the study area were folded into regional isoclinal folds during the early Paleozoic. At this time the rocks were metamorphosed to lower greenschist facies and were penetratively deformed, developing a pervasive slaty cleavage ( $S_1$ ); however, original sedimentary and volcanic features and textures were preserved. During the late Paleozoic (Alleghanian), deformation of the Kiokee belt to the southeast affected adjacent rocks along the southeastern border of the study area in the vicinity of the Modoc zone. Adjacent to the Modoc zone, slaty cleavage is overprinted by a mylonitic foliation, and the rocks have been metamorphosed to upper greenschist to amphibolite facies. The effects of this deformation decrease rapidly northwest of the Kiokee belt, and northwest of the Modoc zone this deformation is expressed as localized shear zones. Subsequently, rocks of the Kiokee belt and study area were folded into a regional antiform and the slaty cleavage of the study area was rotated to its present orientation.

Gold-bearing veins were emplaced into the country rock just prior to the last fold event. These veins were deposited from hydrothermal fluids produced from dehydration and decarbonation of minerals during prograde metamorphism, most likely generated deep within the higher grade rocks of the Kiokee belt. As the hydrothermal fluids migrated up the metamorphic gradient toward lower grade rocks of the Carolina slate belt, gold and other vein minerals precipitated from these fluids near the greenschist/

amphibolite facies transition. Gold most likely was transported in the hydrothermal fluid as a gold thiosulfide complex and precipitated as a result of boiling of the hydrothermal fluid and sulfidization of the host rock.

Gold was mined in the study area intermittently from about 1823 to 1922. Formerly productive mines included the Columbia, Parks, Hamilton, Tatham and Woodall. Most mining activity consisted of underground lode mining of quartz veins.

## ACKNOWLEDGEMENTS

Thanks are extended to Bruce O'Connor, Mark Hall, Earl Shapiro, William McLemore, David Wenner and David Vanko for their reviews of this report. Thanks also are extended to David Wenner for the oxygen isotope analyses and to David Vanko, Phil Newton and Mark Pyle for the fluid inclusion work. The contributions of those listed above greatly improved the quality of this report.

## INTRODUCTION

This study of the McDuffie County gold belt was initiated as part of an on-going study of the former gold-producing regions of the state. The historical record is unclear, but the first discovery and mining of gold reportedly occurred in the McDuffie County belt; however, the significance and mining history of this belt has been overshadowed by the more popularly known Dahlonega belt. Some of the early reports on the gold deposits of Georgia and the region gave little or no information on the gold deposits of the McDuffie County belt (for example: Becker, 1894; Yeates and others, 1896) and as a result, the importance of the McDuffie gold belt may have been overlooked. A published report on the belt as a whole was not available until the work by Jones (1909) although published (Fluker, 1902) and unpublished studies (Jones, 1902; Yeates, 1902) of limited scope were done earlier.

The McDuffie County gold belt (Fig. 1), named for the county where the most extensive mining activity occurred, includes parts of Warren, McDuffie, Wilkes, Lincoln and Columbia Counties. The belt attains a maximum width of 5 miles (8 km) and extends from northeastern Warren county northeastward to the vicinity of the Georgia-South Carolina border in extreme southeastern Lincoln County, a distance of approximately 30 miles (48 km). The average strike of the belt is approximately N65°E. The belt

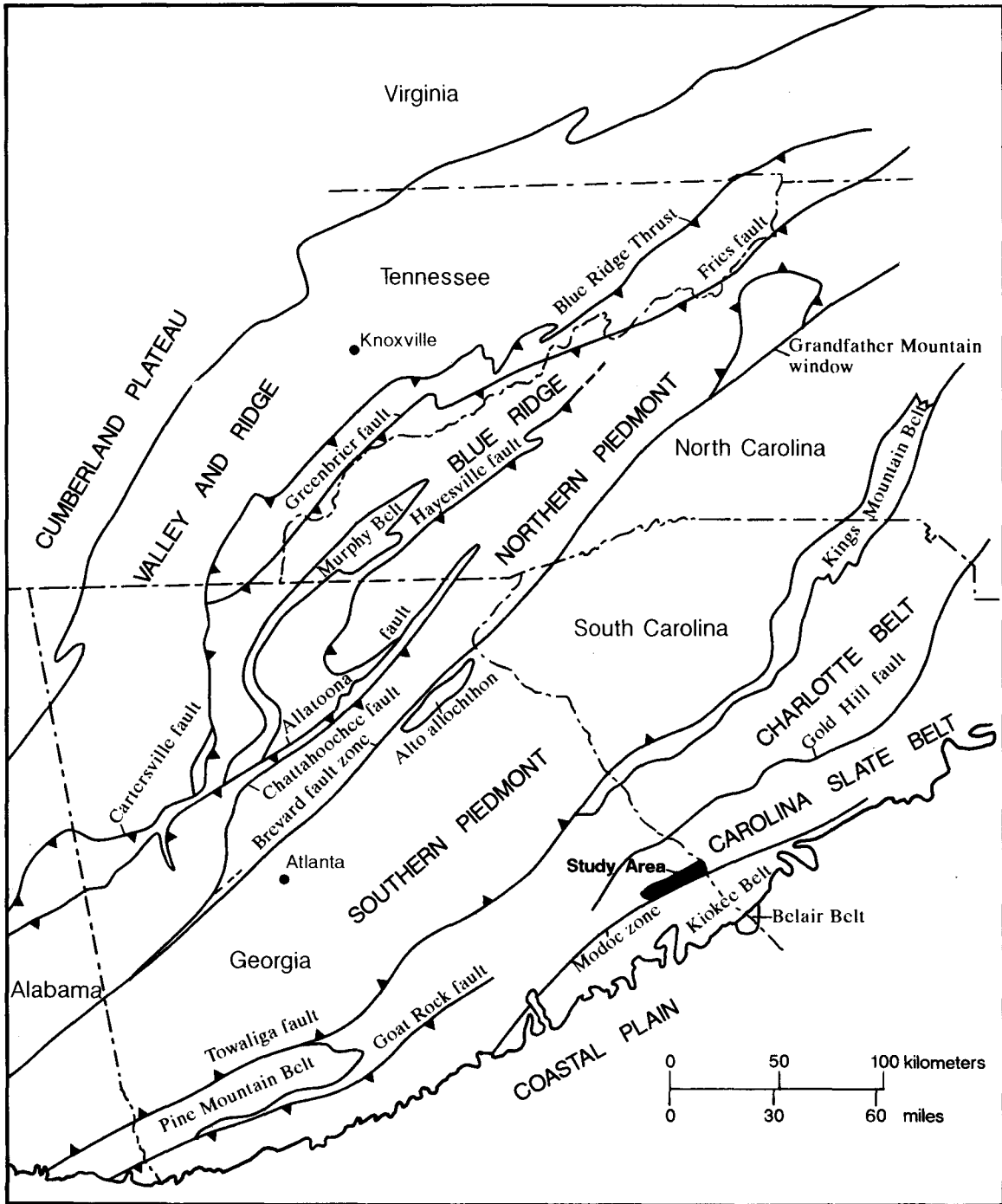


Fig. 1 - Location of the study area in relation to regional geologic features.

is located within the Carolina slate belt province and roughly parallels the Modoc zone, the boundary between the Carolina slate belt and the Kiokee belt. The belt is centered about the Little River section of Clark Hill Reservoir.

## METHODS

Data collection for the study consisted of geologic mapping of portions of seven 7.5-minute quadrangles. The level of geologic mapping consisted of mapping along all roads, primary and secondary drainage and the shoreline of Clark Hill Reservoir. Mapping was done between March 1989 and October 1990 in the Aonia, Cadley, Leah, Plum Branch, Winfield, Woodlawn and Wrightsboro Quadrangles (Plate 1). In addition to the mapping of geologic features, an attempt was made to locate all abandoned mines and prospects. Mine workings were plotted on a large-scale map (Plate 2), and representative ore and host rock samples were collected from mine dumps, where available. Although all mine workings have been abandoned for over fifty years and are generally inaccessible, much data on vein orientation and morphology, ore mineralogy and host rock lithology could be gathered from locally abundant dump material and the distribution and orientation of abandoned workings.

Representative samples were collected of all rock types. One-hundred and twenty-nine thin and polished sections were made and were examined by conventional transmitted and reflected light, petrographic techniques. Chemical analyses were performed on one-hundred and eleven samples. Selected country rock and ore samples were analyzed for major oxides (whole rock), base and precious metals and trace elements. Geochemical analyses were performed by Bondar-Clegg, Inc. Analysis parameters are given in Appendix A. Fluid inclusion studies were conducted on ten selected samples of auriferous and barren quartz veins by David A. Vanko at Georgia State University. Oxygen isotope analyses were provided for 29 samples by David B. Wenner at the University of Georgia Stable Isotope Laboratory.

## PREVIOUS INVESTIGATIONS

Most previous reports encompassing all or parts of the study area have consisted of mineral commodity studies (mainly gold) and general reconnaissance studies. Most of these were conducted prior to 1970, and while most provided somewhat limited data on the overall geology of the McDuffie belt, many of these reports provided considerable information on local geology. Since 1970, several detailed studies have been conducted that have greatly expanded our knowledge of certain aspects of the study area and vicinity. Some of these latest studies have been student theses investigating the geology of selected 7.5-

minute quadrangles mainly along the northern border of the study area, others have been studies involving geologic mapping and geochemical reconnaissance work related to mineral exploration, and, still, others have been structural and tectonic studies.

The earliest investigations encompassing all or part of the study area were reports by Jones (1902, 1909); Yeates (1902); Fluker (1902, 1903, 1907, 1934); Kelly and others (1934a and b) and Pardee and Park (1948) on a few or all of the gold deposits. An early report on brick clays was done by Smith (1931). General stratigraphic and structural features of the study area were described in a report by Crickmay (1952), and the hydrogeology was discussed by LeGrand and Furcron (1956). A comprehensive mineral survey with a general discussion of the geology of the area was completed by Hurst and others (1966). The geology of selected areas was described by Crawford and others (1966), and county geologic maps were prepared by Crawford (1968 a,b,c,d,e, and f). General discussions of the geology of the study area and vicinity were given by Carpenter (1976, 1982). Whitney and others (1978) discussed the tectonic setting and geochemical affinity of volcanic rocks in part of the Carolina slate belt. Studies of the geology of selected 7.5-minute quadrangles were made by Paris (1976), Reusing (1979) and Von der Heyde (1990). Recent work by Secor (1987); Sacks and Dennis (1987); Maher (1987) and Dennis and others (1987) describe the structure and tectonics of a part of the study area and adjacent areas. Higgins and others (1988) briefly discussed the study area in the context of their regional synthesis. Geochemical studies of the study area were provided by Hurst and others (1990) and Hurst (1990). Allard and Whitney (in prep.) recently completed a regional synthesis of the geology of east-central Georgia that includes the study area.

## GEOLOGY

### Introduction

The study area is located within the southern part of the Carolina slate belt near the boundary with the Kiokee Belt. Host rocks for the McDuffie County gold belt were formerly referred to as the Little River series (Crickmay, 1952), but this term has been largely abandoned as specific stratigraphic units have been defined in recent years. The term Little River allochthon has been proposed by Higgins and others (1988) for rocks of the study area.

Informally defined units in Georgia, including the study area, (Carpenter, 1976; Paris, 1976; Whitney and others, 1978) are correlative with formally defined formations in South Carolina (Secor and Wagener, 1968; Secor and Snoke, 1978; Secor, 1987). The formal usage of the names for these rock units in South Carolina is adopted in this study.

## Stratigraphy

The rocks of the study area comprise two formations and numerous intrusive rocks of various ages and compositions. The Richtex Formation is the most extensive stratigraphic unit within the study area and is host for the majority of the gold deposits. Bordering the Richtex Formation on the north and south is the Persimmon Fork Formation. These two formations are intruded by numerous pre- and post-metamorphic igneous rocks varying in size and composition from large granodiorite plutons to very small mafic and felsic dikes. Modal analyses of major rock types are given in Table 1.

### *Persimmon Fork Formation*

Rocks mapped here and in adjacent areas of the Carolina slate belt of Georgia have been referred to as the lower volcanic sequence (Lincolnton metadacite) and the felsic pyroclastic sequence (Carpenter, 1976; Paris, 1976; Whitney and others, 1978). Paris (1976) referred to the lower pyroclastic sequence informally as the Pleasant Grove formation. Correlative rocks in South Carolina were named the Persimmon Fork Formation (Secor and Wagener, 1968) and have been mapped into Georgia (Secor and others, 1986a; Secor, 1987). Since the same rocks formally named in South Carolina can be mapped into Georgia, the formal name as used in South Carolina will be used here.

The Persimmon Fork Formation in South Carolina and Georgia consists of vitric and crystal-vitric metatuffs; coarse-grained dacitic lava flows, domes and tuffs (Lincolnton metadacite); lithic and lithic lapilli metatuffs; meta-agglomerates; mafic metatuffs; quartz sericite schist; and interlayered metasediments including volcanoclastic metagraywackes and meta-argillites (Whitney and others, 1978; Secor, 1987). In the extreme northern portion of the study area the Persimmon Fork Formation consists of fine grained, felsic ash flow metatuffs; felsic lapilli metatuffs; minor mafic phyllites; and meta-dacitic flows. A second occurrence of this formation is near the southeastern border of the study area within and adjacent to the Modoc zone (Plate 1). These rocks of the Persimmon Fork Formation have been subjected to intense shearing associated with development of the Modoc zone and are of slightly higher metamorphic grade.

The source for the pyroclastic rocks that make up the bulk of the Persimmon Fork Formation most likely is the Lincolnton metadacite (Whitney and others, 1978). The Persimmon Fork Formation has been assigned a Cambrian age based on Rb-Sr whole-rock and U-Pb (zircon) ages of  $554 \pm 20$  Ma and 568 Ma, respectively, for the Lincolnton metadacite (Carpenter and others, 1982). Estimates on the thickness of this formation in Georgia vary from approximately 3500 feet (1050 m) to 5000 feet (1500 m) (Paris, 1976; Carpenter, 1976; Whitney and others, 1978).

In the study area, the most common rocks within the Persimmon Fork Formation are the felsic ash flow

metatuffs and felsic lapilli metatuffs. The felsic ash flow metatuffs consist of lithic and vitric fragments in a matrix of very fine grained quartz, plagioclase, sericite and epidote. The lithic fragments are predominantly felsic volcanic rocks with minor amounts of mafic to intermediate volcanic fragments. The felsic lapilli metatuffs consist of lithic and vitric fragments of similar composition as the ash flow metatuffs (Fig. 2). Lapilli are on the average 15 to 20 mm long and are flattened in the plane of the foliation. Matrix material predominantly consists of fine grained quartz, plagioclase, sericite, chlorite and epidote.

The remaining rocks may be abundant locally, but overall are minor components. The mafic phyllites are composed of chlorite, epidote, clinozoisite, calcite, albite and quartz and are chemically similar to basalts. All original minerals have been metamorphosed to a greenschist assemblage. The meta-dacite flows are fine to medium grained, leucocratic and are composed of anhedral to subhedral phenocrysts of albite and blue, opalescent, locally embayed quartz (Fig. 3) in a groundmass of quartz, plagioclase and minor sericite and epidote.

### *Richtex Formation*

Workers in South Carolina, and more recently in Georgia, have described this unit as a sequence of low-grade metasediments (pelites and wackes) with intermediate to mafic tuffs and flows all of which are intruded by sheets and plugs of mafic igneous rocks (Secor and Wagener, 1968; Howell and Pirkle, 1976; Secor, 1987). Investigators working in Georgia have referred to this unit as the upper sedimentary sequence (Carpenter, 1976; Whitney and others, 1978; Carpenter, 1982). Geologic mapping for this study has further extended the Richtex Formation into Georgia and has shown that this formation composes the bulk of the study area (Plate 1) and is host for the majority of the gold deposits.

As observed within the study area, the Richtex Formation consists of light to dark gray, banded meta-argillite; dark gray metasiltstone and metagraywacke; mafic metatuffs and flows; and felsic metavolcanic rocks. These rocks were intruded by sheets, plugs and stocks of intermediate to mafic igneous rocks prior to metamorphism and penetrative deformation (Fig. 4). Original sedimentary structures such as laminated bedding and graded bedding are well preserved in the meta-argillites, metasiltstones and metagraywackes (Fig. 5). Additional original structures observed in other areas include cross-bedding, scour-and-fill and bedding slump (Whitney and others, 1978). Volcanic fragments constitute a high percentage of the clasts within the metasedimentary rocks. Interlayered with the metasedimentary rocks are thin beds of mafic and felsic metavolcanic rocks (tuffs and flows), varying in composition from dacites to basalts. Within the study area, the felsic metavolcanic rocks increase in abundance to the southwest. The estimated minimum thickness of this formation in Georgia is 5000 feet (1500 m) (Carpenter, 1976; Whitney

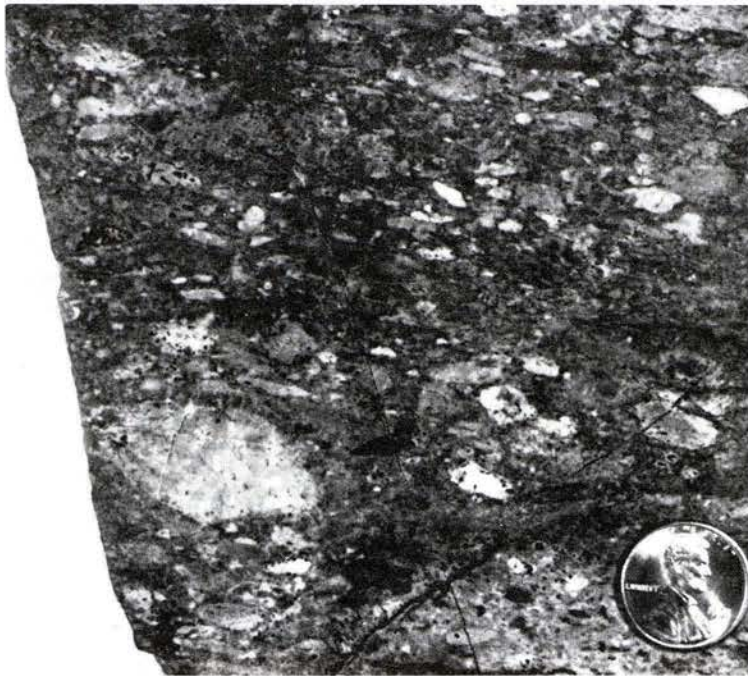


Fig. 2 - Sawed hand sample (top) and outcrop of lapilli metatuffs of intermediate composition (Persimmon Fork Formation).

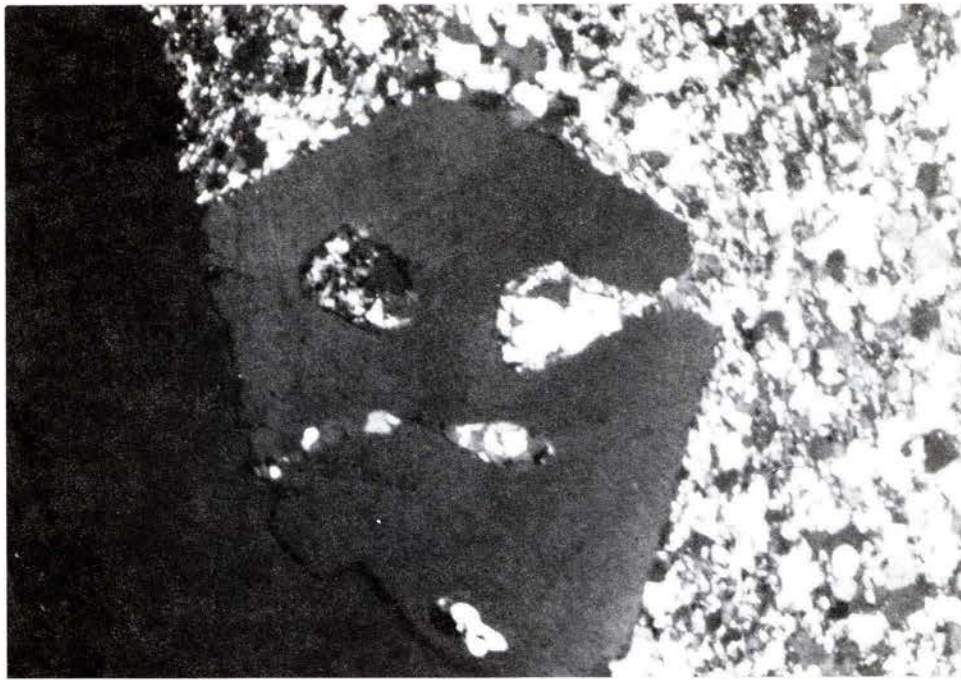


Fig. 3 - Embayed quartz crystals in a matrix of quartz, plagioclase, epidote, sericite and chlorite (metadacite flow Persimmon Fork Formation). Field of view is 3.16 mm.



Fig. 4 - Saprolite exposure (Richtex Formation) along the shoreline of Clark Hill Reservoir of felsic metavolcanic rocks (light colored) intruded by pre-kinematic sheeted mafic bodies. View is to the north. Penetrative slaty cleavage strikes northeast.

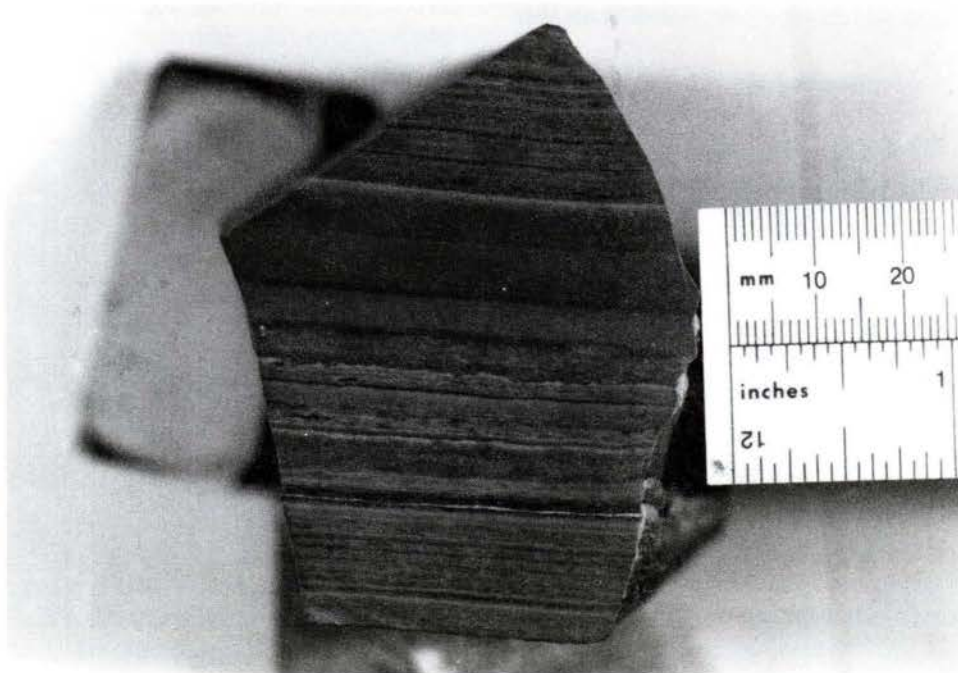


Fig. 5 - Well-preserved original sedimentary structures in metasediments: graded bedding above (Persimmon Fork Formation) and laminated bedding below (Richtex Formation).

Table 1  
Modal Analysis of Representative Rock Types\*

	<u>AO-25</u>	<u>WB-99</u>	<u>AO-183</u>	<u>L-207C</u>	<u>C-151</u>	<u>C-144</u>	<u>WL-200</u>	<u>AO-178</u>	<u>WB-71A</u>	<u>L-53</u>	<u>C-145A</u>	<u>AO-176B</u>
Quartz	44	30	10	10	43	60	20	40	72	<1		40
Plagioclase	44	25	82	82	7		40	41	20	25		10
Epidote	10	5	2				15	10	1	20		10
Clinozoisite										20	40	
Chlorite	2			1	2	18	5	5				35
Amphibole**	<1									15		
K-feldspar		30	3	5								
Biotite		3	1	1				<1	5			
Sericite		7	2	1	47	20	20	3	2	<1		<1
Opauques					1	2		1		2		<1
Garnet									<1			
Actinolite										3		
Serpentine										15	40	
Pyroxene**											20	
Calcite												5

\*Based on visual estimates

\*\*Highly altered; composition unknown

AO-25, WB-99 - metagranodiorite

AO-183, L-207C - metaquartz monzonite

C-151, C-144, WL-200 - metasediments

AO-178, WB-71A - felsic metavolcanic rocks

L-53, C-145A - mafic meta-intrusions

AO-176B - mafic phyllite

Refer to Plate 3 for sample locations.

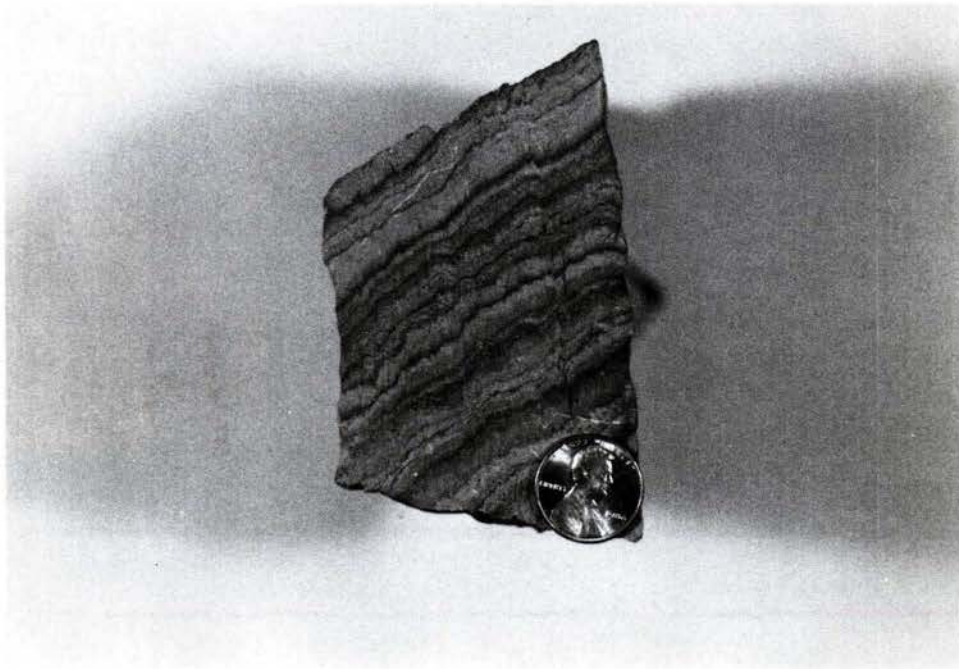


Fig. 6 - Meta-argillite (Richtex Formation) exhibiting a distinct bedding/cleavage relationship.

and others, 1978).

Meta-argillite is the most abundant rock type within the Richtex Formation. Bedding thickness varies from very fine to massive, however, rocks possessing finely laminated bedding are much more abundant. The meta-argillite is predominantly composed of quartz, sericite and chlorite with lesser amounts of plagioclase and epidote. The color of the darker laminations is attributable to a higher chlorite and/or heavy mineral content. The meta-argillite generally exhibits clearly defined bedding/foliation relationships (Fig. 6).

The metasiltsstones and metagraywackes are less abundant than the meta-argillite and were observed only locally. These rocks are medium to dark gray and are composed of quartz, plagioclase and lithic clasts in a fine-grained matrix of quartz, sericite, chlorite and epidote. The lithic clasts are volcanic and sedimentary in origin. Bedding is generally massive although fine bedding is present locally. Graded bedding is distinct, and scour structures can be seen locally (Fig. 7).

Locally, interlayered with the metasedimentary rocks are mafic and felsic metavolcanic rocks which are dacitic to basaltic in composition. Texturally, these rocks vary from very fine-grained tuffs and flows to lapilli and lithic tuffs and are very similar to metavolcanic rocks within the Persimmon Fork Formation.

A Cambrian age is inferred for the Richtex Formation based on the presence of Cambrian fossils in lithologically similar rocks in the Belair belt in South Carolina (Maher and others, 1981). Rocks of the Belair belt occupy the same stratigraphic position as those of the Richtex Formation, but lie on the opposite limb of the Kiokee antiform. Cambrian fossils also have been found in the Asbill Pond formation (informal usage) in South Carolina (Samson and others, 1990; Secor and others, 1983), a lateral equivalent of the Richtex Formation (Secor and others, 1986a).

### *Rocks of the Northern Part of the Modoc Zone*

Bordering the study area on the southeast are a suite of rocks composing a 4-5 km wide ductile shear zone called the Modoc zone (Sacks and Dennis, 1987). Rocks of the northern part of the Modoc zone are within the study area. As the Modoc zone is approached from the northwest, regional greenschist mineral assemblages in the slate belt become overprinted by upper greenschist and amphibolite facies mineral assemblages, and slaty cleavage becomes overprinted by a mylonitic foliation. Zones where shearing has been concentrated are characterized by S-C mylonites, muscovite "fish," and augen gneiss.

Modoc zone rocks within the study area consist of two mappable units. One unit consists of interlayered sericite quartzite and quartz-sericite phyllite. The phyllite in this unit exhibits S-C mylonitic textures indicating that shearing has been particularly intense in these rocks.

Locally, this unit has undergone brecciation and at least two episodes of silicification. Silicification also was accompanied by base and/or precious metal mineralization, and several prospecting pits are present in the silicified horizons. Across the study area, this unit forms a series of elongate hills, locally of high relief where silicification was intense (Plate 1).

The second mappable unit consists of muscovite-biotite-quartz schist, biotite gneiss, biotite augen gneiss and amphibole gneiss. The schist consists of fine- to very fine-grained biotite, muscovite, quartz and plagioclase. Muscovite "fish" porphyroblasts (Fig. 8) are common. The biotite gneiss and biotite augen gneiss are granitic in composition and vary widely in texture from fine-grained and finely laminated to thickly banded and augened. Shearing is pervasive, and most of the gneisses are slightly garnetiferous. Most likely, ortho- and paragneisses are present. The amphibole gneisses possibly are higher grade equivalents of mafic phyllites in the Richtex Formation and/or the Persimmon Fork Formation to the northwest.

## **Intrusive Rocks**

Intruding the Richtex and Persimmon Fork Formations are sheets, plugs and stocks of igneous rocks which are granodioritic to gabbroic in composition. These range in size from dikes less than 10 cm wide to stocks several square kilometers in areal extent. Most of these show the effects of penetrative deformation and greenschist facies metamorphism; others are clearly post-kinematic.

### *Pre- to Syn-metamorphic Intrusions*

These intrusions exhibit the greatest variety of compositions and textures. They include large, medium-grained metagranodiorites, fine-grained metaquartz monzonites and sheeted bodies which are andesitic to gabbroic in composition.

### **Metagranodiorite**

The most areally extensive intrusive rock type is medium-grained metagranodiorite. The largest of these bodies is located in extreme northern McDuffie County and is approximately 12 km long and 2 km wide. Several smaller bodies of this rock are located to the southwest in western McDuffie County and northern Warren County, and another is located near the northeastern end of the study area in Lincoln County (Plate 1).

These intrusions are medium-grained, mesocratic, weakly to well foliated and are locally strongly sheared. Linear features are best observed at weathered outcrops. Contacts with the country rock are sharp (Fig. 9), and fine-grained, dark-colored xenoliths are common (Fig. 10). A



Fig. 7 - Scour features in metagraywacke (Richtex Formation). Note deformed rip-up clasts.

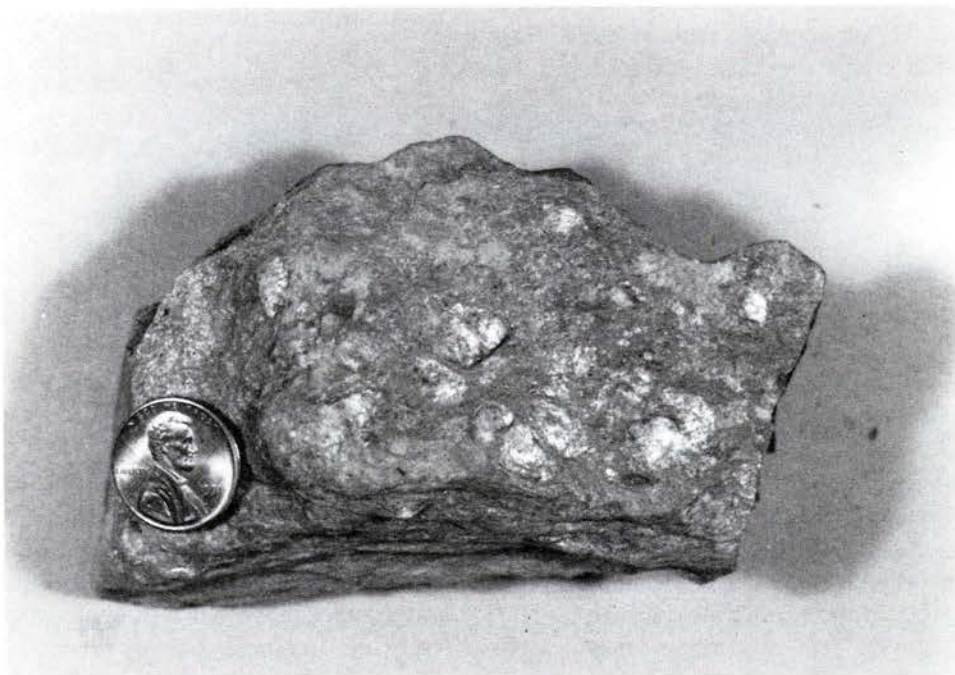


Fig. 8 - "Muscovite fish" (Persimmon Fork Formation) along shears in weathered phyllite adjacent to the Modoc zone.



Fig. 9 - Sawed hand sample containing a contact between metagranodiorite and the phyllite country rock (Richtex Formation). Sample is from the tailings dump at the Columbia Mine.



Fig. 10 - Dark-colored xenoliths within the large metagranodiorite body.

few outcrops display numerous domal features (Fig. 11) representing either original flow texture or a subsequent tectonic fabric. The latter explanation is favored since these features occur in the vicinity of local ductile shear zones. These intrusions are locally cut by leucocratic felsic dikes (Fig. 12).

Microscopically, the metagranodiorites consist of subhedral plagioclase (albite to oligoclase), potassium feldspar and quartz with accessory chlorite, epidote, biotite and sericite. Modal compositions are given in Table 1. Plagioclase crystals are highly altered to epidote and sericite and locally are rimmed by more sodic plagioclase or potassium feldspar. Many of the plagioclase crystals are partially bound by granophyric intergrowths of quartz and potassium feldspar. Locally, this symplectic texture composes up to fifty percent of the rock in some of the smaller bodies. Potassium feldspar is clouded with inclusions and is highly altered to sericite. Most of the biotite has altered to chlorite.

Chemically, these rocks are granodiorites (Table 2) (Fig. 13) although their mineral composition reflects the greenschist facies metamorphism they have undergone. The abundance of granophyric textures strongly suggests that these bodies are hypabyssal intrusions that cooled relatively rapidly.

### Metaquartz Monzonite

A second intrusive rock is metaquartz monzonite. This rock type is present in two separate bodies approximately 7 and 2 square kilometers in size. The larger body is located in the extreme northeastern part of the study area in Lincoln County, and the smaller body is located in the north-central part of the study area in Wilkes County.

The metaquartz monzonites are fine-grained, grayish pink in color and exhibit a tectonic fabric mainly along their peripheries. Upon weathering, these rocks become redder in color and any tectonic fabric is accentuated. Microscopically, these rocks consist of subhedral crystals of plagioclase (albite/oligoclase), potassium feldspar and quartz with accessory chloritized biotite, epidote and muscovite. Sericitization, locally, is intense (Fig. 14). Very little of the quartz and potassium feldspar occurs as individual crystals, instead the two minerals typically are graphically intergrown, locally exhibiting a cuneiform texture (Fig. 15). Most plagioclase crystals are rimmed by potassium feldspar (Fig. 14).

The metaquartz monzonite is chemically similar to the metagranodiorite (Table 3) (Fig. 13) and may be genetically related. The presence of granophyric textures in both intrusive rock types suggests that both are hypabyssal intrusions (Bard, 1986). The lack of a penetrative tectonic fabric, as in the metagranodiorite, suggests that the metaquartz monzonite was intruded tectonically late and is younger than the metagranodiorite. Apparent cross-cutting relationships between bodies of metagranodiorite and metaquartz monzonite in the extreme northeastern part of the study area (Plate 1) suggest that the metaquartz monzonite intruded the metagranodiorite and supports the above conclusion of their relative ages. The metaquartz

monzonite and the metagranodiorite may have shared a common parent magma. Both the metaquartz monzonite and metagranodiorite bodies are locally cut by lamprophyre dikes (discussed below). It has been suggested that similar meta-intrusions in South Carolina were the magma source for the Carolina slate belt volcanic rocks (Secor, 1987).

### Mafic Sheets and Stocks

Less abundant, but widespread, are pre- to syn-metamorphic mafic sheets and stocks which are dioritic to gabbroic in composition. The sheeted mafic bodies (metadikes/sills) intruded the Richtex Formation prior to metamorphism and subsequently were penetratively deformed along with the country rock. Their crosscutting nature can be observed at numerous outcrops (Fig. 4). Fresh outcrops of these sheeted bodies, however, are rare, but the rock bodies appear to be andesitic to basaltic in composition and are composed of a greenschist metamorphic assemblage of chlorite, epidote, calcite and opaque minerals.

The mafic stocks generally have an exposed surface area of less than one square kilometer, however, one body north of Leah (Plate 1) is approximately four square kilometers in size. Most of the stocks crosscut the country rock, but many are elongated parallel to subparallel to the regional strike of  $S_p$ , suggesting that some of these may be thick, deformed dikes or sills. These rocks are dark greenish gray and exhibit a variety of textures, ranging from porphyritic to medium and coarsely equigranular. Most of these bodies are weakly foliated, except along their borders where foliation is well-developed and the mafic bodies blend into the enclosing phyllites.

The mafic stocks are highly altered. Chemically, they are dioritic in composition (Table 4) (Fig. 16); however, their original igneous mineralogy has been metamorphosed to a greenschist facies assemblage. They are composed predominantly of serpentinized clinopyroxene and hornblende, clinozoisite (after calcic plagioclase) and albite/oligoclase with minor amounts of sericite, opaques and chlorite. The stocks clearly intruded the Richtex Formation prior to or coincident with regional deformation.

### *Post-metamorphic intrusive rocks*

Post-metamorphic intrusive rocks represent a very small, but unique component of the rocks of the study area. These rocks consist of cross-cutting diabase and lamprophyre dikes. They are clearly the youngest rocks in the study area and provide an upper age limit for various geologic events.

### Diabase Dikes

Diabase dikes occur intermittently across the study area and are the most abundant of the cross-cutting mafic dikes. At least seven are present within the study area. They are less than one meter in thickness, up to seven kilometers long and strike N 5-35° W. These dikes are



Fig. 11 - Domal features within the large metagranodiorite body. Outcrop is along the shoreline of Clark Hill Reservoir.



Fig. 12 - Sapolite exposure of a leucocratic felsic dike cross-cutting the largest metagranodiorite body. The exposure is along the shoreline of Clark Hill Reservoir, and the view is to the northwest. Notebook is 23 x 30 cm.

Table 2

	Major Oxide, Trace Element and Normative Analyses of Metagranodiorites*									
	AO-1	AO-9	AO-25	AO-34	BV-1	C-86	C-87	C-146	C-147	C-153
SiO <sub>2</sub>	63.4	66.1	62.1	66	63.9	72.7	73	68.2	68.1	68
TiO <sub>2</sub>	0.59	0.5	0.66	0.77	0.57	0.22	0.26	0.5	0.54	0.56
Al <sub>2</sub> O <sub>3</sub>	14.7	14.8	15.7	14.4	14.7	13.5	12.9	14.2	14.4	14.6
Fe <sub>2</sub> O <sub>3</sub>	2.79	2.43	2.99	2.67	2.72	1.24	0.86	2.51	2.45	2.17
FeO	2.7	2.06	3.02	1.65	2.05	0.64	1.15	2.26	2.45	2.1
MnO	0.13	0.11	0.17	0.19	0.11	0.06	0.08	0.13	0.15	0.16
MgO	1.66	1.29	1.72	0.96	1.46	0.43	0.43	0.84	0.99	1.22
CaO	4.21	3.58	4.78	2.83	4.1	1.63	1.64	3.15	3.16	3.46
Na <sub>2</sub> O	3.26	3.95	3.87	4.76	4.12	3.89	4.11	4.1	3.95	4.01
K <sub>2</sub> O	2.96	1.84	2.02	2.56	1.94	3.52	3.44	2.15	2.58	1.94
P <sub>2</sub> O <sub>5</sub>	0.29	0.27	0.25	0.37	0.17	0.08	0.29	0.05	0.17	0.21
S <sub>2</sub> tot	0.02	0.02	0.02	0.02	0.05	0.07	0.02	0.02	0.04	0.02
CO <sub>2</sub>	0.02	0.03	0.03	0.01	0.74	0.07	0.05	0.11	0.05	0.02
LOI	1.62	1.29	1.39	0.99	1.94	0.5	0.34	0.81	0.93	0.89
Total	98.35	98.27	98.72	98.18	98.57	98.55	98.57	99.03	99.96	99.36

## Trace Elements (ppm)

Cu	24	6	27	6	33	2	3	20	16	6
Pb	2	20	2	24	26	15	15	19	21	9
Zn	61	44	83	114	61	24	33	74	68	55
Mo	<1	7	<1	<1	6	<1	<1	1	<1	<1
Ni	3	8	9	3	7	2	1	3	3	3
Co	10	11	10	6	8	2	7	7	9	11
Cd	1	<1	<1	<1	<1	<1	3	<1	<1	<1
Bi	<5	<5	<5	<5	<5	6	<5	<5	10	<5
As	16	<5	<5	14	7	<5	36	27	<5	21
Sb	<5	<5	<5	<5	<5	<5	<5	<5	<5	<5
Te	<10	<10	<10	<10	<10	<10	11	<10	<10	<10
Ba	878	700	555	582	743	962	674	714	706	427
Cr	175	196	217	163	169	137	246	339	190	198
V	78	71	88	20	72	18	13	41	39	54
Sn	<20	<20	<20	<20	23	<20	<20	<20	<20	<20
W	<10	<10	13	<10	<10	<10	<10	<10	<10	<10
Li	4	9	16	5	12	12	10	10	10	6
Be	2.8	2.3	2.3	3.5	5.3	2.2	2.8	2.6	3	2.5
Ga	<2	10	12	11	19	11	5	18	14	14
La	5	15	12	9	16	19	16	8	9	6
Ce	<5	<5	<5	<5	67	<5	<5	<5	<5	<5
Ta	49	9	170	<1	50	<1	53	31	133	<1
Sc	31	30	47	35	17	5	<1	25	38	24
Nb	7	8	10	9	11	11	7	11	6	7
Sr	143	261	284	280	385	165	123	171	146	146
Y	9	20	20	20	18	15	11	25	17	15
Zr	28	57	46	37	51	49	32	79	37	39

## CIPW Norms

Ap	0.65	0.60	0.56	0.82	0.38	0.18	0.64	0.11	0.38	0.47
Il	1.15	0.97	1.29	1.47	1.10	0.42	0.50	0.97	1.05	1.09
Mt	4.15	3.58	4.45	3.74	3.99	1.62	1.26	3.70	3.63	3.21
Or	17.88	11.02	12.22	15.21	11.57	20.76	20.52	12.87	15.53	11.67
Ab	28.2	33.90	33.55	40.50	35.21	32.86	35.11	35.17	34.06	34.56
An	17.11	16.22	19.98	10.42	16.05	7.55	6.30	14.18	14.21	16.09
Di	1.99		2.27	1.13	2.96			1.13	0.54	
Hy	3.01	2.59	3.20	1.28	1.94	0.70	1.14	1.68	2.24	2.59
C		0.91				1.04	0.26			0.24
Q	22.56	27.13	19.76	22.48	22.64	32.67	32.43	28.28	27.31	28.51
Hm				0.11		0.12				
Total	96.69	96.93	97.28	97.16	95.84	97.91	98.16	98.09	98.94	98.43

Ap-apatite, Il-ilmenite, Mt-magnetite, Or-orthoclase, Ab-albite, An-anorthite, Di-diopside, Hy-hypersthene, C-corundum, Q-quartz, Hm-hematite

Table 2 Continued

## Major Oxide, Trace Element and Normative Analysis of Metagranodiorites\*

	C-157	C-162	C-164	C-165	CMH-1	L-208	P-1	WB-95A	WB-98	WB-99
SiO <sub>2</sub>	70.7	73.8	72.5	73.8	58.9	63.3	59.4	67.8	71.3	71.7
TiO <sub>2</sub>	0.63	0.31	0.28	0.26	0.73	0.73	0.47	0.44	0.3	0.3
Al <sub>2</sub> O <sub>3</sub>	13.2	13.2	13.7	12.1	14.6	15.7	12.9	14.8	13.5	14
Fe <sub>2</sub> O <sub>3</sub>	3.43	0.85	1.5	2.14	3.44	3.2	2.07	2.68	1.62	1.82
FeO	1.35	0.6	1.2	1.1	2.9	2.06	3.02	1.42	1.16	1.03
MnO	0.17	0.04	0.05	0.15	0.15	0.15	0.14	0.09	0.07	0.07
MgO	0.5	0.6	0.54	0.13	3.03	1.95	2.1	1.15	0.55	0.62
CaO	2.05	2.02	1.72	0.95	4.82	3.78	5.18	3.72	2.27	2.24
Na <sub>2</sub> O	4.4	5.56	3.84	4.64	3.7	4.39	2.58	4.3	3.72	3.72
K <sub>2</sub> O	2.61	0.68	3.3	2.79	1.12	3.49	2.66	1.78	3.31	3.09
P <sub>2</sub> O <sub>5</sub>	0.26	0.18	0.08	0.14	0.21	0.21	0.25	0.18	0.1	0.1
S <sub>tot</sub>	0.04	0.03	0.02	0.02	0.1	0.02	0.06	0.02	0.02	0.02
CO <sub>2</sub>	0.06	0.03	0.02	0.06	2.81	0.07	3.33	0.03	0.07	0.03
LOI	0.76	0.55	0.65	0.53	4.69	0.93	5.95	0.74	1.04	0.9
Total	100.16	98.45	99.4	98.81	101.2	99.98	100.11	99.15	99.03	99.64

## Trace elements (ppm)

Cu	8	8	7	7	42	24	25	16	11	7
Pb	7	2	6	6	35	10	10	25	2	5
Zn	84	6	32	63	116	84	86	49	26	32
Mo	<1	2	<1	<1	3	6	<1	<1	<1	<1
Ni	1	1	3	2	67	19	19	8	6	1
Co	3	5	6	2	17	14	14	14	3	2
Cd	<1	<1	<1	<1	<1	<1	<1	<1	2	<1
Bi	<5	9	<5	<5	<5	6	<5	10	<5	<5
As	23	26	49	27	<5	<5	64	51	<5	56
Sb	<5	<5	<5	<5	9	7	<5	<5	<5	<5
Te	<10	<10	<10	<10	<10	<10	<10	<10	<10	<10
Ba	726	172	824	787	795	687	690	555	1073	904
Cr	161	223	257	187	170	234	236	172	273	122
V	4	24	24	2	89	90	89	87	30	31
Sn	<20	26	<20	<20	28	<20	<20	<20	<20	<20
W	<10	<10	<10	11	<10	12	<10	<10	<10	<10
Li	5	3	8	5	18	8	10	3	8	11
Be	2.8	2.5	2.6	2.7	4.8	3.4	1.9	2.3	2	2.3
Ga	3	8	<2	<2	15	8	6	<2	13	7
La	8	3	8	15	17	13	13	15	14	12
Ce	<5	<5	<5	<5	93	<5	<5	<5	<5	<5
Ta	46	57	<1	<1	20	72	83	<1	59	13
Sc	23	29	33	26	20	36	26	47	26	23
Nb	9	5	5	8	9	13	13	7	8	10
Sr	160	125	131	93	397	300	302	224	155	140
Y	23	15	10	22	11	21	25	8	20	19
Zr	54	39	34	66	41	86	87	68	50	57

## CIPW Norms

Ap	0.57	0.40	0.18	0.31	0.48	0.47	0.56	0.40	0.22	0.22
Il	1.20	0.59	0.53	0.50	1.43	1.40	0.92	0.84	0.58	0.57
Mt	3.10	1.17	2.18	3.11	5.16	4.68	3.08	3.63	2.37	2.64
Or	15.48	4.03	19.48	16.50	6.83	20.77	16.07	10.58	19.69	18.22
Ab	37.37	47.25	32.47	39.30	32.32	37.42	22.33	36.61	31.69	31.42
An	8.50	8.88	8.00	3.80	20.57	12.92	16.12	15.93	10.43	10.44
Di					2.37	4.08	7.27	1.31	0.22	
Hy	0.82	0.99	1.11	0.25	5.12	2.22	2.95	1.55	1.01	1.02
C	0.06	0.15	1.75	0.11						1.40
Q	30.87	34.33	33.01	34.32	19.32	15.01	21.47	27.31	31.70	32.76
Hm	1.31	0.05						0.20		
Total	99.30	97.84	98.71	98.20	93.60	98.96	90.77	98.36	97.90	98.69

Ap-apatite, Il-ilmenite, Mt-magnetite, Or-orthoclase, Ab-albite, An-anorthite, Di-diopside, Hy-hypersthene, C-corundum, Q-quartz, Hm-hematite

\*See Appendix A for analysis parameters.

Refer to Plate 3 for sample locations.

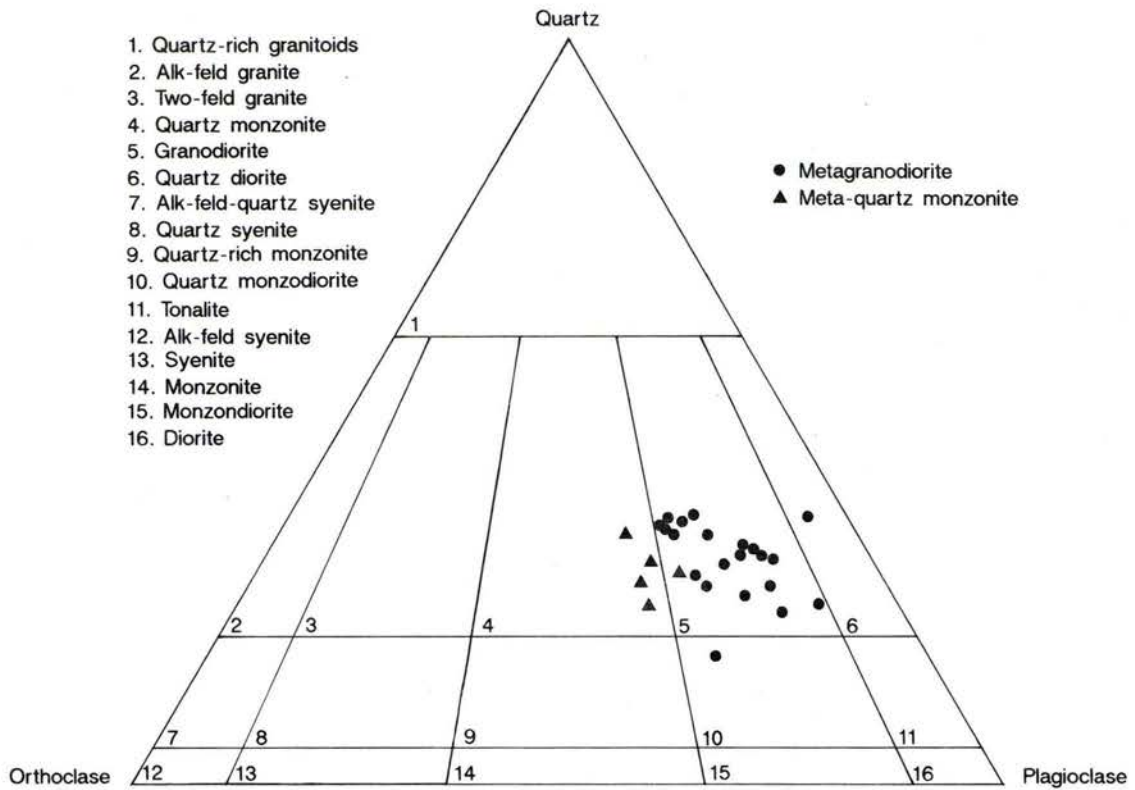


Fig. 13 - Chemical classification of metagranodiorites and metaquartz monzonites from the study area (after Streckeisen, 1976).

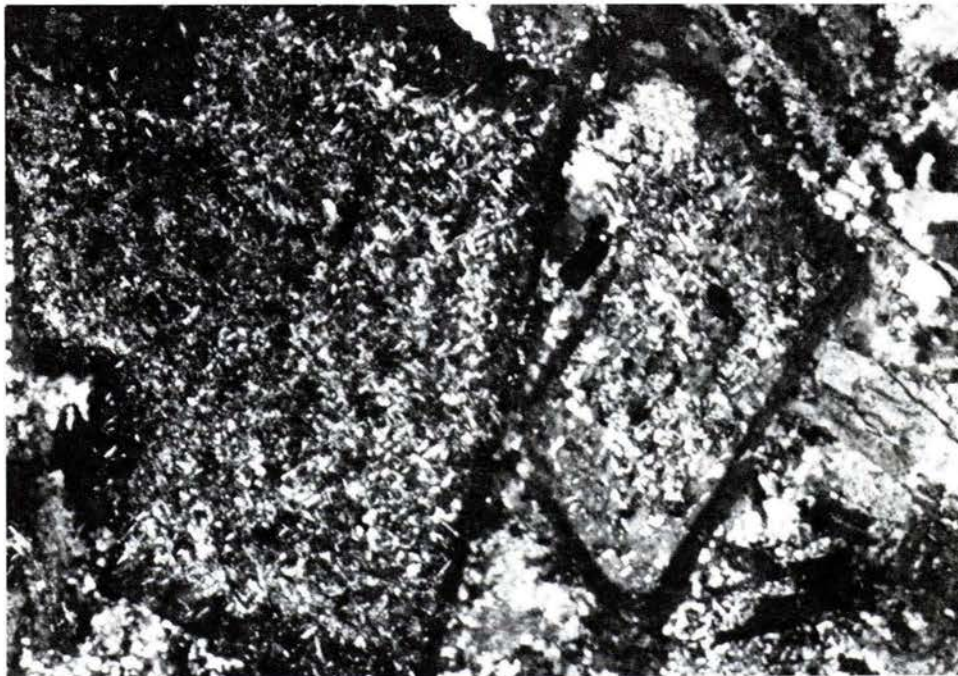


Fig. 14 - Sericitization and feldspar zoning in metaquartz monzonite. Euhedral plagioclase (albite) crystals are highly altered to sericite and are rimmed by potassium feldspar (dark rims). Remainder of sample consists of quartz, chlorite and opaque minerals. Field of view is 3.16 mm.

Table 3  
Major Oxide, Trace Element and Normative  
Analysis of Metaquartz Monzonites\*

	AO-183	L-63	L-207A	AO-183A	L-207C
SiO <sub>2</sub>	71.5	69.3	71.4	75.69	70.53
TiO <sub>2</sub>	0.39	0.52	0.43	0.28	0.42
Al <sub>2</sub> O <sub>3</sub>	13.3	14.2	13.6	12.46	13.39
Fe <sub>2</sub> O <sub>3</sub>	1.48	1.8	1.46	1.94	4.43
FeO	0.7	0.7	0.65	2.51	0.96
MnO	0.1	0.09	0.12	0.10	0.11
MgO	0.32	0.38	0.36	0.13	0.34
CaO	1.2	0.85	0.82	0.57	0.83
Na <sub>2</sub> O	4.39	4.83	5.03	4.27	4.56
K <sub>2</sub> O	4.04	4.46	3.64	4.35	4.45
P <sub>2</sub> O <sub>5</sub>	0.21	0.21	0.25	0.07	0.07
S tot	0.02	0.02	0.02	<0.02	<0.02
CO <sub>2</sub>	0.02	0.43	0.03	0.04	0.03
LOI	0.69	1.05	0.63	0.35	0.45
Total	98.36	98.84	98.44	102.76	100.57
<u>Trace elements</u>					
Cu	5	4	5	8	6
Pb	22	2	2	32	30
Zn	52	52	51	11	18
Mo	3	<1	<1	5	6
Ni	4	1	2	8	9
Co	5	5	5	1	2
Cd	<1	<1	<1	<1	<1
Bi	<5	<5	<5	7	11
As	36	<5	36	14	88
Sb	<5	<5	<5	15	28
Te	<10	<10	<10	<10	<10
Ba	706	681	750	835	849
Cr	248	240	210	245	181
V	7	9	8	4	8
Sn	<20	<20	<20	<20	<20
W	<10	11	<10	<10	<10
Li	1	2	4	<1	9
Be	3	3.6	3.4	3.3	3.5
Ga	<2	<2	5	16	22
La	11	10	13	12	17
Ce	<5	<5	<5	61	75
Ta	15	91	<1	<1	<1
Sc	28	7	7	9.3	11
Nb	5	9	8	8	11
Sr	128	85	106	56	126
Y	22	14	22	16	26
Zr	72	50	104	117	142
<u>CIPW Norms</u>					
Ap	0.46	0.46	0.55	0.16	0.15
Il	0.74	0.99	0.82	0.54	0.80
Mt	1.46	1.04	1.24	2.87	2.24
Or	23.93	26.33	21.46	26.13	26.31
Ab	37.24	40.84	42.48	36.74	38.62
An	4.59	2.84	2.43	2.02	2.93
Di				0.31	0.66
Hy	0.53	0.62	0.59	1.20	0.38
C	0.05	0.77	0.99		
Q	28.15	22.35	26.60	32.40	25.10
Hm	0.48	1.08	0.61		2.90
Total	97.63	97.34	97.76	102.37	100.09

Ap-apatite, Il-ilmenite, Mt-magnetite, Or-orthoclase,  
Ab-albite, An-anorthite, Di-diopside, Hy-hypersthene,  
C-corundum, Q-quartz, Hm-hematite

\*See Appendix A for analysis parameters.  
Refer to Plate 3 for sample locations.

interpreted to be part of the suite of Mesozoic diabase dikes that occur along the eastern flank of the Appalachians from Alabama to Massachusetts. They are, for the most part, unmetamorphosed, exhibiting only slight hydrothermal alteration locally.

The diabase dikes within the study area are relatively typical of diabases elsewhere within the Piedmont and Blue Ridge. At least two varieties, quartz-normative and olivine-normative, are present (Table 5). The olivine-normative diabases exhibit the more typical diabasic texture and consist of subophitic intergrowths of labradorite and augite, interstitial olivine and minor amounts of biotite, magnetite and serpentine. Locally, the labradorite is slightly sericitized. The quartz-normative diabases, on the other hand, consist of euhedral laths of hornblende in a matrix of granophyric andesine and quartz with accessory epidote and magnetite.

Geochemical and petrological studies of diabases of the Appalachian orogen have revealed several subsets based on chemical composition, geographic distribution, strike and age (Lester and Allen, 1950; King, 1961; Weigand and Ragland, 1970; Dooley, 1977; Ragland and others, 1983). Data pertaining to these dikes have been useful in the development of theories on the rifting of Pangea in middle Mesozoic time (Dooley, 1977; Ragland and others, 1983 and references within). The ages of diabase dikes in Georgia were reported to range from 160 to 230 m.y. (Dooley, 1977), but were later re-interpreted to be no older than 195 m.y. (Dooley and Wampler, 1983). Additional studies from other areas of the orogen have suggested two age clusters at 165-175 m.y. and 180-190 m.y. (Deininger and others, 1975; Smith and Noltimier, 1979; Sutter and Smith, 1979). Further work on the diabases of Georgia is warranted in light of other studies of diabases in adjacent states (Ragland and others, 1983).

### Lamprophyre Dikes

Lamprophyres constitute a second suite of post-metamorphic mafic dikes. These types of rocks have been discussed briefly in a few previous studies of portions of the Slate Belt (Fouts, 1966; Crawford and others, 1966; Paris, 1976; Reusing, 1979), but as in the case of the diabases, they constitute only a very small portion of the lithologies present. Possibly for that reason, they have been discussed only briefly in previous studies.

Lamprophyres are not simply textural varieties of plutonic or volcanic rocks. They possess distinct mineralogy, chemistry and textures and have been given their own separate classification (Streckeisen, 1979). Some of their outstanding characteristics include (1) their occurrence as dikes, sills, pipes and diatremes; (2) their unusual chemistry which is primitive (Mg, Cr, and Ni-rich), but also rich in large ion lithophile elements, light rare earth elements and volatiles; (3) their dark color, idiomorphic texture and common content of euhedral mafic phenocrysts; and (4) the common hydrothermal alteration of biotite, olivine,

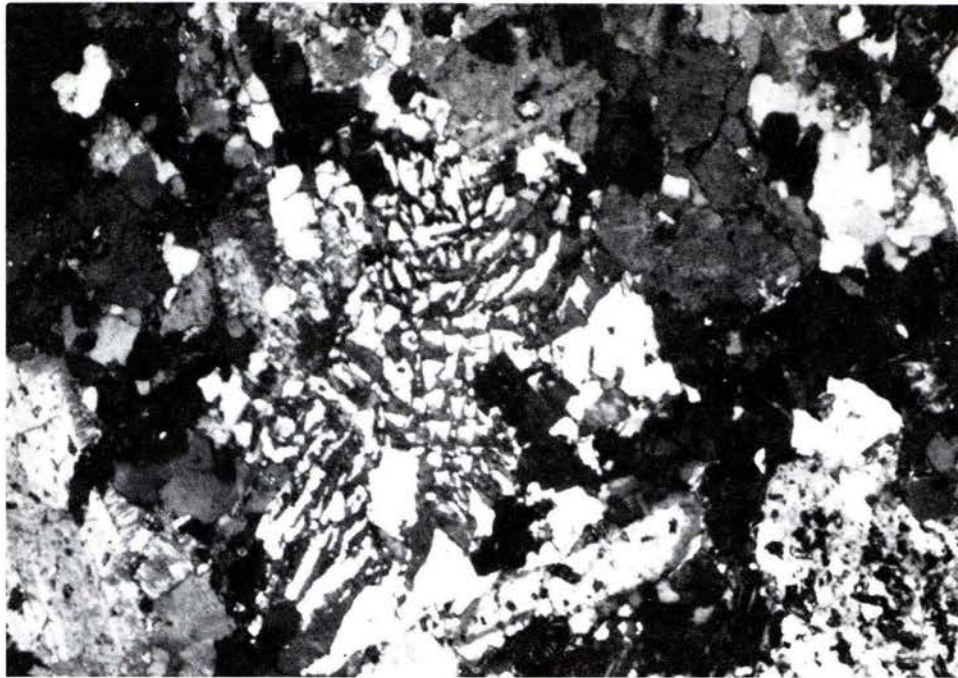


Fig. 15 - Cuneiform intergrowth (granophyre) of quartz (dark) and potassium feldspar in metaquartz monzonite. Groundmass consists of quartz, plagioclase, biotite, sericite and epidote. Field of view is 3.16 mm.

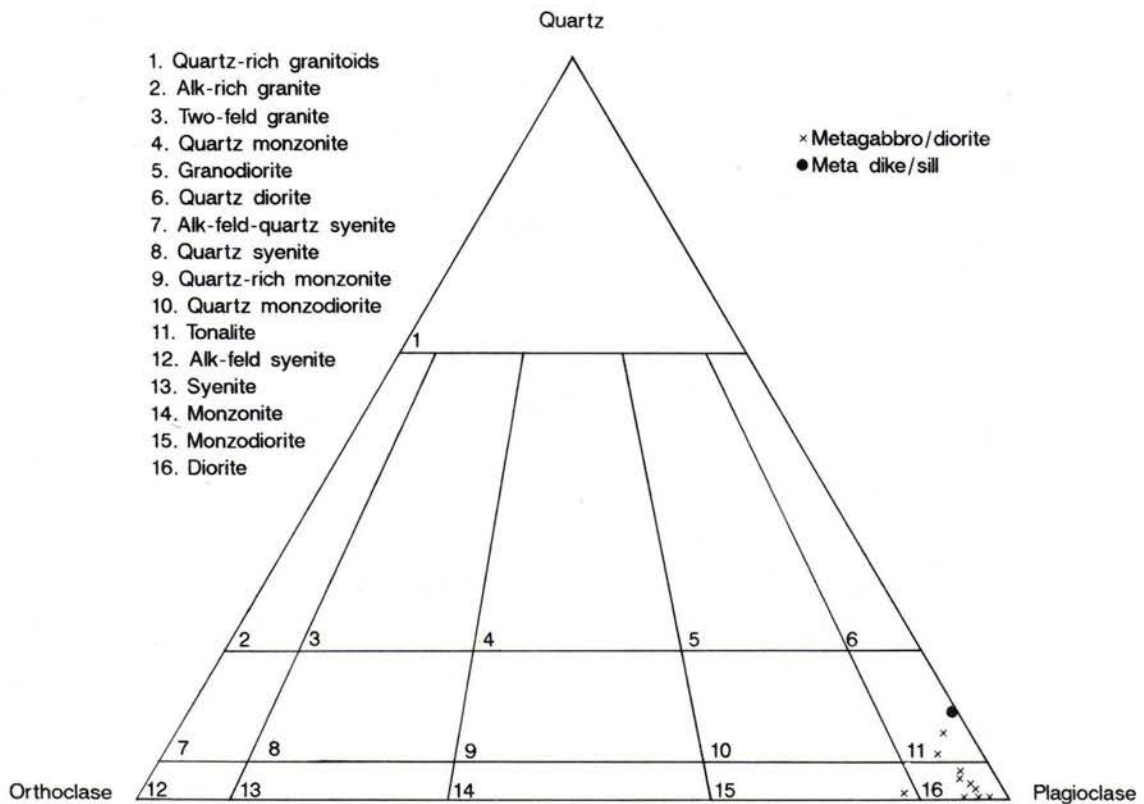


Fig. 16 - Chemical classification of mafic meta-intrusive bodies from the study area (after Streckeisen, 1976).

Table 4

## Major Oxide, Trace Element and Normative Analysis of Mafic Intrusions\*

	AO-180	C-76	C-138	C-145A	C-150A	C-152	C-158	C-161A	C-163	L-53	WB-120
SiO <sub>2</sub>	46.8	49.4	55.8	44.3	47	48	45.9	49.1	49.8	49.9	45
TiO <sub>2</sub>	0.43	0.69	1.02	0.22	0.74	0.73	0.3	0.99	0.82	1.12	0.51
Al <sub>2</sub> O <sub>3</sub>	15.7	15.9	18.2	19.1	19.4	18.7	12.1	16.7	17	16.6	13.8
Fe <sub>2</sub> O <sub>3</sub>	3.08	2.6	2.77	3.73	6.47	3.33	3.47	3.85	2.68	2.78	2.95
FeO	4.45	6.66	6.15	3.75	2.51	5.4	5.65	5.8	6.5	8.75	7.6
MnO	0.15	0.17	0.2	0.13	0.33	0.18	0.19	0.17	0.17	0.23	0.22
MgO	10	8.76	2.71	9.9	6.03	6.31	14.2	6.23	7.07	5.03	11.8
CaO	13.6	10.8	2.49	13.5	12	10.5	12.6	10.3	9.8	9.9	11.9
Na <sub>2</sub> O	1.06	1.92	2.38	0.76	1.42	2.16	0.58	2.57	1.99	2.72	1.21
K <sub>2</sub> O	0.3	0.33	2.05	0.33	0.37	0.5	0.31	1.18	0.53	0.4	0.18
P <sub>2</sub> O <sub>5</sub>	0.18	0.2	0.22	0.19	0.1	0.25	0.21	0.28	0.1	0.26	0.17
S <sub>tot</sub>	0.03	0.02	0.03	0.02	2.09	0.02	0.02	0.02	0.02	0.02	0.03
CO <sub>2</sub>	0.17	0.07	0.03	0.03	0.03	0.03	0.02	0.03	0.04	0.07	0.75
LOI	2.97	1.8	3.24	3.46	3.53	2.73	2.7	1.59	1.69	0.85	3.38
Total	98.92	99.32	97.29	99.42	102.02	98.84	98.25	98.81	98.21	98.63	99.5
<u>Trace elements</u>											
Cu	103	50	48	na	92	39	32	20	65	115	50
Pb	2	14	4	na	43	27	12	6	7	2	2
Zn	41	82	59	na	150	119	64	57	69	89	64
Mo	<1	<1	<1	na	<1	<1	<1	<1	<1	<1	<1
Ni	121	108	30	na	43	28	158	54	78	31	142
Co	47	43	36	na	37	21	57	31	41	37	61
Cd	<1	<1	2	na	<1	<1	<1	<1	<1	<1	<1
Bi	7	17	<5	na	13	6	25	<5	<5	<5	14
As	<5	<5	<5	na	8	7	<5	<5	<5	32	<5
Sb	8	13	<5	na	25	<5	<5	<5	14	7	<5
Te	<10	<10	11	na	<10	11	<10	17	13	12	<10
Ba	50	142	83	na	123	126	84	128	202	67	54
Cr	253	321	157	na	147	261	372	200	192	71	244
V	171	241	220	na	255	251	137	258	224	367	212
Sn	<20	<20	<20	na	<20	<20	<20	<20	<20	<20	<20
W	<10	<10	<10	na	17	<10	<10	<10	<10	<10	17
Li	6	11	9	na	13	12	4	4	7	12	10
Be	1.2	1.6	1.8	na	1.5	1.7	1.1	2.1	1.9	1.8	1.2
Ga	<2	<2	<2	na	8	<2	<2	<2	<2	7	<2
La	3	7	3	na	4	2	3	5	4	6	3
Ce	<5	<5	<5	na	<5	<5	<5	<5	<5	<5	<5
Ta	61	<1	82	na	24	67	126	<1	42	<1	96
Sc	106	86	62	na	81	44	112	59	67	33	96
Nb	3	6	4	na	4	3	4	6	5	5	5
Sr	204	324	316	na	345	235	139	270	276	340	284
Y	6	13	9	na	8	5	9	7	7	16	11
Zr	15	28	5	na	22	39	23	8	14	11	37
<u>CIPW Norms</u>											
Ap	0.42	0.49	0.48	0.42	0.22	0.59	0.48	0.65	0.24	0.63	0.38
Il	0.86	1.45	1.92	0.43	1.44	1.50	0.59	1.99	1.72	2.34	0.98
Mt	4.71	4.17	3.98	5.51	7.18	5.21	5.24	5.89	4.28	4.43	4.34
Or	1.87	2.15	11.98	1.98	2.23	3.18	1.90	7.34	3.44	2.59	1.08
Ab	9.44	17.91	19.92	6.54	12.26	19.69	5.10	22.91	18.51	25.25	10.37
An	39.15	37.27	10.80	48.53	46.40	42.94	30.63	32.18	39.46	35.00	32.09
Di	26.85	17.63		16.12	12.21	9.90	28.81	17.09	11.44	14.37	23.04
Hy	11.98	15.15	7.28	8.61	6.84	11.16	13.44	8.79	13.42	10.56	7.93
Ol	0.47			7.77			9.32				15.13
C			15.98								
Q		1.22	21.64		5.92	1.88		0.33	3.95	2.52	
Hm					1.67						
Total	95.75	97.43	93.99	95.91	96.37	96.06	95.51	97.17	96.46	97.69	95.34

Ap-apatite, Il-ilmenite, Mt-magnetite, Or-orthoclase, Ab-albite, An-anorthite, Di-diopside, Hy-hypersthene, Ol-olivine, C-corundum, Q-quartz, Hm-hematite, na-no analysis

\*See Appendix A for analysis parameters.

Refer to Plate 3 for sample locations.

Table 5

	Major Oxide, Trace Elements and Normative Analyses of Mafic Dikes*											
	AO-35 <sup>1</sup>	AO-38 <sup>1</sup>	AO-41 <sup>2</sup>	AO-172 <sup>2</sup>	AO-173 <sup>1</sup>	AO-184 <sup>1</sup>	AO-196 <sup>1</sup>	C-142B <sup>2</sup>	C-160 <sup>2</sup>	WB-71B <sup>2</sup>	WB-95B <sup>1</sup>	WL-203 <sup>1</sup>
SiO <sub>2</sub>	51.7	51.9	57.3	46.2	52.9	52.1	52.4	46.8	48.4	47.4	58.5	52.8
TiO <sub>2</sub>	1.87	1.11	0.66	1.18	1.29	1.89	2.36	1.52	0.72	1.03	1.02	2.34
Al <sub>2</sub> O <sub>3</sub>	14.5	16.2	16.2	17.1	13.8	14.4	15.1	17.4	16.7	15.9	16.2	14.9
Fe <sub>2</sub> O <sub>3</sub>	3.76	3.71	4.65	2.34	2.98	3.95	4.28	2.2	1.54	2.63	4.25	4.42
FeO	6.15	4.1	4.44	10.4	5.2	5.8	5.15	11.7	7.7	10.05	1.8	4.65
MnO	0.15	0.13	0.16	0.19	0.15	0.15	0.16	0.16	0.18	0.2	0.09	0.14
MgO	5.39	4.99	3.21	6.73	6.11	5.41	4.56	6.39	7.11	7.02	3.35	4.12
CaO	6.44	6.14	8.65	8.73	5.53	6.76	6.54	8.27	11.7	10	4.54	5.84
Na <sub>2</sub> O	2.99	4.17	2.08	3.09	3.15	3.11	3.28	3.68	1.25	2.73	4.24	3.14
K <sub>2</sub> O	2.36	3.18	0.12	0.32	3.06	2.42	2.46	0.28	0.19	0.59	3.88	3.24
P <sub>2</sub> O <sub>5</sub>	0.39	0.6	0.16	0.4	0.47	0.6	0.38	0.24	0.19	0.15	0.2	0.41
S <sub>tot</sub>	0.19	0.3	0.09	0.11	0.06	0.2	0.2	0.04	0.03	0.12	0.11	0.19
CO <sub>2</sub>	0.16	0.03	0.03	0.03	1.66	0.17	0.2	0.03	0.08	0.09	0.25	0.38
LOI	1.6	1.6	0.72	0.65	3.5	1.69	1.99	0.1	2.27	0.67	1.31	2.09
Total	97.65	98.16	98.47	97.47	99.86	98.65	99.06	98.81	98.06	98.58	99.74	98.66
<u>Trace elements (ppm)</u>												
Cu	28	47	46	52	36	36	30	64	7	155	24	25
Pb	45	17	2	2	12	15	19	7	2	14	38	14
Zn	81	72	78	84	98	106	114	89	68	97	59	111
Mo	7	<1	<1	<1	<1	<1	<1	<1	<1	2	<1	<1
Ni	83	69	14	82	130	99	72	86	65	132	47	61
Co	33	30	27	57	39	43	32	65	45	57	17	33
Cd	4	<1	<1	<1	<1	<1	<1	<1	<1	<1	<1	<1
Bi	39	<5	17	13	<5	7	26	<5	17	7	<5	<5
As	99	38	<5	<5	22	<5	<5	36	25	<5	<5	6
Sb	38	<5	8	<5	<5	<5	<5	<5	<5	<5	<5	<5
Te	49	<10	35	20	<10	21	<10	16	13	<10	<10	<10
Ba	586	973	91	91	769	788	870	103	94	182	1424	788
Cr	165	215	178	159	239	298	174	121	328	240	154	165
V	131	170	275	115	135	177	183	124	234	210	122	175
Sn	<20	<20	<20	<20	<20	<20	<20	<20	<20	<20	<20	<20
W	16	10	<10	<10	<10	23	<10	<10	<10	<10	<10	<10
Li	13	2	4	4	15	14	14	6	6	4	17	13
Be	2.8	3.1	1.2	1.6	3.3	2.8	3.4	1.8	1.8	1.3	4.9	3.1
Ga	27	7	3	<2	3	15	<2	<2	<2	3	4	<2
La	20	11	5	2	24	29	24	2	2	6	10	12
Ce	<5	<5	<5	<5	<5	<5	<5	<5	<5	<5	<5	<5
Ta	61	170	160	35	112	<1	<1	143	158	75	123	<1
Sc	98	19	23	55	33	31	14	59	85	<1	33	30
Nb	22	8	5	7	13	24	23	9	5	7	8	24
Sr	462	947	337	212	716	662	786	228	234	119	982	668
Y	8	13	12	16	10	16	10	14	7	19	9	9
Zr	87	75	15	24	90	162	123	47	8	70	87	110
Rb	120	113	7	11	97	101	71	10	4	18	119	126
Cl	100	100	<100	100	<100	100	100	<100	<100	<100	100	100
F	771	218	160	90	425	606	912	107	122	126	665	735
<u>CIPW Norms</u>												
Ap	0.91	1.30	0.36	0.90	1.11	1.39	0.86	0.52	0.47	0.33	0.44	0.92
Il	3.78	2.08	1.30	2.29	2.63	3.79	4.63	2.87	1.53	1.99	1.96	4.56
Mt	5.81	5.31	6.99	3.47	4.64	6.05	6.41	3.17	2.49	3.88	3.18	6.57
Or	14.82	18.49	0.73	1.93	19.36	15.06	14.98	1.64	1.25	3.54	23.18	19.58
Ab	26.89	34.72	18.21	26.71	28.54	27.72	28.60	29.86	11.77	23.44	36.28	27.18
An	20.38	15.84	35.70	32.53	15.50	19.16	19.80	29.87	43.85	29.82	13.86	17.38
Di	9.41	9.00	6.57	7.65	9.20	10.47	9.72	7.78	16.55	16.56	6.77	8.40
Hy	9.12	1.60	5.13	3.67	10.46	8.44	6.07		13.82	3.43	3.75	5.19
Ol		7.91		17.52				22.41		14.72		
Ne								0.54				
Q	4.58		22.64		3.20	4.52	5.60		3.96		6.53	6.21
Hm											2.11	
Total	95.70	96.23	97.63	96.68	94.64	96.59	96.67	98.67	95.68	97.70	98.07	96.00

\*See Appendix A for analysis parameters. Refer to Plate 3 for sample locations.

Ap-apatite, Il-ilmenite, Mt-magnetite, Or-orthoclase, Ab-albite, An-anorthite, Di-diopside, Hy-hypersthene, Ol-olivine, Ne-nepheline, Q-quartz, Hm-hematite <sup>1</sup>Lamprophyre dikes; <sup>2</sup>Diabase dikes

pyroxene and plagioclase (Streckeisen, 1979; Rock and others, 1989). They are normally divided into calc-alkaline, alkaline and melilitic (ultramafic) subgroups (Streckeisen, 1979) with a possible fourth subgroup consisting of lamproites and kimberlites (Rock, 1987).

Within the study area, three varieties of lamprophyres are recognized. They are all within the calc-alkaline subgroup and chemically are classified as kersantites and spessartites (Fig. 17), but all do not neatly fit into published mineralogical classifications of lamprophyres (Williams and others, 1954; Streckeisen, 1979).

The first variety of lamprophyre dike is a classic spessartite in texture and mineralogy. This rock consists of prismatic hornblende phenocrysts and clusters of euhedral augite in a groundmass of hornblende and plagioclase microlites with accessory chlorite and magnetite. The plagioclase (andesine?) is rimmed with more sodic feldspar and is clouded with inclusions of unknown composition. Two of these dikes were observed within a few meters of each other just east of Kemp Creek on the Aonia Quadrangle cutting rocks of the Richtex and Persimmon Creek Formations. These dikes strike N53°W and N60°W and appear to dip vertically. Rocks with the same mineralogy and from the same vicinity have been described as hornblende andesites (Crawford and others, 1966). A lamprophyre just north of the study area with the same mineralogy was described by Reusing (1979).

The second variety of lamprophyre dikes is a kersantite. This rock consists of an aphanitic assemblage of augite, diopside, sericitized andesine and/or labradorite with minor pyrite, magnetite, chloritized biotite, quartz and serpentine. These very fine-grained minerals are embedded in a clouded, glassy groundmass. Within this assemblage are somewhat rounded quartz and albite xenocrysts up to 7 mm long. The albite xenocrysts are zoned and partially sericitized, and both types of xenocrysts are rimmed by sericite(?) aligned perpendicular to the xenocryst boundaries (Fig. 18). In hand specimen, the light gray to white xenocrysts are in contrast to the black, aphanitic matrix (Fig. 19). Three dikes of this composition were found, two in the vicinity of the spessartite dikes near Kemp Creek (described above) and another on a tributary of the Little River, all on the Aonia Quadrangle. One of these dikes strikes N20°W, another N15°W, and both apparently dip vertically. The third dike, however, strikes N50°E and dips 47°NW. These dikes crosscut the metaquartz monzonite intrusion and felsic metavolcanic rocks of the Persimmon Fork Formation.

The third variety of lamprophyre dikes also are kersantites, but differ in that their chief mafic mineral is biotite. These dikes consist of an aphanitic assemblage dominated by chloritized, green biotite and altered plagioclase (andesine?) with subordinate amounts of green hornblende, carbonate, epidote, quartz, chlorite, sphene, apatite and magnetite. The plagioclase is highly altered to epidote and sericite and is rimmed by more sodic feldspar. These lamprophyres are dark gray in color and locally contain

rounded, mafic xenoliths(?), consisting predominantly of biotite. Three dikes of this composition were found, all cross-cutting the large metagranodiorite body on the Aonia and Wrightsboro Quadrangles (Plate 1). Two dikes strike N15°W and dip steeply to the southwest, whereas the third dike strikes N30°W and dips 30° southwest.

The above lamprophyres, in contrast to the diabases, are enriched in phosphorus, potassium, strontium, barium, rubidium, carbon dioxide, sulfur and fluorine (Table 5) (Fig. 20). This type of chemical enrichment, along with standard petrographic techniques, can serve as a means of distinguishing between diabases and lamprophyres since some are megascopically similar. Lamprophyres have been misidentified in the past, and many so called diabases, andesite basalts, hornblende diorites and microdiorites found in many gold districts worldwide may actually be lamprophyres (Rock and others, 1989).

Lamprophyres are commonly found cross-cutting calc-alkaline intrusions and volcanic assemblages and are intimately associated with many gold deposits worldwide (Rock and others, 1989). Lamprophyres, themselves, are characteristically enriched in gold, and this fact has led some researchers to suggest that they are the source of the gold in the deposits with which they are associated (Rock and others, 1989; Rock and Groves, 1988). Those lamprophyres present within the study area also are enriched in gold relative to the other host rocks (Fig. 39), but these dikes represent such a small portion volumetrically, relative to the entire study area, that their functioning as the gold source seems unlikely.

### *Veins and Silicified Breccia Zones*

Post-dating most structural features and lithologies within the study are quartz veins and silicified breccia zones. The quartz veins include gold-bearing veins mined for their gold content and barren veins with no economic mineral concentrations. These veins were introduced into the country rock late in the deformational history of the area, just preceding, or contemporaneous with, the last fold event. These veins exhibit the same distinct orientations (see section on gold deposits), but it is not known why some are mineralized and others are not. The gold-bearing veins are discussed in detail in the section on gold deposits.

Two silicified breccia zones are found in Warren and McDuffie Counties on the Cadley 7.5 minute quadrangle. These zones consist of silicified, reddish-brown to tan clasts of country rock(?) interspersed in a matrix of clear to milky, void-filling quartz crystals (Fig. 21). The breccia's texture is accentuated upon weathering. Multiple episodes of brecciation and silicification are apparent.

These two breccia zones cross-cut the country rock; but it is not known whether they post-date all geologic features within the study area. These zones have been prospected locally for precious metals, but chemical analyses did not reveal economic concentrations of any elements

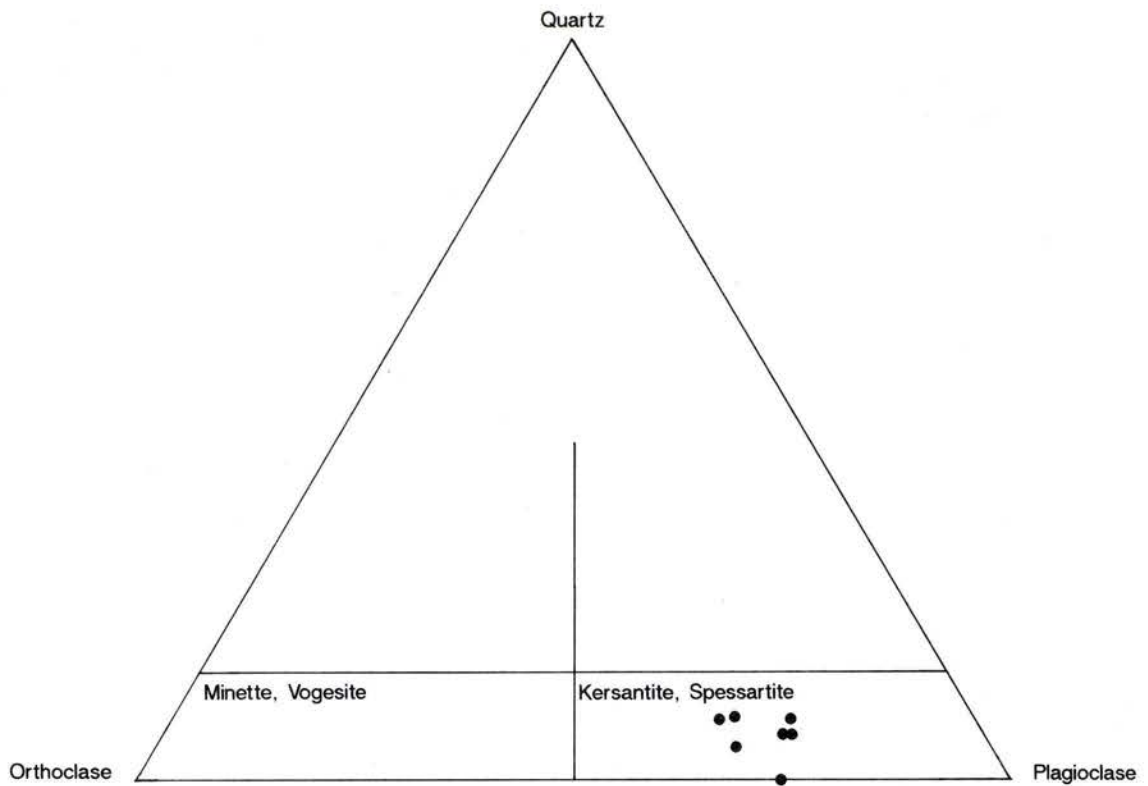


Fig. 17 - Chemical classification of lamprophyres from the study area (after Streckeisen, 1979).

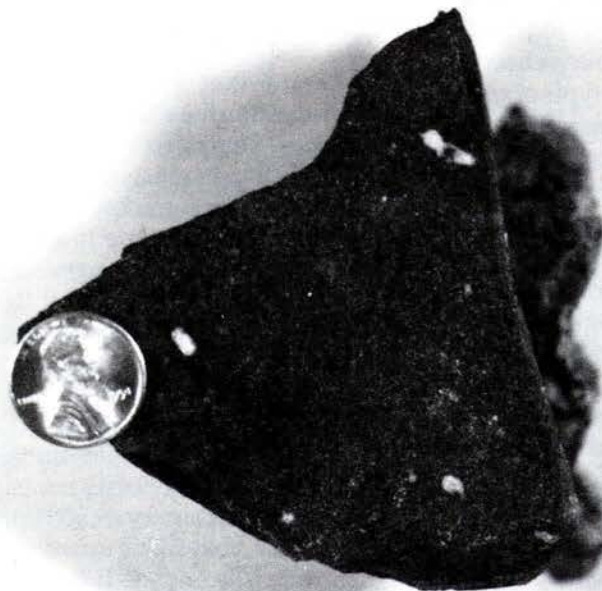


Fig. 19 - Hand sample of the kersantite from Fig. 18. Note light-colored xenocrysts in black, aphanitic groundmass.

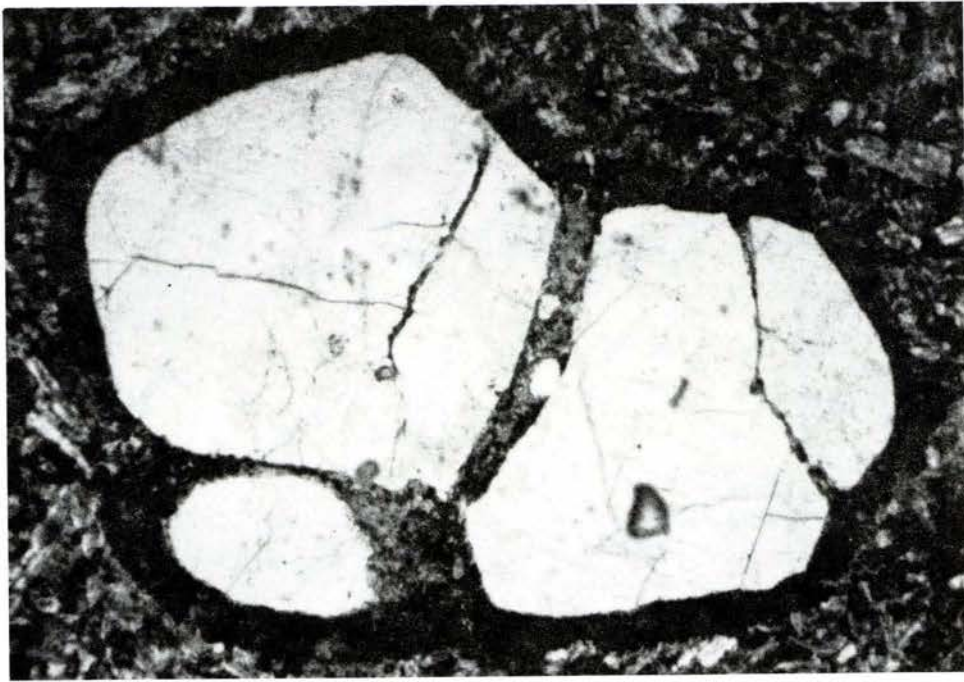


Fig. 18 - Quartz (above) and feldspar (albite) xenocrysts in a kersantite lamprophyre dike. Both xenocrysts are sericitized along their boundaries and are partially resorbed. Groundmass consists of augite, diopside, plagioclase, sericite, opaque minerals, serpentine and biotite. Field of view is 3.16 mm.

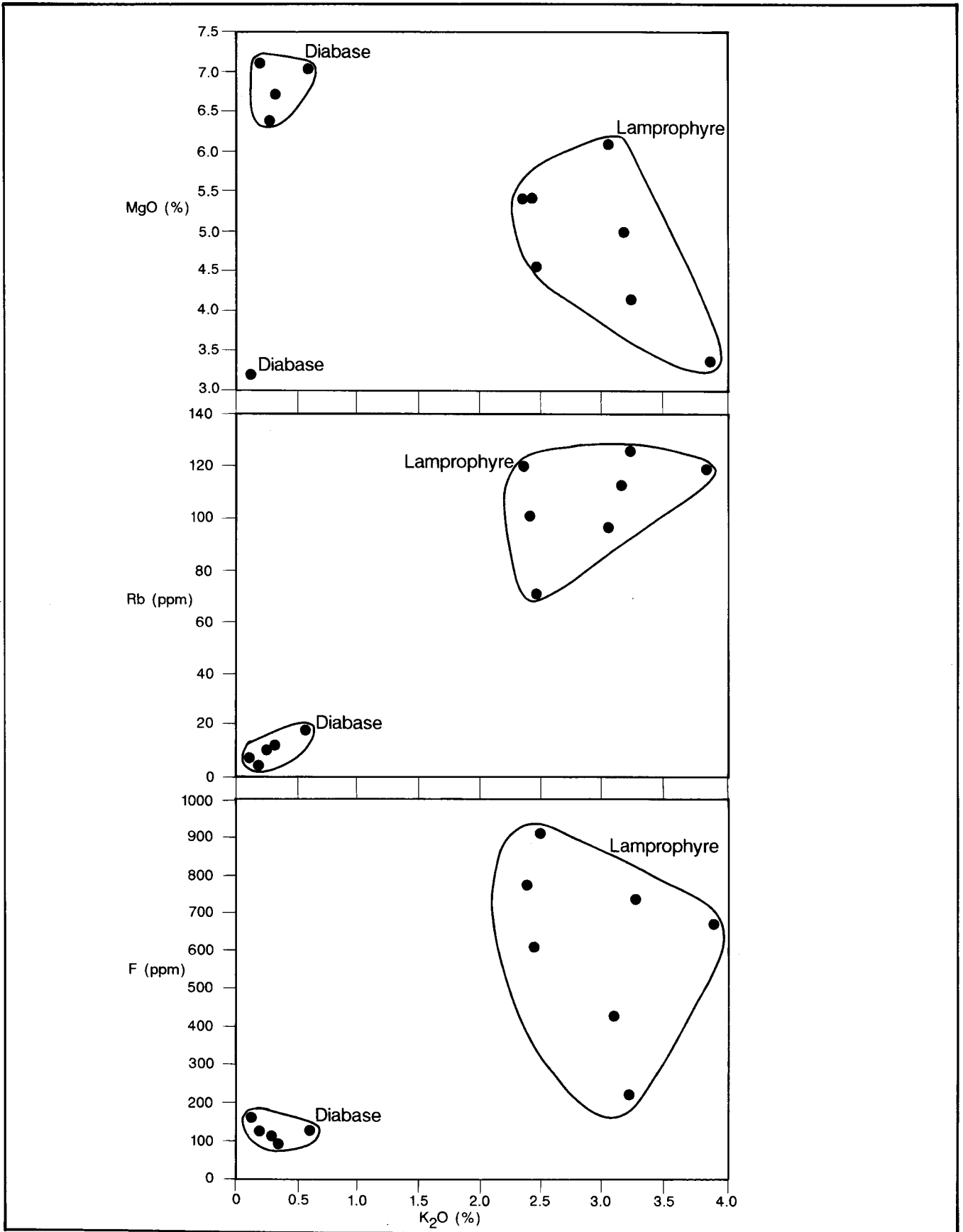


Fig. 20 - Comparison of major and trace element chemistry of the lamprophyre and diabase dikes.(Fig. 20 continued on next page.)

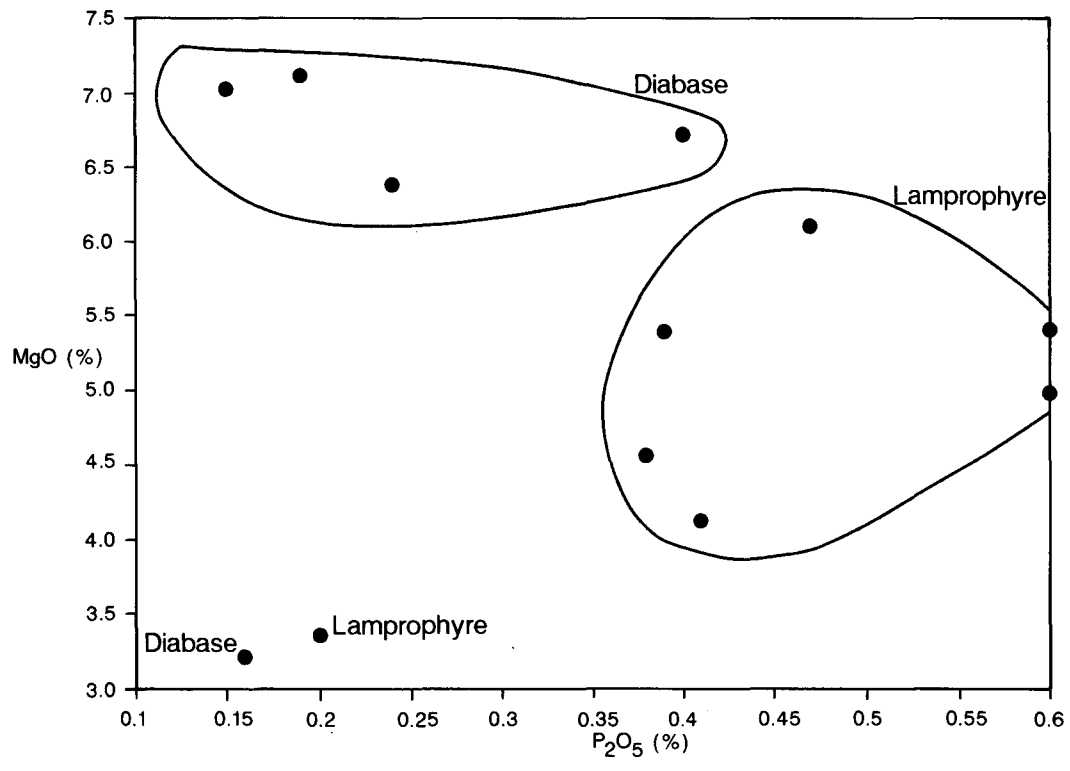
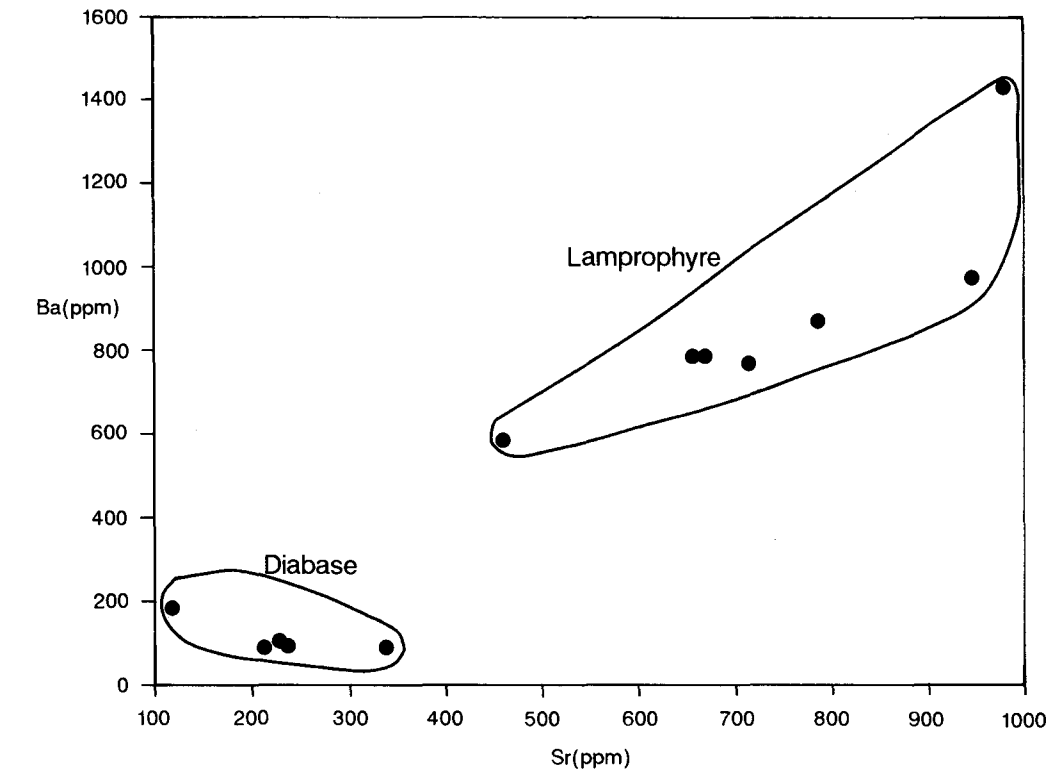


Fig. 20 - Comparison of major and trace element chemistry of the lamprophyre and diabase dikes.

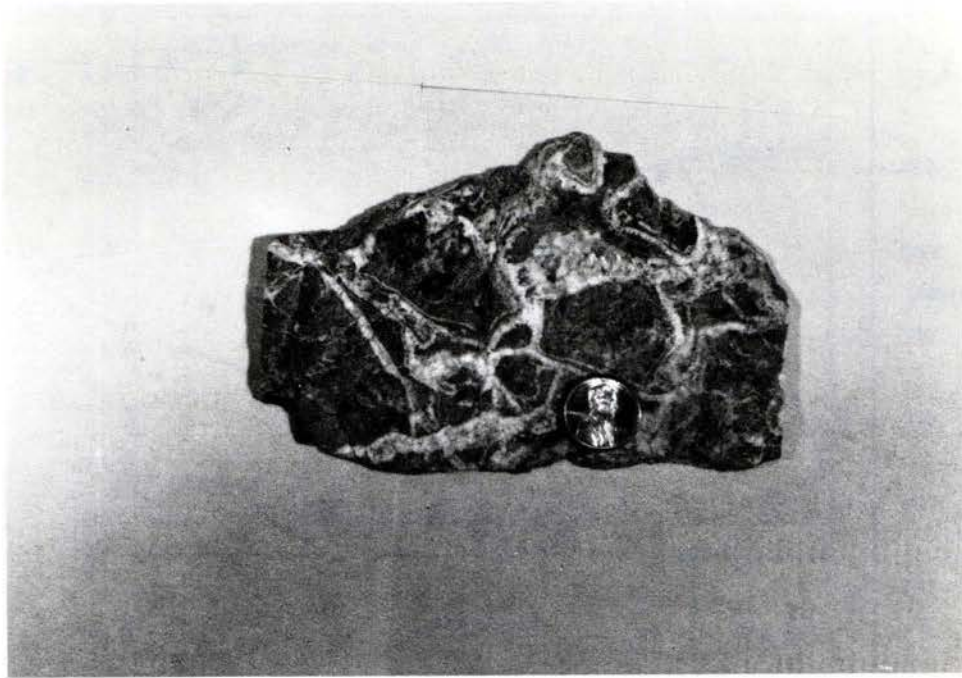


Fig. 21 - Hand sample of the silicified breccia zone near Fountain Campground, McDuffie and Warren Counties. Angular, silicified fragments of host rock (?) are cemented by light-colored quartz.

Table 6  
Assays of Silicified Breccia - Fountain Campground Vicinity\*

	<u>C-81A</u>	<u>C-81B</u>	<u>C-81AA</u>	<u>C-81AB</u>	<u>C-131</u>
Au**	16	7	13	18	8
Ag	<0.02	1.7	0.5	<0.02	<0.02
Cu	12	129	19	70	18
Pb	5	15	3	43	3
Zn	9	162	8	331	8
Mo	7	8	8	7	3
Ni	5	30	8	83	4
Co	1	18	2	40	<1
Bi	<5	<5	<5	23	<5
As	<5	18	<5	<5	6
Sb	<5	5	<5	8	<5
Hg	<0.010	0.120	<0.010	0.046	0.034
Ba	150	<20	1100	80	<20
Cr	314	194	528	206	135
W	<10	21	<10	<10	<10

\*Warren and McDuffie Counties, Cadley 7.5 minute quadrangle.  
 \*\*Au values are in ppb; all others are in ppm.  
 See Appendix A for analysis parameters.  
 Refer to Plate 3 for sample locations.

(Table 6). Preliminary oxygen isotopic analyses suggests that hydrothermal fluids that produced these zones were distinct from those that deposited the gold ores (See section entitled "Gold Ore").

## Metamorphism and Deformation

The eastern Piedmont of Georgia has been characterized as a series of alternating high and low-graded metamorphic belts (Crickmay, 1952). The study area lies within the Carolina slate belt which is a belt of low-grade metamorphic rocks flanked by two higher-grade metamorphic belts, the Charlotte belt on the north and the Kiokee belt on the south. The study area lies adjacent to the Kiokee belt and is separated from the Kiokee belt by the Modoc zone. Regional metamorphism and deformation has affected all rocks within the two belts to various degrees.

Metamorphic isograds were drawn for the study area (Plate 1) based on the first appearance of index minerals in pelitic metasediments and, to a lesser extent, in felsic metavolcanic rocks whose mineralogical proportions were similar to the metasediments. Due to the paucity of exposures of unweathered rock in some areas, the isograds are somewhat approximate. Also, the isograds should be offset by subsequent northwest-striking faults; however, data points are not of sufficient density to show this reliably. The general outline of the isograds, however, shows a greenschist facies assemblage throughout the study area with a chlorite zone in the center increasing to biotite and garnet zones to the north, west and south. A steep gradient is revealed between the study area and the Modoc zone to the south. The overall configuration of the isograds suggests a synformal structure.

### Early Paleozoic Deformation

Rocks within the study area have been metamorphosed to the greenschist facies of regional metamorphism and have been affected, at least in part, by three episodes of deformation. The earliest deformation ( $D_1$ ) recorded in these rocks is characterized by large-scale, isoclinal folds. These folds ( $F_1$ ) are responsible for most outcrop patterns throughout the Carolina slate belt (Secor and others, 1986a) and were accompanied by an axial planar slaty cleavage ( $S_1$ ) that is the dominant foliation within the study area. The study area is part of the Saluda synclinorium, an  $F_1$  fold (Secor and others, 1986a).  $D_1$  deformation affected both the Kiokee and Carolina slate belts and, reportedly, the Charlotte belt (Secor and others, 1986a). This event postdates deposition of the Cambrian slate belt strata and reportedly predates the intrusion of a suite of 385- to 415-Ma plutons in the Charlotte belt that do not record a  $D_1$  fabric (Butler and Fullagar, 1978; Fullagar, 1981).

In most exposures,  $S_1$  is parallel to original bedding ( $S_0$ ). However, in fold axes, incipient transposition of  $S_0$  is evident (Fig. 6).  $S_1$  developed under conditions of greenschist facies metamorphism, producing a mineral assemblage of chlorite, epidote, sericite, albite, calcite and

quartz. As the Modoc zone on the southeast is approached, biotite and rare garnet become a part of the mineral assemblages. These two minerals also appear near the southwestern and northwestern borders of the study area (Plate 1).

### Late Paleozoic Deformation

Included within the study area is the northern portion of the Modoc zone. The Modoc zone has been described as a fault zone (Howell and Pirkle, 1976; Hatcher and others, 1977), a gradational boundary between suprastructure (Carolina slate belt) and infrastructure (Kiokee belt) (Secor and others, 1986a; 1986b) and as a ductile shear zone (Sacks and Dennis, 1987). Rocks of the Modoc zone have been affected by a late Paleozoic (Alleghanian) deformation ( $D_2$ ) that was mainly restricted to the adjacent Kiokee belt (Secor and others, 1986a; Secor, 1987). Development of the Modoc zone as a steep metamorphic gradient between the Kiokee and Carolina slate belts reportedly occurred at this time (Secor and others, 1986a). Deformation in the northern portion of the Modoc zone is characterized by local overprinting of the  $S_1$  slaty cleavage by a mylonitic foliation and the development of an upper greenschist to amphibolite facies mineral assemblage. Shearing is widespread, but is concentrated in certain stratigraphic intervals. Areas of intense shearing are characterized by the development of muscovite "fish," S-C mylonites and augen gneiss. In somewhat less deformed horizons,  $D_2$  is characterized by small-scale folds ( $F_2$ ) that are accompanied by an axial planar foliation ( $S_2$ ) which locally partially transposes  $S_0$  and  $S_1$ . Evidence of  $D_2$  overprinting of  $D_1$  fabric and mineral assemblages diminish rapidly northwest of the Kiokee belt and was not observed northwest of the Modoc zone. Available geochronological data suggest that  $D_2$  deformation occurred about 295-315 Ma (Secor and others, 1986a).

Slaty cleavage ( $S_1$ ) in the Carolina slate belt and  $S_2$  foliation in the Kiokee belt have been folded by a later episode of deformation ( $D_3$ ) characterized by open folds ( $F_3$ ) that plunge gently to the southwest. These folds probably are parasitic on the Kiokee antiform (an  $F_3$  fold of Secor and others, 1986a). Weakly developed crenulations locally accompany these folds. Development of the Kiokee antiform resulted in the rotation of foliations within the study area to their present northwest-dipping orientation.

In the Kiokee and Carolina slate belts in South Carolina and extreme eastern Georgia, Secor and others (1986a) recognized a fourth deformational event manifested by the development of a regional shear zone (Irmo shear zone, Dennis and others, 1987) that overprints structures within the Modoc zone. Mapping for this study indicates that the Irmo shear zone passes southeast of the study area. Small, discordant shear zones observed within the study area probably are related to the development of the Irmo shear zone.

Based on work in the Kiokee and Carolina slate belts in South Carolina and extreme eastern Georgia, Secor

and others (1986a) recognized four deformational events that have affected these belts together or individually. Table 7 is a comparison of deformation observed by Secor and others (1986a) with that observed in the present study.

### *Shear zones*

Several narrow shear zones were recognized within the study area northwest of the Modoc zone. The existence of these shear zones appears to be independent of shearing associated with the Modoc zone. At least two (and possibly three) shear zones were recognized in extreme northern McDuffie County near the northern boundary of the largest metagranodiorite body. The shear zones vary in size from outcrop scale to zones nearly 100 meters wide and up to 5 kilometers long. The largest of these extends from near Broom Creek in an arcing fashion northeastward to near the McDuffie/Wilkes County line, roughly parallel to the Little River (Plate 1). The zone strikes from N45-70°E and, as other observed shear zones, dips moderately to the north-northwest.

The shear zones are characterized by a mylonitic foliation that is subparallel to and overprints  $S_1$  slaty cleavage in the metagranodiorite. Sheared metagranodiorite develops phyllitic bands composed mainly of chlorite and quartz separated by largely undeformed bands or augens of metagranodiorite. Locally, in the center of the shear zones, the metagranodiorite is totally altered to chlorite and quartz. The large shear zone mentioned above is locally mineralized and has been prospected for gold on a small scale near workings of the Porter Mine.

The age of these shear zones is late Paleozoic since they overprint early Paleozoic tectonic fabrics. Displacement along these zones is minimal; therefore, their timing relative to other late tectonic features is uncertain. They may be related to development of the Irmo shear zone (Dennis and others, 1987) immediately south of the study area.

### *Faulting*

Rocks within the study area have been affected by at least four episodes of faulting differing in orientation, age and magnitude. Evidence of the existence of pre-metamorphic faulting can be observed at the contact between the Richtex and Persimmon Fork Formations. Secor (1987) tentatively concluded that the contact is tectonic and cited several lines of evidence to support his conclusion. Mapping for this study also supports his conclusion. The most compelling argument for the existence of a fault between the Richtex and Persimmon Fork Formations, and also cited by Secor (1987), is the relative absence of sheeted mafic intrusive bodies within the Persimmon Fork Formation. The mafic bodies are conspicuously absent upon crossing from the Richtex Formation into the Persimmon Fork Formation. One would expect the mafic bodies to be present throughout the upper part of the Persimmon Fork

Formation as well, if the contact between the two formations is depositional. Since the effects of  $D_1$  penetrative deformation are expressed equally in both formations, faulting would have to have preceded regional metamorphism.

The various characteristics of rocks of the Modoc zone, including interpretations of its origin were discussed previously. Mapping for this study revealed that within the Modoc zone higher-grade gneisses are in close proximity to lower-grade rocks of the Carolina slate belt, suggesting a fault contact. However, investigators working in an adjacent area to the northeast (Secor and others, 1986a) have been able to map stratigraphic units and  $D_1$  structures across the Modoc zone, thus ruling out the possibility of a major fault between the Carolina slate belt and the Kiokee belt. The above evidence does not, however, rule out the possibility of at least some displacement at points within the Modoc zone. Secor (1987) interprets components of normal and dextral strike slip resulting in a net slip on the order of tens of kilometers over the Modoc zone's complex history.

Cross-cutting all tectonic features within the study area are several northwest-striking, strike-slip faults and rare northeast-striking normal faults. The strike-slip faults strike from N25-45°W and dip vertically or approximately 80°SW. Strike-slip displacement varies from a few centimeters in outcrop-scale faults (Fig. 22) to up to 600 meters (2000 feet) in map-scale faults (Plate 1). The magnitude of dip-slip displacement is unknown. Both right-lateral and left-lateral faults are present.

The northwest-striking faults are easily mappable where they cut contrasting lithologies such as metagranodiorite and the surrounding Richtex Formation; otherwise they can be difficult to delineate in the field. Aeromagnetic maps from the Georgia Geologic Survey files (aeromagnetic maps [unpublished], 1975) were helpful in delineating some of these faults where they offset rock units with persistent aeromagnetic signatures. The occurrence of these faults throughout the Slate belt (Paris, 1976; Reusing, 1979; Von Der Heyde, 1990; Allard and Whitney, in prep.) suggests that they may be present throughout the Piedmont, but as yet largely unrecognized. Most likely, these faults are Triassic to Jurassic in age and are a result of extensional stress during the breakup of Pangea and the opening of the proto-Atlantic Ocean.

A second set of post-metamorphic faults were observed in a few outcrops. These are normal faults that strike approximately parallel to regional foliation, but dip more steeply than the foliation to the northwest. Dip-slip displacement on these faults, where observed, is less than 2 meters. Strike-slip displacement, if present, is unknown.

### **Tectonic Environment**

Previous studies on the tectonic environment in which rocks of the Carolina slate belt were deposited have focused on the chemistry of the metavolcanic rocks, the

Table 7

## Comparison of Structural Fabric Elements

	<u>Secor and others (1986a)</u>	<u>This study</u>
D <sub>1</sub>	Isoclinal folding (F <sub>1</sub> ) on a regional scale; Development of regional slaty cleavage (S <sub>1</sub> ); Postdates deposition of Cambrian strata and predates intrusion of 385 to 415 Ma plutons in Charlotte belt.	Isoclinal folding (F <sub>1</sub> ); Responsible for regional outcrop patterns; Development of regional slaty cleavage (S <sub>1</sub> ).
D <sub>2</sub>	Isoclinal folding (F <sub>2</sub> ); Development of S <sub>2</sub> foliation that overprints previous S-surfaces; Development of the Modoc zone as a steep metamorphic gradient between Kiokee and slate belts; Amphibolite grade metamorphism; Reportedly occurred about 295-315 Ma; Restricted to the Kiokee belt and Modoc zone.	Affected only rocks immediately adjacent to the Modoc zone; Development of incipient S <sub>2</sub> foliation; Partial transposition of S <sub>1</sub> in local folds (F <sub>2</sub> ).
D <sub>3</sub>	Formation of the Kiokee antiform; Rotation of previous S-surfaces.	Rotation of foliation to present orientation; Development of numerous small-scale folds (F <sub>3</sub> ); Folding of gold-bearing quartz veins; Development of subdued crenulations.
D <sub>4</sub>	Development of late ductile shear zone (Irmo shear zone).	Probably responsible for numerous small shear zones.

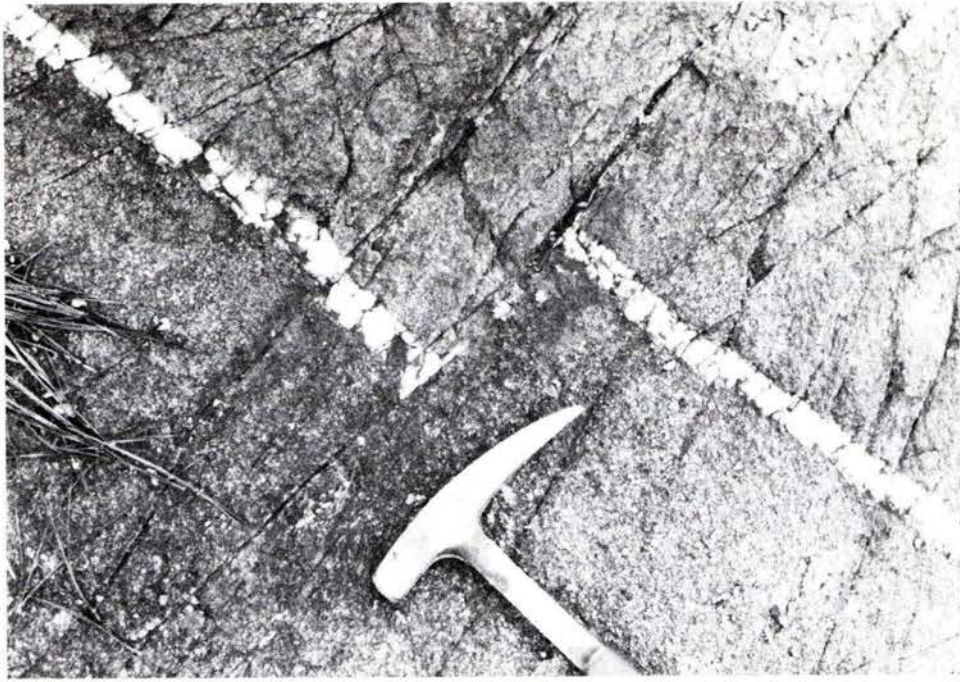


Fig. 22 - Quartz vein in largest metagranodiorite body offset by a northwest-striking fault. Exposure is along the shoreline of Clark Hill Reservoir.

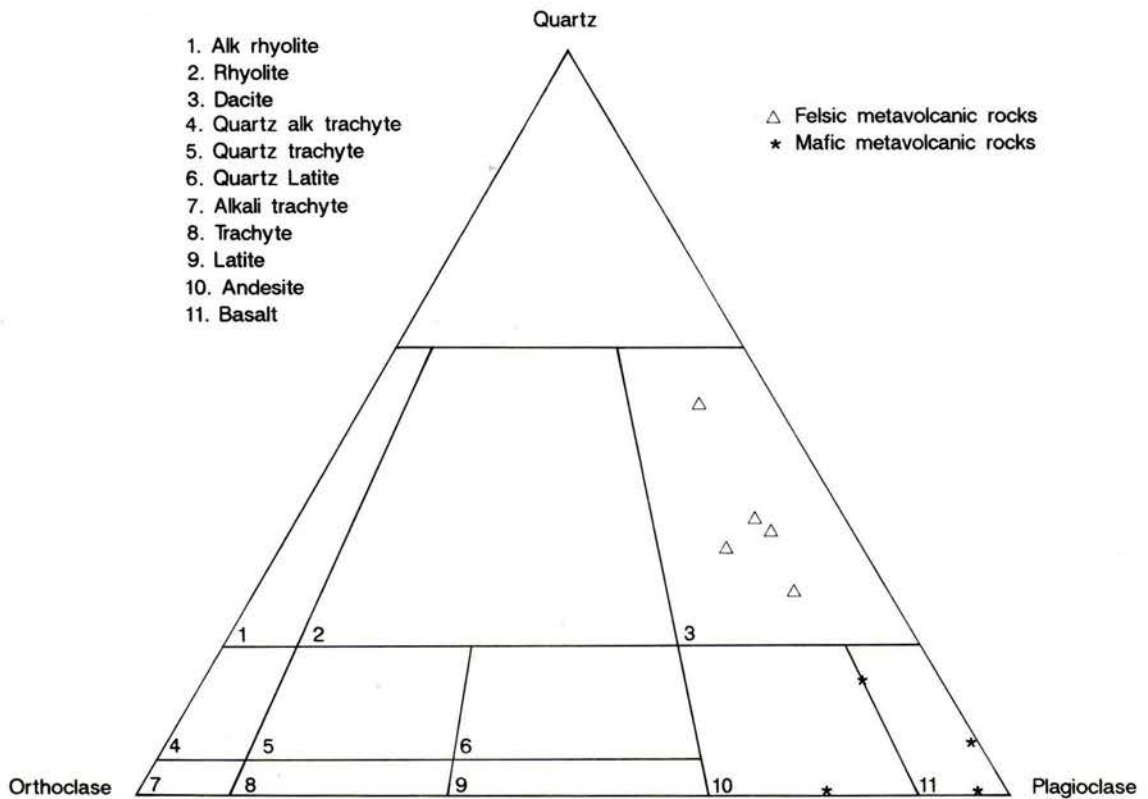


Fig. 23 - Chemical classification of felsic and mafic metavolcanic rocks from the study area (after Streckeisen, 1979).

relative proportions of mafic versus felsic metavolcanic rocks, and the occurrence and characteristics of the interlayered clastic metasediments. Whitney and others (1978) concluded that rocks of the Carolina slate belt in the Georgia-South Carolina area originated in a primitive island arc environment. This interpretation was based on major element chemistry of the metavolcanic rocks and the presence of marine sediments, even though mafic rocks are not the predominant volcanic rock type as would be expected for island arcs. They postulated that volcanic rocks currently exposed in the slate belt represent the younger felsic end members that are produced as the island arc develops and that the older, more primitive mafic components are not exposed. Rogers (1982) disagreed with Whitney and others' conclusion, contending that their cited evidence is not adequate to conclude that these rocks were deposited in an island arc environment or even on oceanic crust. Rogers (1982) proposed deposition in an environment that included both oceanic and continental characteristics, possibly on continental crust thin enough to accommodate the deposition of abundant marine sediments. Feiss (1982), after examining geochemical data from throughout the Carolina slate belt, concluded that the data was ambiguous with respect to environment of deposition and could conclude with confidence only that the Carolina slate belt rocks were deposited over a subduction zone.

This study has corroborated some of the conclusions of the previous investigators, concerning the stratigraphic and lithologic make up of the slate belt; however, conclusions from this study regarding environment of deposition cannot be considered definitive considering the limited stratigraphic interval of the slate belt covered by this study. Some preliminary conclusions based on major and trace element chemistry and lithologic associations, however, are inferred below.

Major element and selected trace element analyses were obtained from four mafic phyllites and five felsic metavolcanic rocks (tuffs and flows) from the study area (Table 8). The mafic phyllites are predominantly basaltic, and the felsic metavolcanic rocks are dacitic (Fig. 23). The chemistry of most of the mafic phyllites plotted utilizing both major and trace elements suggests affinities to oceanic basalts deposited at an oceanic ridge or in a back-arc basin; however, the chemistry of one sample suggests an active continental margin environment (Fig. 24). Other trace element plots (Fig. 25) are ambiguous concerning environment of deposition. The general lack of significant mafic volcanic rocks throughout the entire Carolina slate belt is not indicative of deposition in an island arc environment as defined from previous studies. The chemistry of the mafic and felsic metavolcanic rocks and the presence of interlayered marine sediments suggests that deposition most likely occurred peripheral to an active arcs system in an area overlying crust transitional between an oceanic and a

continental environment.

## GOLD DEPOSITS

### Introduction

The significance of the gold deposits of the McDuffie County gold belt has been overshadowed historically by the more commonly known deposits of the Dahlonega gold belt. It is claimed (Fluker, 1902) that the first discovery of gold in Georgia was made by Cornish miners in 1823 on the present site of the Columbia Mine and that one of the first stamp mills to operate in the United States was subsequently located nearby on the Little River.

Most of the mining activity within the McDuffie County gold belt has been confined to the vicinity of an area referred to as the Forty-acre Lot (Fluker, 1902; Yeates, 1902; Jones, 1909). This lot encompassed most of the properties of the Columbia and Hamilton Mines. The names, locations, types of workings present and recorded production of all mines and prospects in the McDuffie County gold belt are given in Appendix B.

### Mining History and Production

Gold was mined in the McDuffie County belt intermittently from as early as 1823 to about 1922. In contrast to the evolution of mining methods from placer mining to hydraulic mining to underground lode mining that occurred in the Dahlonega, Carroll County and Hall County belts (Yeates and others, 1896; Jones, 1909; Pardee and Park, 1948; Allen, 1986; German, 1985; 1988; 1989), mining in the McDuffie County belt seems to have consisted of lode mining from the beginning. This probably is a reflection of the differing geometry of the ore bodies in that those in the Dahlonega, Carroll County and Hall County belts are very irregular and small, while those in the McDuffie County belt are more uniform and larger and tended to be more easily found as outcrops.

As in most gold mining districts within Georgia, production records are practically non-existent. Production was recorded at the Parks and Columbia mines for the years 1891-1896, 1899-1901 and 1908-1909 while these mines were operated by W.H. Fluker (Yeates, 1902; Jones, 1909; Fluker, 1910). Total recorded production for the Parks and Columbia mines for those time periods was 4,628 oz.

### Gold Ore

#### *Vein Mineralogy and Geometry*

Ore bodies within the McDuffie County gold belt are distinct cross-cutting veins emplaced late in the deformational history of the host rocks. The veins are generally tabular bodies that continue with regular strike

Table 8  
Major Oxide, Trace Element and Normative Analysis  
of Felsic and Mafic Metavolcanic Rocks\*

	AO-176C <sup>1</sup>	AO-177 <sup>1</sup>	AO-178 <sup>1</sup>	AO-197 <sup>1</sup>	WB-71A <sup>1</sup>	AO-176B <sup>2</sup>	AO-193A <sup>2</sup>	C-159 <sup>2</sup>	WL-205 <sup>2</sup>
SiO <sub>2</sub>	70.7	79	61.6	68.1	72	48.6	33.7	47.7	50.7
TiO <sub>2</sub>	0.43	0.24	0.6	0.37	0.26	0.84	1.31	0.72	0.9
Al <sub>2</sub> O <sub>3</sub>	14.1	9.49	15.3	14.5	13.7	15.8	23	16.8	14.8
Fe <sub>2</sub> O <sub>3</sub>	1.86	1.1	3.43	2.24	1.02	3.75	4.37	2.63	1.31
FeO	1.35	0.9	2.7	0.75	1.1	6.25	11.36	6.72	8.9
MnO	0.11	0.06	0.15	0.06	0.09	0.2	0.29	0.18	0.18
MgO	0.89	0.36	1.97	0.57	0.42	6.97	8.43	7.79	3.98
CaO	2.45	1.18	4.91	2.93	1.68	7.75	5.34	11.3	7.42
Na <sub>2</sub> O	4.6	3.71	3.55	5.33	4.8	1.19	0.62	2.07	3.61
K <sub>2</sub> O	1.42	1.46	1.32	1.66	2.49	0.9	1.38	0.34	0.05
P <sub>2</sub> O <sub>5</sub>	0.11	0.05	0.31	0.18	0.19	0.41	0.35	0.12	0.22
S <sub>tot</sub>	0.03	0.02	0.02	0.02	0.02	0.05	0.05	0.03	0.04
CO <sub>2</sub>	0.03	0.02	0.42	0.01	0.02	1.41	0.03	0.07	4.03
LOI	1.37	0.79	2.35	1.09	0.52	5.64	7.73	2.98	6.35
Total	99.45	98.38	98.63	97.81	98.31	99.76	97.96	99.45	102.49
<u>Trace elements</u>									
Cu	15	9	37	14	11	51	8	55	64
Pb	15	2	31	15	2	10	22	6	2
Zn	56	26	85	31	33	87	202	70	76
Mo	<1	<1	<1	<1	<1	<1	<1	<1	<1
Ni	5	7	11	2	1	61	108	79	12
Co	4	4	18	5	1	34	54	43	36
Cd	3	<1	<1	2	<1	<1	<1	<1	<1
Bi	<5	<5	11	<5	<5	19	13	14	6
As	28	35	<5	<5	23	<5	<5	<5	36
Sb	<5	<5	<5	9	<5	<5	8	<5	23
Te	<10	<10	<10	<10	<10	<10	<10	12	15
Ba	513	484	421	520	452	878	300	48	10
Cr	180	504	175	200	166	175	256	254	63
V	38	18	116	42	11	78	316	256	310
Sn	<20	<20	<20	<20	<20	<20	<20	<20	<20
W	<10	<10	<10	<10	<10	<10	<10	<10	<10
Li	4	4	8	5	8	4	58	11	21
Be	2.1	1.4	1.8	2.3	2.5	2.8	2.2	1.6	1.4
Ga	12	4	8	4	10	<2	8	<2	8
La	13	8	8	7	13	5	16	3	4
Ce	<5	<5	<5	<5	<5	<5	<5	<5	<5
Ta	24	65	166	<1	<1	49	156	19	69
Sc	4	20	26	27	22	39	<1	53	6
Nb	6	4	8	6	7	6	12	5	3
Sr	213	102	300	197	128	322	292	312	238
Y	22	10	18	6	16	13	25	14	5
Zr	26	40	18	38	29	5	36	27	5
<u>CIPW Norms</u>									
Ap	0.24	0.11	0.67	0.40	0.42	1.02		0.28	0.54
Il	0.82	0.46	1.12	0.70	0.50	1.80	2.32	1.46	1.92
Mt	2.71	1.61	4.89	1.54	1.49	6.14	5.91	4.06	2.13
Or	8.41	8.66	7.65	9.79	14.77	5.99	7.59	2.14	0.33
Ab	39.00	31.52	29.48	45.03	40.78	11.34	4.88	18.62	34.18
An	11.46	4.95	9.94	10.72	7.12	39.54	24.67	37.79	26.89
Di		0.52		2.34		0.64		18.09	10.59
Hy	1.63	0.63	3.69	0.31	1.04	15.84	6.59	10.25	10.65
Ol							17.75	3.68	
C	1.61		8.49		1.02		20.09		
Q	32.14	49.09	27.45	24.68	30.60	10.35			4.84
Hm				1.18					
Total	98.02	97.55	93.38	96.69	97.75	92.66	89.80	96.37	92.07

<sup>1</sup>Felsic metavolcanic rocks; <sup>2</sup>Mafic metavolcanic rocks

Ap-apatite, Il-ilmenite, Mt-magnetite, Or-orthoclase, Ab-albite, An-anorthite  
Di-diopside, Hy-hypersthene, Ol-olivine, C-corundum, Q-quartz, Hm-hematite

\*Analysis parameters are given in Appendix A. Refer to Plate 3 for sample locations.

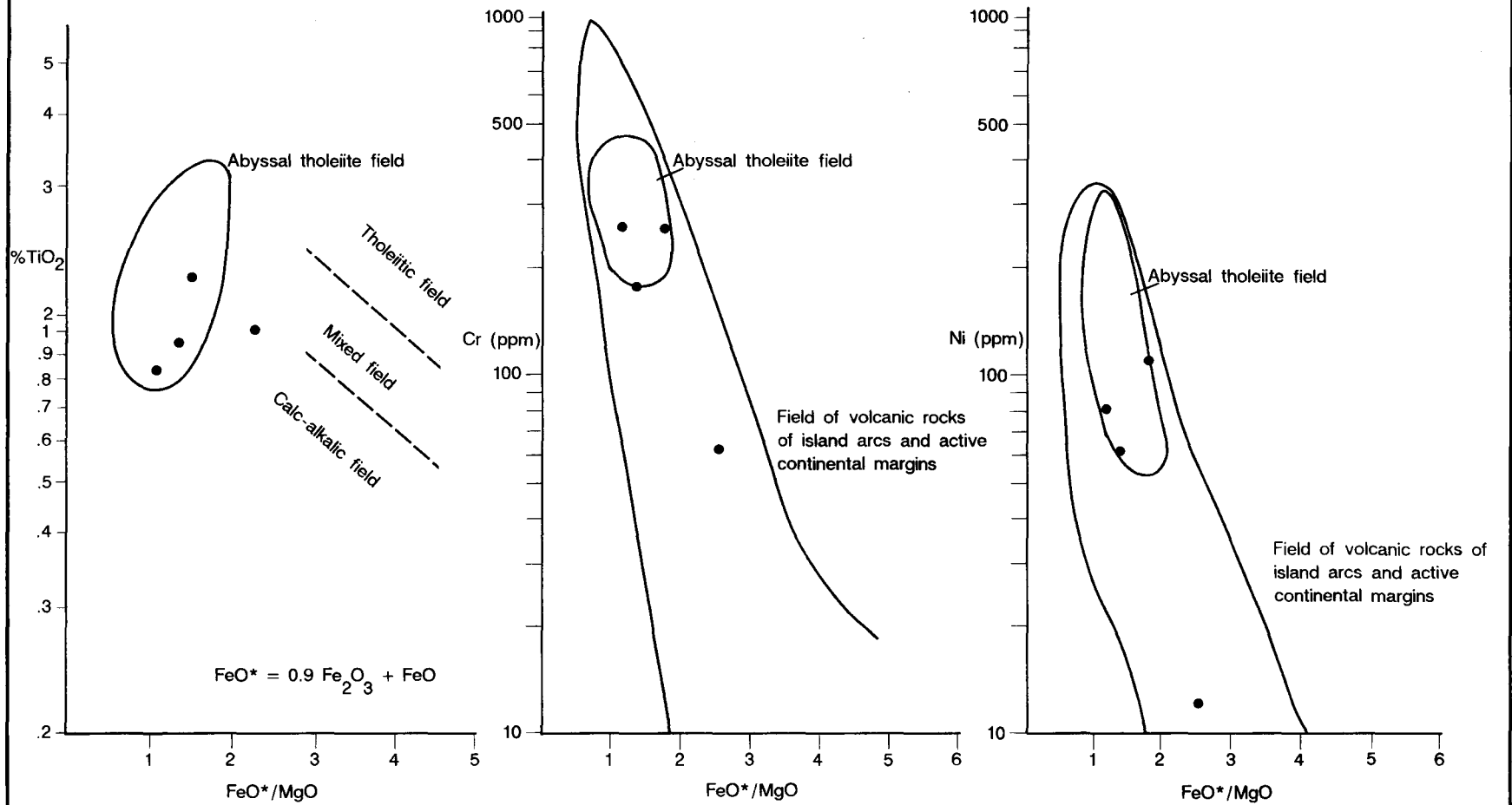


Fig. 24 - Discrimination of mafic phyllites using major trace element chemistry (after Miyashiro and Shido, 1975).

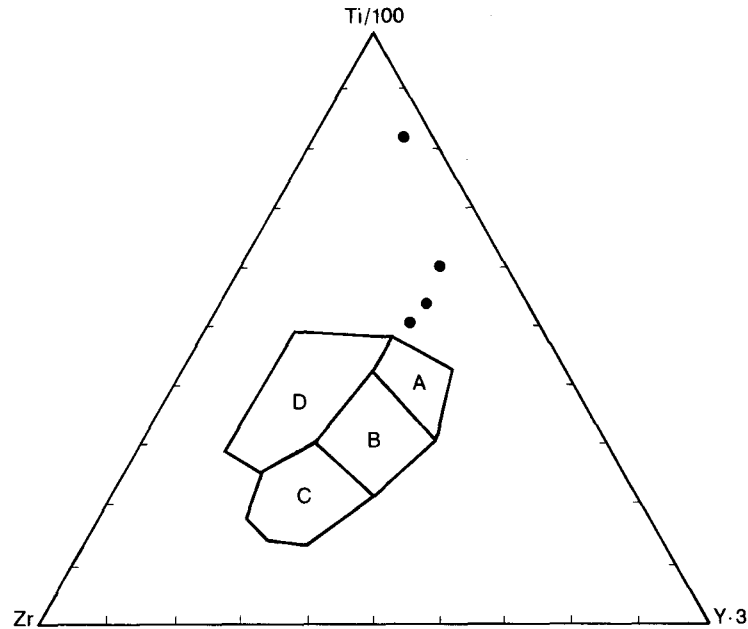


Fig. 25 - Plot of trace element chemistry of mafic phyllites on a standard discrimination diagram (Pearce and Cann, 1973). Note atypical trace element signatures. D - Ocean islands or continental basalts, B - Ocean floor basalts (abyssal tholeiites), A and B - Low-potassium tholeiites, C and B - Calc-alkalic basalts.

Table 9  
Ore Sample Assays<sup>1</sup>

	TAT-1	TAT-1A	COL-1	TMO	PM-N1	PM-N2	PM-E	C-137	P-2	GM-1	C-136	B-1	ED-A	LAN-E
Au	*54	*560	*121	*298	0.49 <sup>2</sup>	2.04 <sup>2</sup>	*841	*22	*13	*361	*<5	*69	*9	6.46 <sup>2</sup>
Ag	0.6	1.1	0.4	1.2	11.4	27.1	0.7	1.6	0.2	<0.2	0.3	1.7	<0.2	14.9
Cu	32	101	56	34	563	589	47	65	4	4	10	1290	4	190
Pb	265	487	6	611	3408	13400	27	4	6	4	4	2	4	1759
Zn	105	83	32	462	28	42	19	6	14	5	16	2	3	1241
Mo	<1	1	<1	<1	<1	5	7	4	1	2	1	<1	<1	4
Ni	10	20	18	10	14	10	78	10	6	7	14	5	5	17
Co	3	8	17	7	14	10	18	428	2	3	12	1	1	9
Cr	187	287	309	140	322	277	379	201	389	370	170	371	544	170
Mn	1500	2800	300	1400	<100	<100	<100	<100	400	100	1300	<100	<100	<100
W	<10	10	<10	<10	<10	<10	<10	12	<10	<10	<10	<10	<10	<10
Bi	<5	<5	<5	<5	8	7	<5	19	<5	<5	<5	<5	<5	11
As	14	<5	8	17	11	14	18	<5	<5	<5	<5	<5	<5	387
Sb	<5	<5	<5	<5	<5	<5	<5	<5	<5	<5	<5	<5	<5	8
Hg	<0.010	<0.010	<0.010	0.051	0.038	0.052	0.081	0.060	0.059	<0.010	0.061	<0.010	0.040	0.427
Ba	590	60	30	470	<20	<20	<20	<20	100	<20	170	<20	<20	<20
Fe	35700	83500	19200	43500	20300	12900	22600	>100000	16800	7500	26400	8600	6000	42700
Te	<0.2	<0.2	<0.2	<0.2	5.2	20.0	<0.2	8.9	<0.2	<0.2	na	<0.2	na	1.0
Tl	0.6	<0.1	<0.1	0.5	<0.1	<0.1	<0.1	<0.1	<0.1	<0.1	na	<0.1	na	<0.1

<sup>1</sup>Assays are in ppm unless otherwise noted. All samples are from mine dumps.

<sup>2</sup>Ounces per ton

\*ppb

na - no analysis

TAT-1, TAT-1A, TMO - Tatham Mine; COL-1 - Columbia Mine; PM-N1, PM-N2, - Parks Mine (north workings); PM-E - Parks Mine (east workings); C-137 - Unnamed prospect; P-2 - Porter Mine; GM-1 - Green Mine; C-136 - Unnamed prospect; B-1 - Bussey Mine; ED-A - Edmunds Mine; LAN-E - Landers Mine

Analysis parameters are given in Appendix A.

Refer to Plate 3 for sample locations.

and dip over considerable distances. The thickness of the veins, however, varies from as much as 6 meters (20 feet) to as little as one or two centimeters. The veins consist primarily of massive quartz with subordinate amounts of ankerite, galena, pyrite, chalcopyrite, sphalerite, calcite, gold, silver, sericite, azurite, barite, cerussite, covellite, chalcocite, malacite, pyromorphite, pyrrhotite and scheelite (Hurst and others, 1966; Cook, 1978; this study). Quartz, ankerite, galena, pyrite, chalcopyrite and sphalerite are primary gangue minerals, whereas the remainder of those listed above are either supergene in origin or occur sporadically in trace amounts. Quartz and ankerite are the most common gangue mineral, but the relative abundances of the remaining gangue minerals varies among the mines in the belt and between clusters of workings at individual mines. For example, sphalerite and galena are the most common gangue minerals at the northern cluster of workings of the Parks Mine (Plate 2), whereas pyrite is the most abundant gangue mineral at the eastern cluster of workings. The relative differences in vein mineralogy may be due to the mining of different vein sets at the above two locations. Locally, at the Parks and Landers Mines, galena and sphalerite approach ore grade concentrations (Table 9).

The bulk of each vein is made up of milky white to bluish gray quartz, generally highly fractured and massive. Locally, the veins exhibit a banded or ribbon texture indicating cracking and sealing during vein formation, and it is along these bands that the best specimens of free gold were found (Fluker, 1902). Other veins are basically breccias consisting of angular fragments of host rock cemented by quartz and ankerite (Fig. 26) in which a thin zone of ankerite separates the quartz and other vein minerals from the host rock (Fig. 27). In thin section, individual quartz grains exhibit undulose extinction, and the boundaries between some grains are mutually penetrative, while the boundaries between other grains are granulated and sheared. The traces of previously healed fractures are defined by numerous fluid inclusions. Some quartz grains have euhedral terminations exhibiting successive overgrowths indicating several episodes of growth and etching (Fig. 28). The boundaries between successive overgrowths are marked by sericitization and abundant fluid inclusions.

The gold (Fig. 29) and sulfides of the veins occur within granulated areas between larger quartz grains and along clean fractures. Much of the gold occurs apart from the sulfides and is readily visible to the unaided eye on fresh breaks and sawn surfaces. Much of the pyrite also is auriferous (Fluker, 1902). Gold ore from mines within the belt consistently assayed around one ounce per ton (Fluker, 1902; Yeates, 1902; Jones, 1909). Dump samples collected for this study contained gold in amounts up to 6 ounces per ton (Table 9). Samples assaying up to 20 ppm tellurium suggest the presence of some gold as tellurides although no tellurides were identified. To the miners, the presence of abundant galena and pyromorphite was an indication of very rich ore (Fluker, 1902).

Pyrite is the most abundant sulfide gangue mineral followed by galena and sphalerite in approximately equal proportions, and then by chalcopyrite. Pyrite occurs interstitial to quartz and other minerals within the veins and is disseminated unevenly in the adjacent host rock replacing the host rock and filling fractures (Fig. 30). Pyrite appears to have formed throughout the process of vein formation (Fig. 31). Early euhedra of pyrite are surrounded by other gangue minerals and locally late pyrite has overgrown early aggregates of pyrite and sphalerite (Fig. 32). Many of the pyrite euhedra are zoned (Fig. 32).

Galena and sphalerite were the latest of the primary gangue minerals to form (Fig. 33). These two minerals occur interstitial to pyrite and chalcopyrite and are common in late fractures and cross-cutting veins, and often accompany gold. Sphalerite locally contains aligned inclusions of chalcopyrite (Fig. 34).

Chalcopyrite formed closely in time to the early pyrite. Individual crystals are euhedral to subhedral and are locally embayed by late-forming galena and sphalerite (Fig. 35). Of the most common primary sulfides, chalcopyrite is the most commonly altered. It is commonly rimmed by covellite and is rarely accompanied by bornite (Fig. 36). Locally, chalcopyrite contains minute inclusions of chalcocite.

### *Vein Orientation*

At least four sets of auriferous veins were recognized in the McDuffie belt when the mines were active (Yeates, 1902; Fluker, 1902). Veins striking east-west, northwest, northeast and north-south were worked at various times. All underground workings are now inaccessible; therefore, recorded observations made when the mines were active were relied upon for the strike of the vein sets (Yeates, 1902; Fluker, 1902; Fluker, 1907; Jones, 1909). In addition, the alignments of abandoned surface workings also were useful in delineating the various vein sets (Plate 2). Vein sets strike approximately E-W ( $\pm 10^\circ$ ), N40-70°W, N-S ( $\pm 10^\circ$ ) and N45-60°E. Dips of the veins are variable, but the northeast-striking set reportedly dips 45-60° northwest, the northwest-striking set reportedly dips 45-50° northeast (Yeates, 1902; Fluker, 1902), and the north-striking set reportedly are vertical or dip to the east (Fluker, 1907; Jones, 1909). The dip of the nearly E-W set is unknown. The most productive veins, at least at the Parks Mine, were the E-W and N-S sets (Fluker, 1907). The variety of vein orientations probably indicates a changing stress field during vein formation.

### *Alteration*

Host rock alteration associated with the emplacement of the ore bodies consisted of carbonatization and

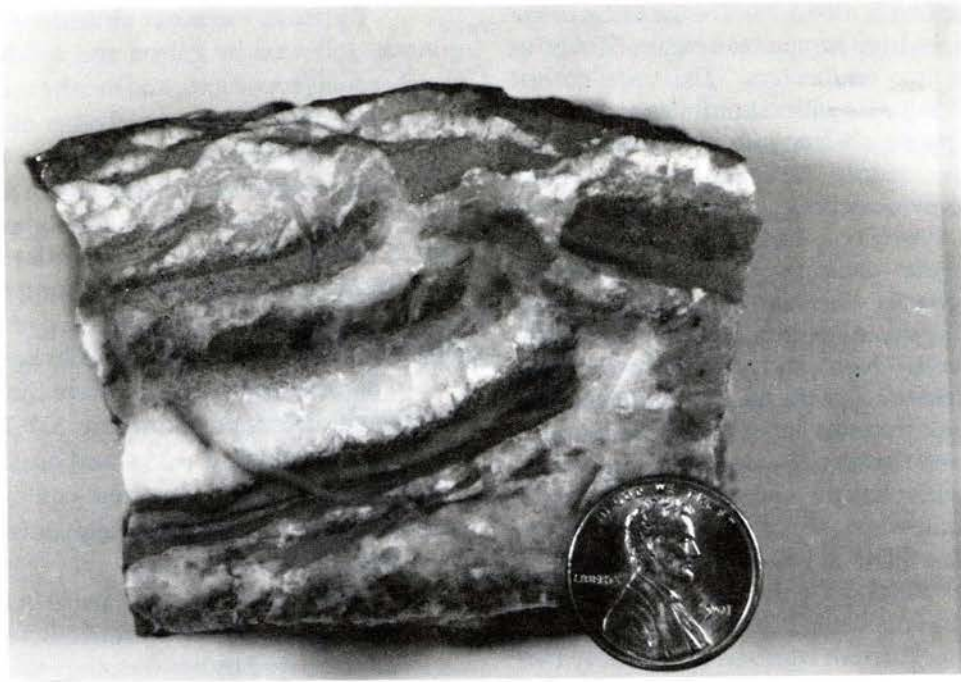


Fig. 26 - Sawed brecciated auriferous vein from the Phillips Mine. Angular fragments of host rock (phyllite) are in a matrix of ankerite (white) and quartz.

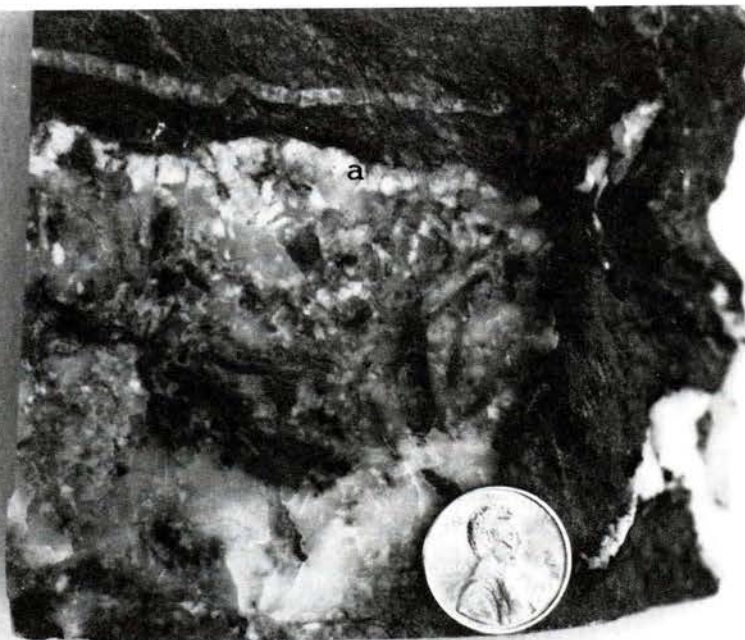


Fig. 27 - Sawed brecciated auriferous vein from the Tatham Mine showing ankerite (a) zoning along its borders. Sericitized host rock fragments, quartz, very fine-grained sulfides and ankerite make up the remainder of the vein.

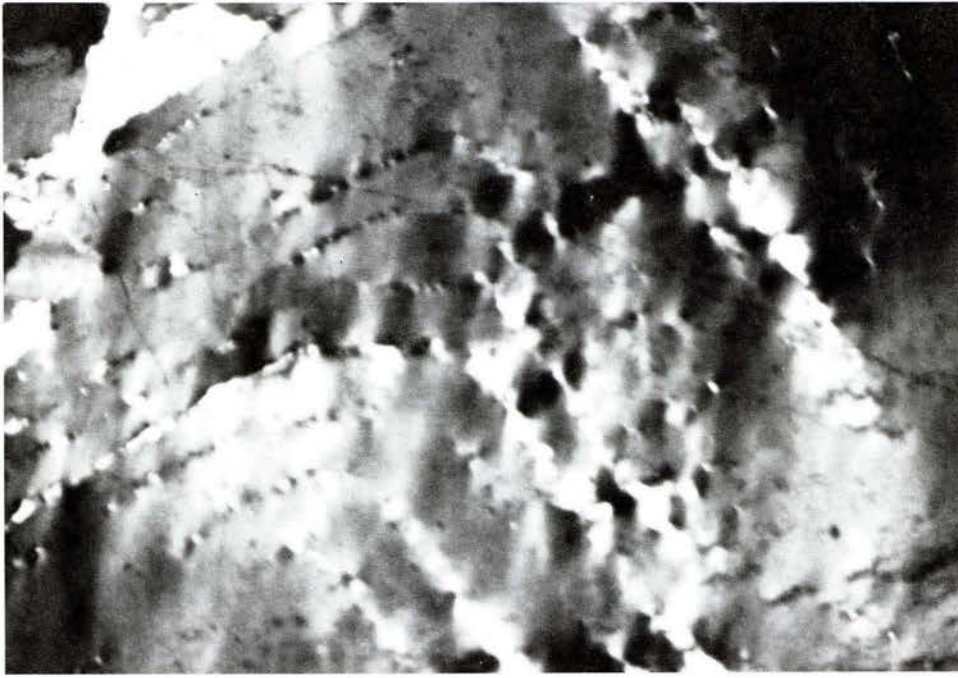


Fig. 28 - Vein quartz from the Landers Mine showing successive euhedral overgrowths. An etched surface separating successive overgrowths is defined by sericite and numerous fluid inclusions. Field of view is 3.16 mm.

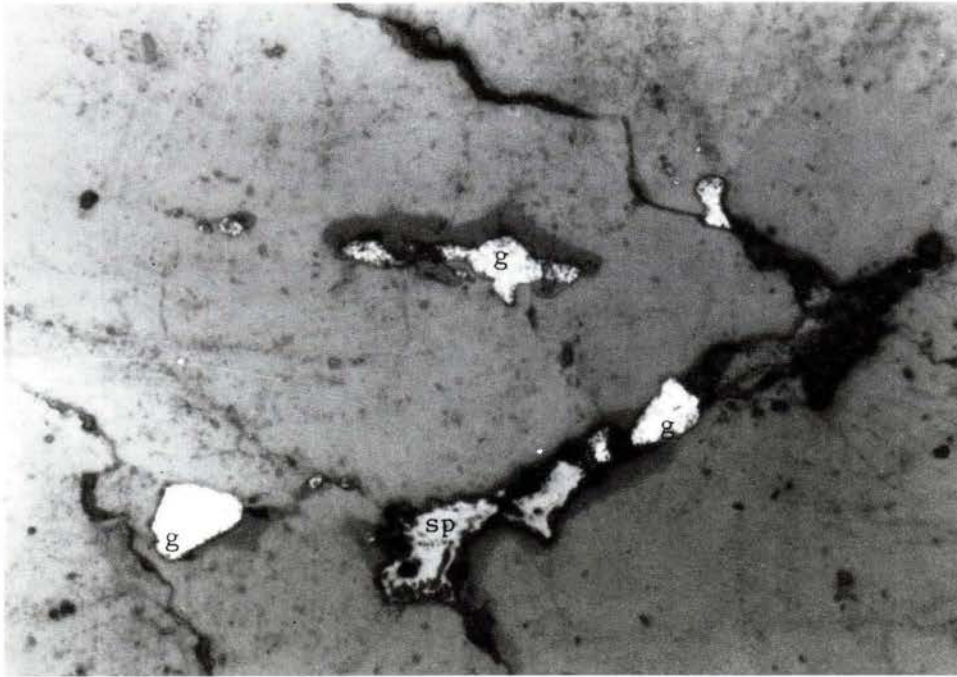


Fig. 29 - Polished thin section from the Landers Mine showing gold grains (g) and sphalerite (sp) in quartz . Field of view is 1.82 mm.



Fig. 30 - Sawed (phyllite?) host rock and ore from the Tatham Mine, McDuffie County showing euhedral pyrite crystals (py) disseminated throughout the host rock around veinlets (above) and localized along a healed fracture (below). Late veinlet (LV) cuts larger vein in lower part of lower photograph.

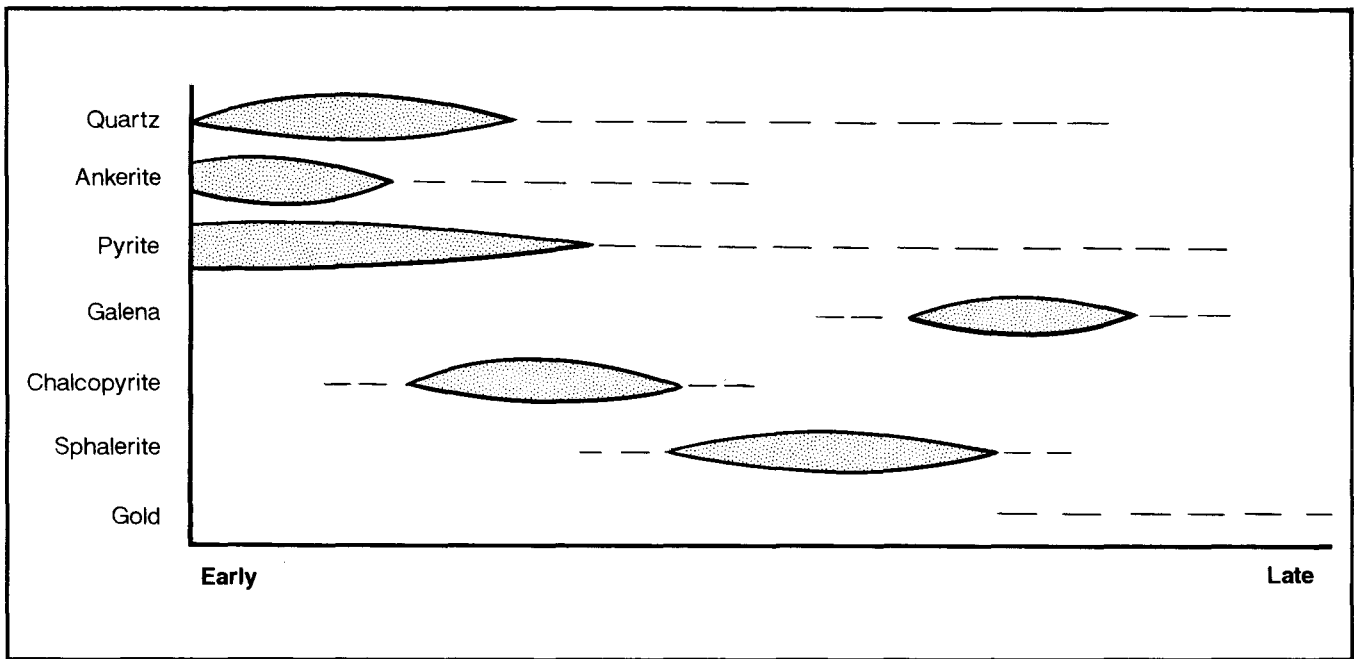


Fig. 31 - Vein mineral paragenesis of ore bodies in the McDuffie County gold belt.

pyritization. Carbonatization consisted of replacement of portions of the host rock by ankerite which also is a common vein mineral. Ankerite is evenly distributed within the host rock adjacent to the veins, and thin zones of ankerite separate the veins from the host rocks. Samples from mines throughout the study area showed varying degrees of carbonatization and pyritization.

Samples exhibiting alteration representative of the gold belt as a whole were collected from the dump at the Tatham Mine. In these samples of vein and host rocks, the most visible alteration is replacement of the phyllite and metagranodiorite host rocks by pyrite and ankerite. Sparry ankerite crystals line the borders of the veins, and the host rocks adjacent to the veins have been replaced by very fine-grained ankerite and disseminated, euhedral pyrite (Fig. 30). Pyrite also is localized along fractures in the host rock adjacent to the veins. Samples of the metagranodiorite host rock have been partially replaced by as much as 35 percent ankerite.

#### *Fluid Inclusions*

The types of alteration that the host rocks have undergone and the mineralogy of the ore bodies suggest the ore-forming fluids were rich in  $\text{CO}_2$  and reduced sulfur. To confirm this hypothesis, fluid inclusion studies were conducted on ore samples from the Columbia, Parks, Landers and Tatham Mines by two Georgia State University

students under the supervision of Dr. David A. Vanko (Newton and Pyle, 1991). The results of their study provided preliminary data on fluid inclusions and is summarized in the following paragraphs. All data were collected with a modified USGS-type gas flow heating and freezing stage manufactured by Fluid, Inc.

Primary and secondary (or pseudo-secondary) inclusions were observed. The primary inclusions vary in size (2-20 microns) and shape and generally contain 5-15 percent vapor phase. Some primary inclusions are elongated by roughly 5 to 10 times in one direction. Some equant primary inclusions occur in chevron patterns.

The secondary or pseudo-secondary inclusions are generally smaller and more equant than the primary inclusions and range in size from 0.5 to 15 microns. They are oriented in certain planes assumed to be fractures that have been annealed to various degrees (Newton and Pyle, 1991).

Approximately 40 fluid inclusions from samples of the Parks mine were observed during heating and freezing. Many inclusions contain three phases at room temperature: aqueous liquid, vapor (generally 5-15 percent), and a liquid carbonic phase (generally 30 volume percent). Melting temperatures for the carbonic phase ranged from  $-58.4^\circ\text{C}$  to  $-56.4^\circ\text{C}$  with the majority falling between  $-57.2^\circ\text{C}$  to  $-57.0^\circ\text{C}$  indicating that the carbonic phase is almost pure  $\text{CO}_2$  ( $\text{CO}_2$  melting temperature =  $-56.6^\circ\text{C}$ ). Ice melting was not observed, however, a slight expansion of the vapor phase of some inclusions occurred



Fig. 32 - Polished thin section from the Tatham Mine showing zoned pyrite (py) overgrowth on an aggregate of sphalerite (sp) and pyrite (py). Field of view is 4.40 mm.

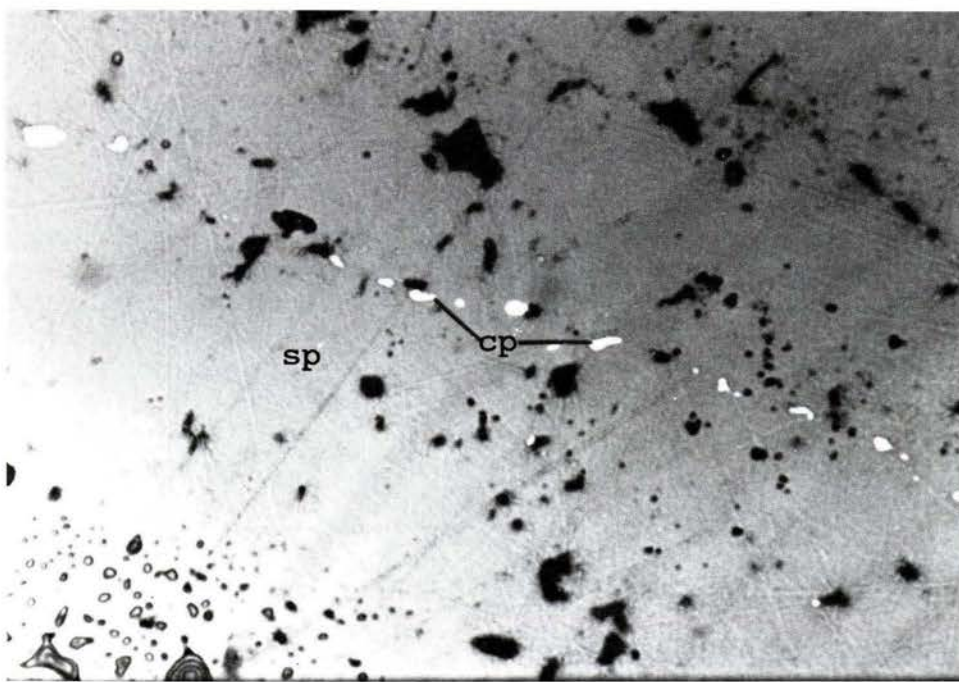


Fig. 34 - Polished thin section from the Landers Mine showing aligned inclusions of chalcopryite (cp) in sphalerite (sp). Field of view is 0.33 mm.

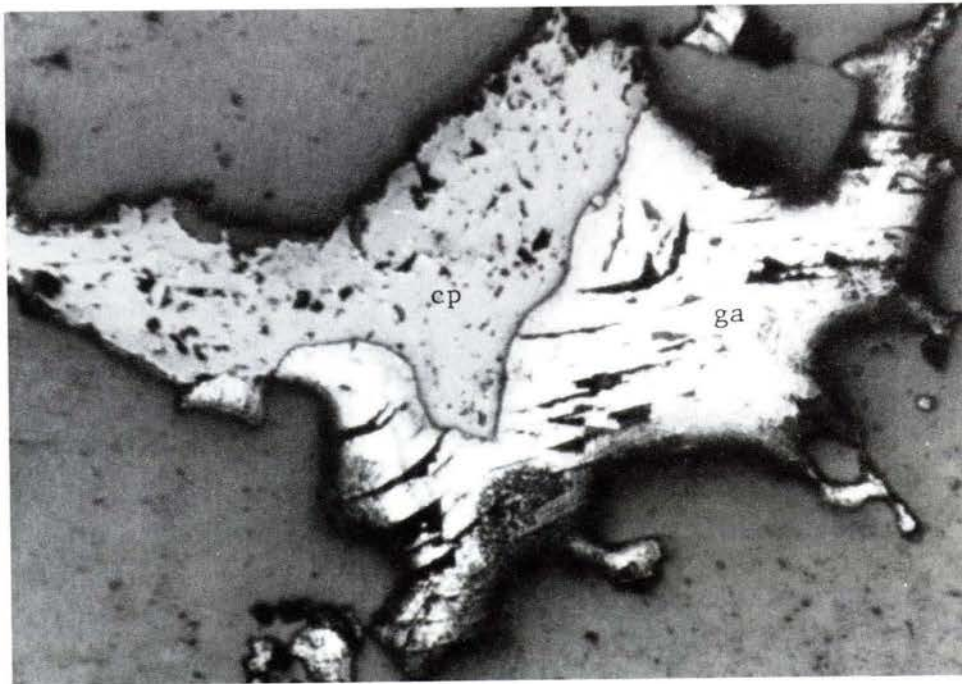
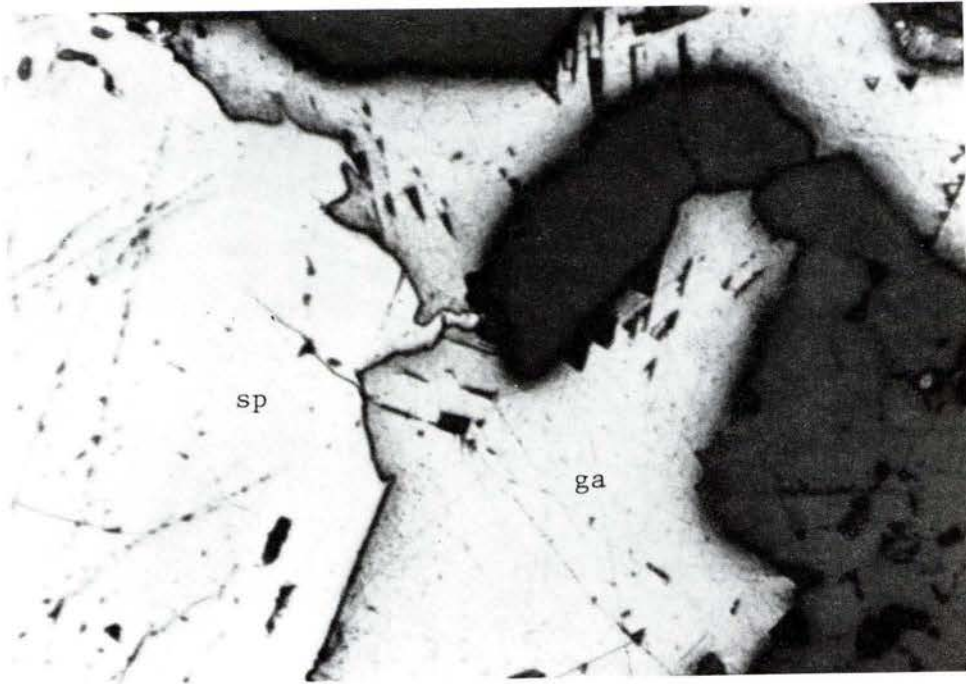


Fig. 33 - Polished thin section from the Landers Mine showing interpenetration boundaries between sphalerite (sp) and galena (ga) (above) and between galena (ga) and chalcopyrite (cp) (below). Field of view is 4.40 mm.

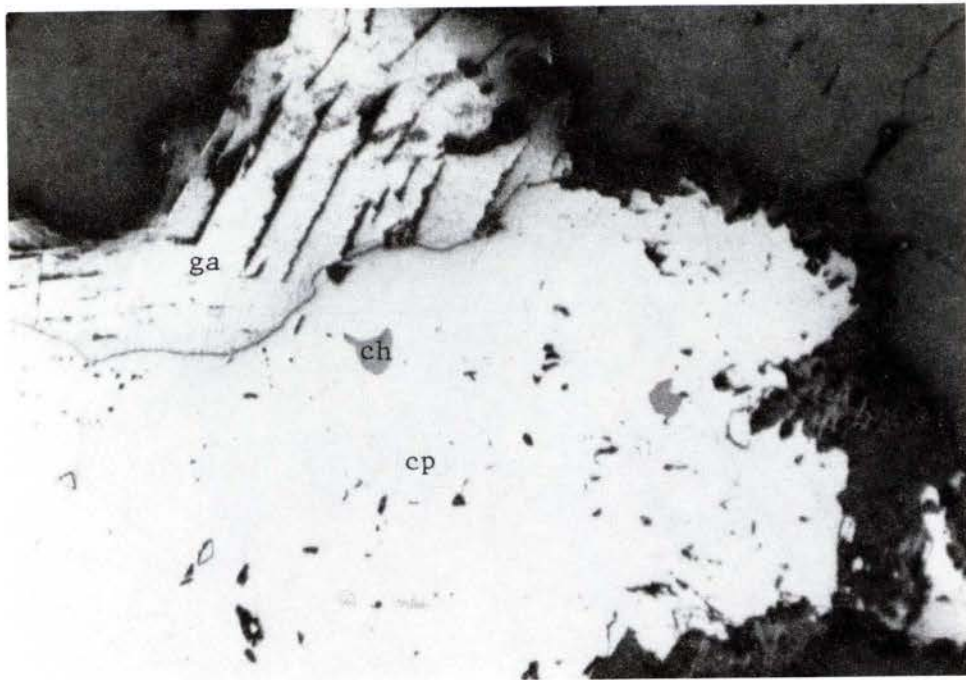


Fig. 35 - Polished thin section from the Landers Mine showing galena (ga) embaying chalcopyrite (cp). Note inclusions of chalcocite (ch) in chalcopyrite. Field of view is 4.40 mm.

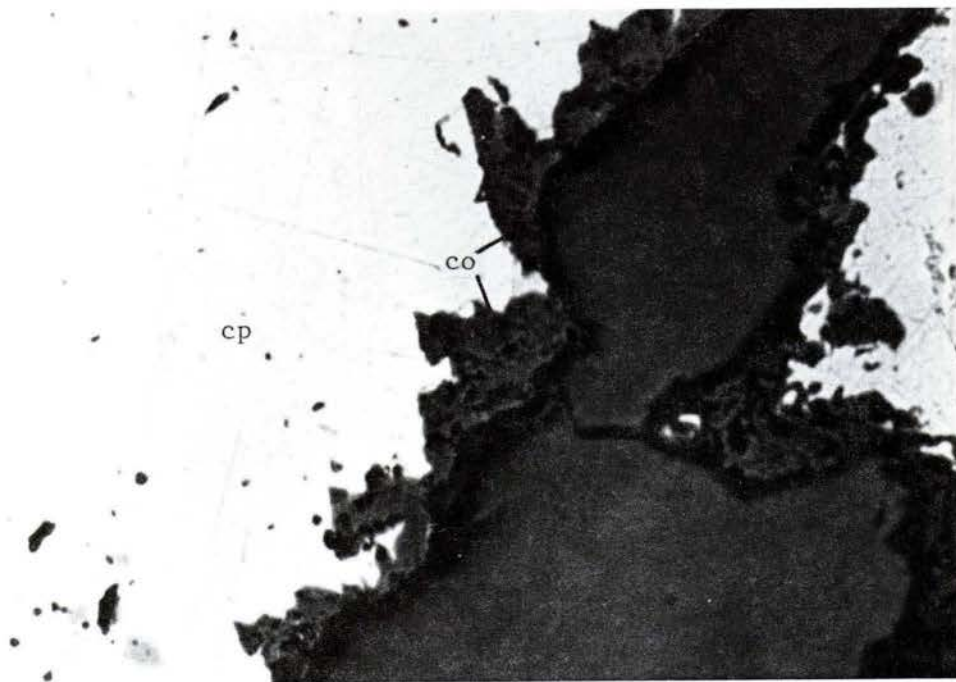


Fig. 36 - Polished thin section from the Landers Mine showing chalcopyrite (cp) altered to covellite (co) along grain boundaries with quartz. Field of view is 0.33 mm.

upon heating at around  $-1.1^{\circ}\text{C}$ . Assuming that this expansion indicates the melting temperature of ice in the inclusions, the salinity of the water is at least 2 to 4 weight percent NaCl.

One clathrate melting point of  $7.7^{\circ}\text{C}$  was obtained. The value of  $7.7^{\circ}\text{C}$  corresponds to 4.5 weight percent NaCl in the aqueous phase and is consistent with the inferred ice melting temperatures.

Recorded homogenization temperatures for  $\text{CO}_2$  ranged from  $18^{\circ}$  to  $30^{\circ}$  with two maxima at  $18^{\circ}$  to  $19^{\circ}$  and  $28^{\circ}$  to  $29^{\circ}$ . The range of total homogenization temperatures was from  $153^{\circ}$  to  $301^{\circ}$  with the majority falling between  $180^{\circ}$  and  $240^{\circ}$ . Using the preliminary data for the carbonic phase melting point of  $-57^{\circ}\text{C}$ , the clathrate melting point of  $7.7^{\circ}\text{C}$ , and the carbon dioxide homogenization temperature of  $28^{\circ}\text{C}$  and comprising 30 volume percent of the inclusions, a typical fluid can be postulated. Using the program FLINCOR, this fluid is calculated to have 10 molecular percent  $\text{CO}_2$  and a bulk density of 0.91 (assuming a  $\text{CO}_2\text{-H}_2\text{O-NaCl}$  fluid). The fluid pressure is 2.0 kb at  $200^{\circ}\text{C}$ , 3.2 kb at  $300^{\circ}\text{C}$ , and 4.3 kb at  $400^{\circ}\text{C}$ . If the temperature of ore formation can be constrained by an independent geothermometer, the ore fluid pressure may be estimated. Assuming ore formation took place under greenschist grade conditions (i.e., around  $250^{\circ}\text{C}$ ), the fluid pressure was 2.5 kb. Depending on whether fluids were under hydrostatic or lithostatic pressure, this implies a crustal depth of 25 km or 8.3 km, respectively. The values obtained by Newton and Pyle (1991) are consistent with trapping temperatures and pressures obtained from auriferous veins in the Slate Belt of North Carolina (Ford, 1981; Ford and Feiss, 1982), and also are consistent with greenschist facies metamorphic conditions.

### *Oxygen Isotopes*

Twenty-nine samples were analyzed at the Stable Isotope Laboratory of the University of Georgia under the supervision of Dr. David B. Wenner to determine their  $\delta^{18}\text{O}$  values. The samples included quartz vein ore bodies, barren quartz veins, silicified zones, host rocks immediately adjacent to the ore bodies and host rocks considerable distances from known ore bodies. Quartz separates were analyzed from the veins and silicified zones, whereas  $\delta^{18}\text{O}$  determinations of the country rocks were made from whole rock samples. The  $\delta^{18}\text{O}$  determinations were made on a Finnigan MAT model delta E isotope ratio mass spectrometer. Results are reported relative to SMOW with a precision on the order of  $\pm 0.1\text{-}0.15$  per mil. Although the number of  $\delta^{18}\text{O}$  analyses may not be statistically significant, some preliminary conclusions can be drawn.

Rocks within the study area occurring immediately adjacent to the ore bodies as well as those far removed from the ore bodies consistently have  $\delta^{18}\text{O}$  values ranging from 3.1 to 5.5 per mil with only one sample falling outside this range (Fig. 37) (Table 10). The above host rock samples

included several different rock types including metasediments, felsic to intermediate metavolcanic rocks, mafic phyllite, metagranodiorite and metaquartz monzonite. The  $\delta^{18}\text{O}$  values for these rocks are  $^{18}\text{O}$  depleted compared to their unmetamorphosed equivalents ( $\delta^{18}\text{O} >$  approximately 6.0) (Taylor, 1968). Similar  $^{18}\text{O}$  depletion has been reported for plutons, volcanic rocks and mineral deposits from various parts of the Carolina slate belt (Wesolowski and others, 1985; Feiss and Wesolowski, 1986; Klein and Criss, 1988) and has been attributed to interaction with meteoric waters during a premetamorphic hydrothermal event. Field evidence of a premetamorphic hydrothermal event is found in samples of the host rock at the Parks Mine (Fig. 38). In these samples an early episode of quartz veining that cross-cuts original textures is transposed into the  $S_1$  foliation. This field evidence, coupled with the isotopic data, strongly suggest that rocks within the study area also have experienced an early hydrothermal event that was strongly influenced by meteoric water, causing the  $^{18}\text{O}$  depletion.

All quartz vein ore bodies have  $\delta^{18}\text{O}$  values ranging from 6.7 to 8.7 per mil (Fig. 37). These values are consistent with published values for metamorphic fluids (Taylor, 1974). These values are distinctly higher than those of their host rocks. However, since the whole rock samples contain a large proportion of feldspar which is typically  $^{18}\text{O}$ -depleted at equilibrium and, therefore, depresses the whole rock  $\delta^{18}\text{O}$  value, the  $\delta^{18}\text{O}$  value of quartz separated from the whole rock sample of the host rock most likely would have an  $\delta^{18}\text{O}$  value closer to the quartz from the quartz veins.

A series of late silicified breccia zones (discussed previously) in the vicinity of Fountain Campground in Warren County show the highest  $\delta^{18}\text{O}$  values (Fig. 37). The fluids that caused the silicification of these zones also appear to be of metamorphic origin, but of a different source and possibly much younger.

### *Time of Emplacement*

The ore bodies within the study area have been mildly deformed. They have been folded only by the last fold event ( $F_3$ ) and apparently locally have been offset by the northwest-striking faults. This would put the emplacement of the ore bodies just prior to  $F_3$  folding in the late Paleozoic (Alleghanian).

### *Genesis of the Gold Deposits*

The gold deposits of the McDuffie County gold belt bear many similarities to other gold deposits from many locations worldwide and of various geologic ages. The temperature and pressure ranges determined by the study of fluid inclusions fall within the lower part of the ranges for temperature of formation and depth of emplacement for deposits classified as mesothermal gold deposits

Table 10  
 $\delta^{18}\text{O}$  Values for Rock Types Within the Study Area

<u>Sample #</u>	<u><math>\delta^{18}\text{O}</math> value (‰)</u>	<u>Sample description</u>
PM-N*	6.7	Parks Mine ore - north workings.
PM-E	8.3	Parks Mine ore - east workings.
LAN-1	7.9	Landers Mine ore
LAN-2	8.7	Landers Mine ore
COL-1	7.0	Columbia Mine ore
TAT-1A	8.3	Tatham Mine ore
TAT-1B	8.7	Tatham Mine ore
PM-EH	5.2	Parks Mine host rock - east workings.
PM-NH	3.6	Parks Mine host rock - north workings.
COL-M	3.3	Columbia Mine host rock.
BV-2	3.1	Bell Vein host rock.
PH-H	3.2	Phillips Mine host rock.
LM-H	5.4	Landers Mine host rock.
AO-5	7.5	Siliceous zone
AO-39	3.4	Barren quartz vein
C-81AA	11.2	Silicified zone near Fountain Campground.
C-131	11.5	Silicified zone near Fountain Campground.
AO-178	5.5	Country rock - felsic metavolcanic
AO-176A	5.0	Country rock - felsic metavolcanic
AO-176B	1.5	Country rock - Mafic phyllite
C-134	7.2	Country rock - Meta-argillite
AO-9	4.1	Country rock - Metagranodiorite
AO-25	3.3	Country rock - Metagranodiorite
L-63	4.5	Country rock - Metaquartz monzonite

\*Refer to Plate 3 for sample locations.

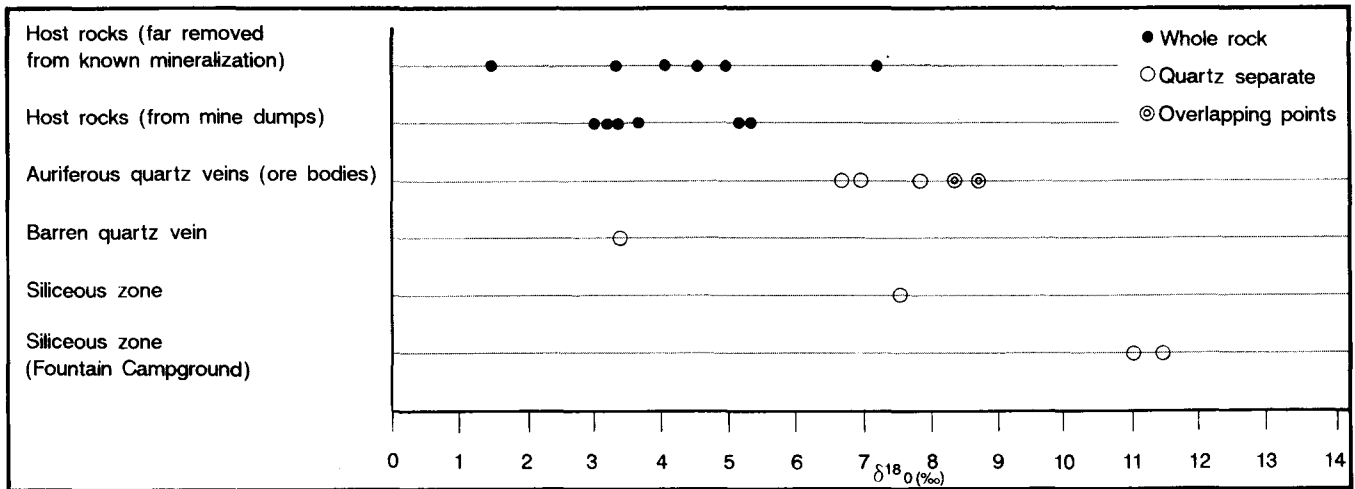


Fig. 37 - Oxygen isotope values for host rocks, veins and silicified zones within the study area.

(Park and MacDiarmid, 1975). Deposits that share many common characteristics with those of the McDuffie County belt include those of the Superior province of Canada (Colvine, 1989), the Mother Lode of California (Knopf, 1929; Berger, 1986), the Alaska-Juneau and Treadwell deposits in southeastern Alaska (Light and others, 1989), and the those of the Yilgarn Block of Western Australia (Groves and others, 1989). Although the above deposits share many common characteristics with the McDuffie County belt, notable differences seen in the McDuffie County belt deposits include generally lower oxygen isotope values for ore and host rocks and lack of a significant amount of mafic host rocks.

Three basic models have been proposed over the years to explain the origin of hydrothermal gold deposits. These include: the magmatic model, which proposes that hydrothermal gold deposits are derived from fluids emanating from acidic intrusions that are spatially or temporally related to the deposits; the metamorphic model which proposes that circulating metamorphic fluids remove gold from mafic volcanic rocks and/or interflow sediments and precipitate gold by reaction with high Fe-Mg host rocks; and the degassing model which proposes that gold is deposited by fluids emanating from the mantle and/or crust in the vicinity of major shear zones.

Preliminary fluid inclusion data strongly suggest that the CO<sub>2</sub>-rich, low salinity fluids that deposited the ore bodies were of metamorphic origin, most likely produced by breakdown of minerals during prograde dehydration and decarbonation. The oxygen isotopic data also supports a metamorphic source for the aqueous ore-forming fluids and argues against a meteoric water source. The localization of many of the deposits along the southeastern flank of

the largest metagranodiorite intrusion and the alignment of all the deposits approximately equidistant northwest of the Modoc zone (Plate 1) strongly suggest that the ore bodies were deposited at their particular positions by fluids migrating up the metamorphic gradient from the Modoc zone and Kiokee belt. As these fluids reached the vicinity of the amphibolite/greenschist facies transition, corresponding to the brittle/ductile deformation transition, the vein minerals were deposited. The drawing of approximate metamorphic mineral isograds (Plate 1) shows that most deposits are located within the lowest grade rocks (chlorite zone). This ore genesis model is consistent with the interpretation (Secor and others, 1986a; 1986b) that rocks of the Carolina slate belt (including the study area) compose a superstructure complex of low-grade rocks overlying an infrastructure complex of high-grade rocks of the Kiokee belt separated by the Modoc zone, a regional shear zone and steep metamorphic gradient.

Gold most likely was transported in the ore fluids as the relatively stable gold thiosulfide complex Au(HS)<sub>2</sub><sup>-</sup>. Vein mineral precipitation most likely was initiated as confining pressure approached equilibrium-saturation vapor pressure of the hydrothermal fluids causing phase separation (boiling) and by a decrease in temperature, and immediately followed sulfidization of the host rock by reaction with H<sub>2</sub>S. Boiling of the auriferous hydrothermal fluids is possible since many of the fluid inclusions are almost entirely composed of vapor (D. Vanko, personal communication, 1992).

Study of the Ohaaki-Broadlands geothermal system in New Zealand (Seward, 1989) has revealed that boiling of hydrothermal fluids plays an important role in the deposition of gold (from thiosulfide complexes) from

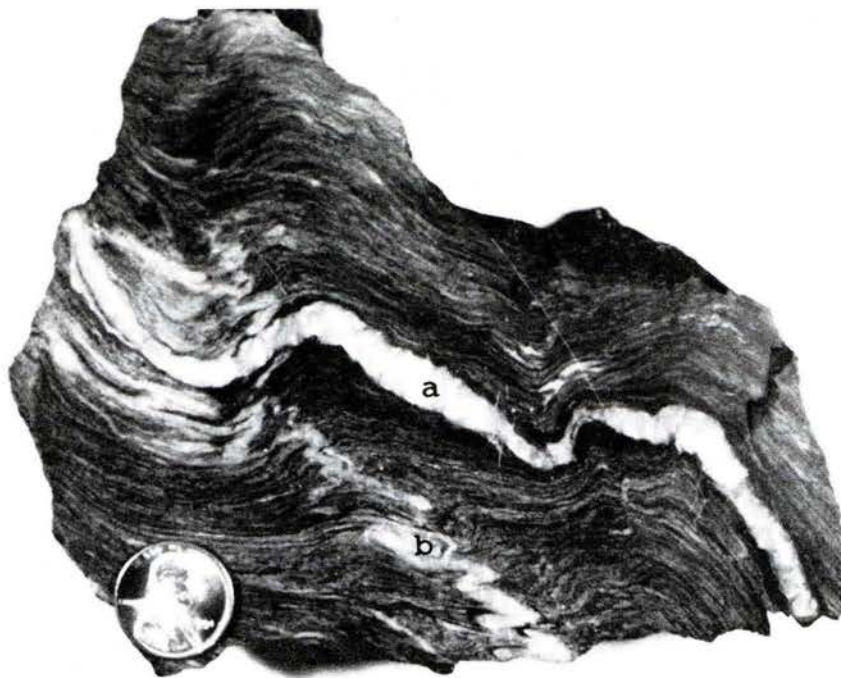


Fig. 38 - Sawed sample of phyllite host rock (Richtex Formation) from the Parks Mine. Late-kinematic quartz/ankerite veinlet (A) is deformed by late folding. Pre-kinematic veinlet (B) is transposed into  $S_1$ .

such fluids, and that if base metals are present in hydrothermal fluids in sufficient quantities, they would precipitate as sulfides followed by gold. The decrease in reduced sulfur ( $H_2S$ ) concentration as sulfides are deposited, combined with loss of  $CO_2$  by reaction with wallrock, lowers the solubility of gold causing its precipitation (Seward, 1989). This is supported by the occurrence of much of the gold in late fractures within the ore separate from the base metal sulfides and the abundance of the gangue minerals pyrite and ankerite.

The observation (Fluker, 1902) that some of the highest grade ore was normally galena-rich suggests that locally the ore-forming fluids were rich enough in lead so that if boiling was an important factor in mineral precipitation, galena precipitation accelerated the decline in sulfur concentration and caused gold to precipitate more closely in time to the galena. Slight variations in ore body mineralogy, gold content and mineral suites within the ore bodies throughout the gold belt suggest there were local variations in the physio-chemical conditions of the ore-forming fluids either within the same vein set or among the various sets.

Ponding of the hydrothermal fluid may have occurred adjacent to the largest metagranodiorite body as the relatively impermeable rock mass acted as a barrier to fluid migration and dispersion. This may account for the concentration of the most productive mines on the southeastern flank of the meta-intrusive body (Plate 1).

The source of the gold in hydrothermal gold deposits has been debated for years. Various types of rocks have been proposed as sources, ranging from mafic to ultramafic rocks, felsic to intermediate intrusions, volcanic

rocks, sediments and lamprophyre dikes and sills. All of these types of rocks are present in the study area, and many contain gold in trace amounts (Fig. 39, Appendix C). However, the gold values are small and no particular rock type is sufficiently enriched in gold or is volumetrically significant enough to be the sole source of gold for these deposits. The mineralizing fluids most likely extracted gold from a variety of source rocks, becoming increasingly enriched in gold and other constituents as they migrated from deep within the crust.

### Future Production Outlook

The discovery and subsequent mining of large low-grade gold deposits in recent years in South Carolina has spurred exploration efforts throughout the region. Most of the exploration effort, however, is directed at finding large tonnage, low-grade, disseminated gold deposits like the South Carolina deposits that can be mined by open-pit methods. It is unknown if the McDuffie County gold belt deposits are amenable to this type of mining method since they occur as distinct, relatively high-grade veins. Conceivably, the McDuffie County belt deposits could be mined by open-pit methods if the veins were of sufficient density and grade to make the overall bulk grade high enough. The alternative is to pursue underground mining of individual veins or vein stockworks. According to old reports cited in this report, some of the veins were of sufficient grade, size and continuity to be mined profitably. An exploration program would be necessary to adequately determine the feasibility of the above two options.

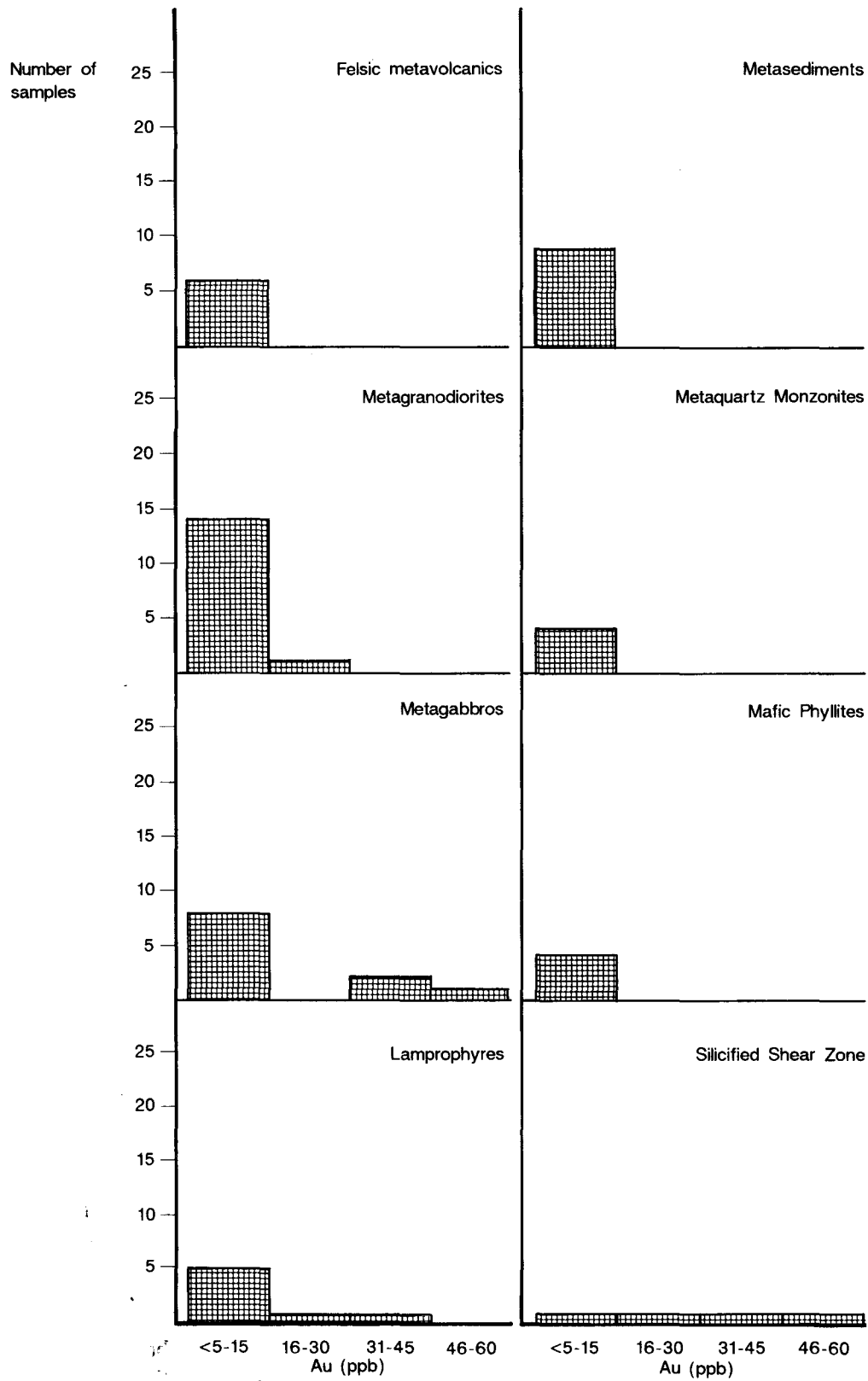


Fig. 39 - Gold content of representative rock types within the study area.

## SUMMARY

The McDuffie County gold belt is located within the Slate belt geologic province just northwest of the Modoc zone, the boundary between the Slate belt and the Kiokee belt. Rocks within the study area consist of felsic to mafic composition extrusive metavolcanic rocks and argillite to wacke metasedimentary rocks. These rocks most likely were deposited peripheral to a back-arc basin over crust transitional between oceanic and continental environments. These volcanic and sedimentary rocks were intruded by pre-metamorphic granodiorites, quartz monzonites and sheeted mafic bodies and by post-metamorphic mafic dikes. The rocks within the study area have been assigned a Cambrian age based on ages of intrusive rocks and the presence of Cambrian fossils in the metasediments.

Rocks within the study area were folded into regional isoclinal folds during the early Paleozoic. At that time the rocks were metamorphosed to lower greenschist facies and were penetratively deformed, developing a pervasive slaty cleavage, but preserving original sedimentary and volcanic features. During the late Paleozoic (Alleghanian), deformation of the Kiokee belt to the southeast affected adjacent rocks along the southeastern border of the study area in the vicinity of the Modoc zone. Adjacent to the Modoc zone, slaty cleavage is overprinted by a mylonitic foliation and the rocks have been metamorphosed to upper greenschist to amphibolite facies. The effects of this deformation diminish rapidly northwest of the Kiokee belt, and northwest of the Modoc zone this deformation is expressed as localized shear zones. Finally, rocks of the Kiokee belt and the study area were folded into a regional antiform and the slaty cleavage of the study area was rotated to its present orientation. Rocks of the Carolina slate belt are interpreted to be a suprastructure complex of greenschist facies rocks overlying amphibolite facies infrastructure rocks of the Kiokee belt. Suprastructure and infrastructure rocks are separated by the Modoc zone, a steep metamorphic gradient and the locus of regional shearing (Secor and others, 1986a; 1986b).

Gold-bearing veins were emplaced into the country rock just prior to the last fold event. These veins were deposited from hydrothermal fluids produced by dehydration and decarbonation of minerals during prograde metamorphism. Gold and other vein minerals precipitated from these fluid as they migrated up the metamorphic gradient to the greenschist/amphibolite facies transition. Gold most likely was transported in the hydrothermal fluid as a gold thiosulfide complex and precipitated as a result of boiling of the hydrothermal fluid and sulfidization of the host rock.

Gold was mined in the study area intermittently from about 1823 to 1922. Formerly productive mines included the Columbia, Parks, Hamilton, Tatham and Woodall. Most mining activity consisted of underground lode mining of quartz veins.

## REFERENCES

- Allard, G.O. and Whitney, J.A., in prep., Geology of the Inner Piedmont, Carolina Terrane, and Modoc Zone in Northeast Georgia.
- Allen, N.E., 1986, The geology of base and precious metal-bearing quartz veins in Hall and Gwinnett Counties, Georgia [M.S. thesis]: Auburn, Auburn University, 98 p.
- Aeromagnetic maps of a part of the Carolina slate belt and vicinity of Georgia: 1975, Unpublished maps in the files of the Georgia Geologic Survey. Scale 1:24,000.
- Bard, J.P., 1986, Microtextures of igneous and metamorphic rocks: D. Reidel Publishing Company, Boston, 264 p.
- Becker, G.F., 1894, Reconnaissance of the gold fields of the Southern Appalachians: U.S. Geological Survey 16th Annual Report, pt. 3, p. 251-319.
- Berger, B.R., 1986, Descriptive model of low-sulfide Au-quartz veins, in Cox, D.P., and Singer, D.A., Mineral deposit models: U.S. Geological Survey Bulletin 1693, p. 239.
- Butler, J.R., and Fullagar, P.D., 1978, Petrochemical and geochronological studies of plutonic rocks in the southern Appalachians: III. Leucocratic adamellites of the Charlotte belt near Salisbury, North Carolina: Geological Society of America Bulletin, v. 89, p. 460-466.
- Carpenter, R.H., 1976, General geology of the Carolina slate belt along the Georgia-South Carolina border, in Chowns, T.M., ed., Stratigraphy, structure, and seismicity in Slate belt rocks along the Savannah River: Georgia Geologic Survey, Guidebook 16, p. 9-12.
- Carpenter, R.H., 1982, Mineralization and alteration in the Lincolnton, Georgia - McCormick, South Carolina area, in Allard, G.O., and Carpenter, R.H., conveners, Exploration for metallic resources in the southeast, symposium: The University of Georgia Department of Geology and Continuing Education, p. 120-138.
- Carpenter, R.H., Odom, A.L., and Hartley, M.E., III, 1982, Geochronological investigation of the Lincolnton meta-dacite, Georgia and South Carolina, in Bearce, D.N., Black, W.W., Kish, S.A., and Tull, J.F., eds., Tectonic studies in the Talladega and Carolina slate belts, southern Appalachian orogen: Geological Society of America Special Paper 191, p. 145-152.
- Colvine, A.C., 1989, An empirical model for the formation of Archean gold deposits: Products of final

- cratonization of the Superior Province, Canada, in Keays, R.R., Ramsay, W.R.H., and Groves, D.I., eds., *The geology of gold deposits: The perspective in 1988: Economic Geology Monograph 6*, p. 37-53.
- Cook, R.B., Jr., 1978, *Minerals of Georgia: their properties and occurrences: Georgia Geologic Survey Bulletin 92*, 189 p.
- Crawford, T.J., Hurst, V.J., and Ramspott, L.D., 1966, *Extrusive volcanics and associated dike swarms in central-east Georgia: Geological Society of America Southeastern Section Guidebook*, University of Georgia, Athens, 53 p.
- Crawford, T.J., 1968a, *Geologic map of Warren County, Georgia: Central Savannah River Area Planning and Development Commission, Augusta, Georgia. Scale - 1" = 9600'.*
- \_\_\_\_\_, 1968b, *Geologic map of McDuffie County, Georgia: Central Savannah River Area Planning and Development Commission, Augusta, Georgia. Scale - 1" = 9600'.*
- \_\_\_\_\_, 1968c, *Geologic map of Wilkes County, Georgia: Central Savannah River Area Planning and Development Commission, Augusta, Georgia. Scale - 1" = 9600'.*
- \_\_\_\_\_, 1968d, *Geologic map of Lincoln County, Georgia: Central Savannah River Area Planning and Development Commission, Augusta, Georgia. Scale - 1" = 9600'.*
- \_\_\_\_\_, 1968e, *Geologic map of Columbia County, Georgia: Central Savannah River Area Planning and Development Commission, Augusta, Georgia. Scale - 1" = 9600'.*
- \_\_\_\_\_, 1968f, *Geologic map of Taliaferro County, Georgia: Central Savannah River Area Planning and Development Commission, Augusta, Georgia. Scale - 1" = 9600'.*
- Crickmay, G.W., 1952, *Geology of the crystalline rocks of Georgia: Georgia Geologic Survey Bulletin 58*, 54 p.
- Deininger, R.W., Dallmeyer, R.D., and Neathery, T.L., 1975, *Chemical variations and K-Ar ages of diabase dikes in east-central Alabama: Geological Society of America Abstracts with Programs, V. 7*, p. 482.
- Dennis, A.J., Sacks, P.E., and Maher, H.D., 1987, *Nature of the Late Alleghanian strike-slip deformation in the eastern South Carolina Piedmont: The Irmo shear zone, in Secor, D.T., ed., Anatomy of the Alleghanian orogeny as seen from the Piedmont of South Carolina and Georgia: Carolina Geological Society Guidebook*, p. 49-66.
- Dooley, R.E., 1977, *K-Ar relationships in dolerite dikes of Georgia [M.S. thesis]: Atlanta, Georgia Institute of Technology*, 185 p.
- Dooley, R.E., and Wampler, J.M., 1983, *Potassium-Argon relations in diabase dikes of Georgia - the influence of excess <sup>40</sup>Ar on the geochronology of early Mesozoic igneous and tectonic events, in Gohn, G.S., ed., Studies related to the Charleston, South Carolina, earthquake of 1886 - tectonics and seismicity: U.S. Geological Survey Professional Paper 1313*, p. M1-M24.
- Feiss, P.G., 1982, *Geochemistry and Tectonic Setting of the Volcanics of the Carolina Slate Belt: Economic Geology, v. 77*, p. 273-293.
- Feiss, P.G., and Wesolowski, D., 1986, *Oxygen isotopic evidence for the interaction of meteoric-hydrothermal waters with granites and subaerial volcanics in pyrophyllite/Au deposits of the Carolina slate belt [abs]: Geological Society of America Abstracts with Programs, v. 18*, p. 600
- Fluker, W.H., 1902, *Gold mining in McDuffie County, Georgia: Engineering and Mining Journal, v. 73*, p. 725.
- \_\_\_\_\_, 1903, *Gold mining in McDuffie County, Georgia: American Institute of Mining Engineers Transactions, v. 33*, p.119-125.
- \_\_\_\_\_, 1907, *A report on the Parks gold mine, McDuffie County, Georgia: Unpublished report in the Georgia Geologic Survey files*, 21 p.
- \_\_\_\_\_, 1910, *Addendum to: A report on the Parks gold mine, McDuffie County, Georgia: Unpublished report in the Georgia Geologic Survey files*, p. 16-21.
- \_\_\_\_\_, 1934, *The Hamilton gold mine, McDuffie County, Georgia: Unpublished report in the Georgia Geologic Survey files*, 27 p.
- Ford, M.M., 1981, *A fluid inclusion and petrographic study of barren and gold-mineralized quartz veins in the central and southern Carolina slate belt, North Carolina [M.S. thesis]: Chapel Hill, The University of North Carolina*, 72 p.
- Ford, M.M., and Feiss, P.G., 1982, *Fluid inclusion studies of Au-bearing and barren quartz veins in the Carolina slate belt, central and southern North Carolina [abs]: Geological Society of America Abstracts with Pro-*

- grams, v. 14, p.18.
- Fouts, J.A., 1966, The geology of the Metasville area, Wilkes and Lincoln Counties, Georgia [M.S. thesis]: Athens, The University of Georgia, 61 p.
- Fullagar, P.D., 1981, Summary of Rb-Sr whole-rock ages for South Carolina: South Carolina Geological Survey, South Carolina Geology, v. 25, p. 29-32.
- German, J.M., 1985, The geology of the northeastern portion of the Dahlonga gold belt: Georgia Geologic Survey Bulletin 100, 41 p.
- \_\_\_\_\_, 1988, The geology of gold occurrences in the west-central Georgia Piedmont: Georgia Geologic Survey Bulletin 107, 48 p.
- \_\_\_\_\_, 1989, Geologic setting and genesis of gold deposits of the Dahlonga and Carroll County gold belts, Georgia: Economic Geology, v. 84, p. 903-923.
- Groves, D.I., Barley, M.E., and Ho, S.E., 1989, Nature, genesis, and tectonic setting of mesothermal gold mineralization in the Yilgarn Block, western Australia, in Keays, R.R., Ramsay, W.R.H., and Groves, D.I., eds., The geology of gold deposits: The perspective in 1988: Economic Geology Monograph 6, p. 71-85.
- Hatcher, R.D., Jr., Howell, D.E., Talwani, P., and Zeitz, I., 1977, Eastern Piedmont fault system: Some speculations on its extent [abs]: Geological Society of America Abstracts with Programs, v. 9, p. 145.
- Higgins, M.W., Atkins, R.L., Crawford, T.J., Crawford, R.F., III, Brooks, R., and Cook, R.B., 1988, The structure, stratigraphy, tectonostratigraphy, and evolution of the southernmost part of the Appalachian orogen: U.S. Geological Survey Professional Paper 1475, 173 p.
- Howell, D.E., and Pirkle, W.A., 1976, Geologic section across the Modoc fault zone, Modoc, South Carolina, in Chowens, T.M., ed., Stratigraphy, structure, and seismicity in slate belt rocks along the Savannah River: Georgia Geologic Survey, Guidebook 16, p. 16-20.
- Hurst, V.J., 1990, Gold in east-central Georgia: Georgia Geologic Survey Bulletin 112, 60 p.
- Hurst, V.J., Crawford, T.J., and Sandy, J., 1966, Mineral resources of the central Savannah River area, v. 1-2: Central Savannah River Area Planning and Development Commission, Augusta, Georgia.
- Hurst, V.J., Kremer, T., and Bush, P.B., 1990, A geochemical reconnaissance for gold in east-central Georgia: Georgia Geologic Survey Information Circular 83, 18 p.
- Jones, S.P., 1902, Gold deposits of Lincoln, Warren, Oglethorpe, Wilkes, Madison, Elbert, Hart, Greene, Taliaferro, Newton, Clarke, and Baldwin Counties, Unpublished report in Georgia Geologic Survey files, 19 p.
- Jones, S.P., 1909, Second report on the gold deposits of Georgia: Georgia Geologic Survey Bulletin 19, 283 p.
- Kelly, S.F., Zuschlag, T., and Low, B., 1934a, Report on the electrical exploration of the Woodall, Hamilton and Columbia properties, McDuffie County, Georgia: Unpublished report in Georgia Geologic Survey files, 32 p.
- \_\_\_\_\_, 1934b, Discovering gold quartz veins electrically: Mining and Metallurgy, v. 15, p. 251-256.
- King, P.B., 1961, Systematic pattern of Triassic dikes in the Appalachian region: U.S. Geological Survey Professional Paper 424-B, p. B93-B95.
- Klein, T.L., and Criss, R.E., 1988, An oxygen isotope and geochemical study of meteoric-hydrothermal systems at Pilot Mountain and selected other localities, Carolina slate belt: Economic Geology, v. 83, p. 801-821.
- Knopf, A., 1929, The Mother Lode system of California: U.S. Geological Survey Professional Paper 73, 226 p.
- LeGrand, H.E., and Furcron, A.S., 1956, Geology and ground-water resources of central-east Georgia: Georgia Geologic Survey Bulletin 64, 174 p.
- Lester, J.G., and Allen, A.T., 1950, Diabase of the Georgia Piedmont: Geological Society of America Bulletin, v. 61, p. 1217-1224.
- Light, T.D., Brew, D.A., and Ashley, R.P., 1989, The Alaska-Juneau and Treadwell lode gold system, southeastern Alaska, in Shawe, D.R., and Ashley, R.P., eds., Gold deposits in metamorphic rocks - part I: U.S. Geological Survey Bulletin 1857-D, p. 27-36.
- Maher, H.D., 1987, D<sub>3</sub> folding in the eastern Piedmont associated with Alleghanian thrusting, in Secor, D.T., ed., Anatomy of the Alleghanian orogeny as seen from the Piedmont of South Carolina and Georgia: Carolina Geological Society Guidebook, p. 35-48.
- Maher, H.D., Palmer, A.R., Secor, D.T., Jr., and Snoke, A.W., 1981, New trilobite locality in the Piedmont of South Carolina, and its regional implications: Geology, v. 9, p. 34-36.
- Miyashiro, A., and Shido, F., 1975, Tholeiitic and calc-alkalic series in relation to the behaviors of titanium, vanadium, chromium, and nickel: American Journal

- of Science, v. 275, p. 265-277.
- Newton, P., and Pyle, M., 1991, Fluid inclusion study of gold bearing quartz veins, Columbia gold mine area, McDuffie County, Georgia [Senior thesis]: Atlanta, Georgia State University, 13 p.
- Pardee, J.T., and Park, C.F., 1948, Gold deposits of the southern Piedmont: U.S. Geological Survey Professional Paper 213, 156 p.
- Paris, T.A., 1976, The geology of the Lincoln 7.5 minute quadrangle, Georgia-South Carolina [M.S. thesis]: Athens, The University of Georgia, 191 p.
- Park, C.F., Jr., and MacDiarmid, R.A., 1975, Ore Deposits: W.H. Freeman and Company, San Francisco, 530 p.
- Pearce, J.A., and Cann, J.R., 1973, Tectonic setting of basic volcanic rocks determined using trace element analyses: Earth and Planetary Science Letters, v. 19, p. 290-300.
- Ragland, P.C., Hatcher, R.D., Jr., and Whittington, D., 1983, Juxtaposed Mesozoic diabase dike sets from the Carolinas: A preliminary assessment: Geology, v. 11, p. 394-399.
- Reusing, S.P., 1979, Geology of the Graves Mountain area, Lincoln and Wilkes Counties, Georgia [M.S. thesis]: Athens, The University of Georgia, 121 p.
- Rock, N.M.S., 1987, The nature and origin of lamprophyres: An overview, in Fitton, J.G., and Upton, B.G.J., eds., Alkaline igneous rocks: Geological Society of London Special Publication, v. 30, p. 191-226.
- Rock, N.M.S., and Groves, D.I., 1988, Do lamprophyres carry gold as well as diamonds?: Nature, v. 332, p. 253-255.
- Rock, N.M.S., Groves, D.I., Perring, C.S., and Golding, S.D., 1989, Gold, lamprophyres, and porphyries: What does their association mean?, in Keays, R.R., Ramsay, W.R.H., and Groves, D.I., eds., The geology of gold deposits: The perspective in 1988: Economic Geology Monograph 6, p. 609-625.
- Rogers, J.J.W., 1982, Criteria for recognizing environments of formation of volcanic suites: application of these criteria to volcanic suites in the Carolina slate belt, in Bearce, D.N., Black, W.W., Kish, S.A., and Tull, J.F., eds., Tectonic studies in the Talladega and Carolina Slate Belts, Southern Appalachian orogen: Geological Society of America Special Paper 191, p. 99-107.
- Sacks, P.E., and Dennis, A.J., 1987, The Modoc zone - D<sub>2</sub> (Early Alleghanian) in the eastern Appalachian Piedmont, South Carolina and Georgia, in Secor, D.T., Jr., ed., Anatomy of the Alleghanian orogeny as seen from the Piedmont of South Carolina and Georgia: Carolina Geological Society Guidebook, p. 19-34.
- Samson, S., Palmer, A.R., Robison, R.A., Secor, D.T., Jr., 1990, Biogeographical significance of Cambrian trilobites from the Carolina slate belt: Geological Society of America Bulletin, v. 102, p. 1459-1470.
- Secor, D.T., Jr., 1987, Regional overview, in Secor, D.T., Jr., ed., Anatomy of the Alleghanian orogeny as seen from the Piedmont of South Carolina and Georgia: Carolina Geological Society Guidebook, p. 1-18.
- Secor, D.T., Jr., and Wagener, H.D., 1968, Stratigraphy, structure, and petrology of the Piedmont in central South Carolina: South Carolina Geological Survey Geologic Notes, v. 12, p. 67-84.
- Secor, D.T., Jr., and Snoke, A.W., 1978, Stratigraphy, structure and plutonism in the central South Carolina Piedmont, in Snoke, A.W., ed., Geological investigations of the eastern piedmont, southern Appalachians: South Carolina Geological Survey, Carolina Geological Society Guidebook, p. 65-123.
- Secor, D.T., Jr., Samson, S.L., Snoke, A.W., and Palmer, A.R., 1983, Confirmation of the Carolina slate belt as an exotic terrane: Science, v. 221, p. 649-651.
- Secor, D.T., Jr., Snoke, A.W., Bramlett, K.W., Costello, O.P., and Kimbrell, O.P., 1986a, Character of the Alleghanian orogeny in the southern Appalachians: Part I. Alleghanian deformation in the eastern Piedmont of South Carolina: Geological Society of America Bulletin, v. 97, p. 1319-1328.
- Secor, D.T., Jr., Snoke, A.W., and Dallmeyer, R.D., 1986b, Character of the Alleghanian orogeny in the southern Appalachians: Part III. Regional tectonic relations: Geological Society of America Bulletin, v. 97, p. 1345-1353.
- Seward, T.M., 1989, The hydrothermal chemistry of gold and its implications for ore formation: Boiling and conductive cooling as examples, in Keays, R.R., Ramsay, W.R.H., and Groves, D.I., eds., The geology of gold deposits: The perspective in 1988: Economic Geology Monograph 6, p. 398-404.
- Smith, R.W., 1931, Shales and brick clays of Georgia: Georgia Geologic Survey Bulletin 45, 348 p.
- Smith, T.E., and Noltimier, H.C., 1979, Paleomagnetism of the Newark trend igneous rocks of the north central Appalachians and the opening of the central Atlantic

Ocean: *American Journal of Science*, v. 279, p. 778-807.

Streckeisen, A., 1976, To each plutonic rock its proper name: *Earth Science Review*, v. 12, p. 1-33.

\_\_\_\_\_, 1979, Classification and nomenclature of volcanic rocks, lamprophyres, carbonatites, and melilitic rocks: Recommendations and suggestions of the IUGS Subcommittee on the Systematics of Igneous Rocks: *Geology*, v. 7, p. 331-335.

Sutter, J.F., and Smith, T.E., 1979,  $^{40}\text{Ar}/^{39}\text{Ar}$  ages of diabase intrusions from Newark trend basins in Connecticut and Maryland: Initiation of central Atlantic rifting: *American Journal of Science*, v. 279, p. 808-831.

Taylor, H.P., Jr., 1968, The oxygen isotope geochemistry of igneous rocks: *Contributions to Mineralogy and Petrology*, v. 19, p. 1-71.

\_\_\_\_\_, 1974, The application of oxygen and hydrogen isotope studies to problems of hydrothermal alteration and ore deposition: *Economic Geology*, v. 69, p. 843-883.

Von der Heyde, W.S., 1990, The Geology of the Washington East 7.5 minute quadrangle, Wilkes County, Georgia [M.S. thesis]: Athens, The University of Georgia, 130 p.

Wesolowski, D., Sans, J.R., Thornton, C.P., and Ohmoto, H., 1985, Regional trends in the oxygen isotopic compositions of granitoid plutons, central and southern Appalachians [abs.]: *Geological Society of America Abstracts with Programs*, v. 17, p. 465.

Weigand, P.W., and Ragland, P.C., 1970, Geochemistry of Mesozoic dolerite dikes from eastern North America: *Contributions to Mineralogy and Petrology*, v. 29, p. 195-214.

Whitney, J.A., Paris, T.A., Carpenter, R.H., and Hartley, M.E., III, 1978, Volcanic evolution of the southern slate belt of Georgia and South Carolina: A primitive oceanic island arc: *Journal of Geology*, v. 86, p. 173-192.

Williams, H., Turner, F.J., and Gilbert, C.M., 1954, *Petrography, An Introduction to the Study of Rocks in Thin Section*: San Francisco, W.H. Freeman and Company, 406 p.

Yeates, W.S., 1902, A preliminary report on the Columbia gold mine, McDuffie County, Georgia: Unpublished report in the Georgia Geologic Survey files, 23 p.

Yeates, W.S., McCallie, S.W., and King, F.P., 1896, A preliminary report on a part of the gold deposits of Georgia: *Georgia Geologic Survey Bulletin 4-A*, 535 p.

APPENDIX A  
GEOCHEMICAL ANALYSIS PARAMETERS

<u>Element</u>	<u>Analytical Method*</u>	<u>Detection Limit</u>
SiO <sub>2</sub>	DCP	0.01%
Al <sub>2</sub> O <sub>3</sub>	DCP	0.01%
Fe <sub>2</sub> O <sub>3</sub>	DCP	0.01%
FeO	Titration	0.01%
MgO	DCP	0.01%
CaO	DCP	0.01%
Na <sub>2</sub> O	DCP	0.01%
K <sub>2</sub> O	DCP	0.01%
TiO <sub>2</sub>	DCP	0.01%
P <sub>2</sub> O <sub>5</sub>	DCP	0.01%
MnO	DCP	0.01%
CO <sub>2</sub>	DCP	0.01%
S	DCP	0.02%
LOI	Gravimetric	
Au	ICP or FA/AA	5 ppb
Ag	ICP	0.2 ppm
Cu	ICP	1 ppm
Pb	ICP	2 ppm
Zn	ICP	1 ppm
Be	ICP	0.5 ppm
Ba	ICP	5 ppm
Cd	ICP	1 ppm
Cr	ICP	1 ppm
La	ICP	1 ppm
Li	ICP	1 ppm
Mo	ICP	1 ppm
Nb	ICP	1 ppm
Ni	ICP	1 ppm
Sc	ICP	1 ppm
Sr	ICP	1 ppm
V	ICP	1 ppm
Y	ICP	1 ppm
Zr	ICP	1 ppm
Bi	ICP	5 ppm
Co	ICP	1 ppm
Ga	ICP	2 ppm
As	ICP	5 ppm
Ce	ICP	5 ppm
Sb	ICP	5 ppm
Ta	ICP	10 ppm
Te	ICP	10 ppm
W	ICP	10 ppm
Sn	ICP	20 ppm
Rb	XRF	1 ppm
F	Specific Ion	20 ppm
B	DCP	10 ppm
Se	OEX/AA	0.1 ppm
Hg	CVAA	10 ppb

APPENDIX A Continued

<u>Element</u>	<u>Analytical Method*</u>	<u>Detection Limit</u>
Tl	ICP	0.1 ppm
Pt	FA/DCP	5 ppb
Pd	FA/DCP	1 ppb

\*DCP - Direct Current Plasma Emission Spectroscopy

XRF - X-ray Fluorescence

CVAA - Cold Vapor Atomic Absorption

FA/DCP - Fire Assay/Direct Current Plasma Emission Spectroscopy

AA - Atomic Absorption

OEX/AA - Organic Extraction/Atomic Absorption

INAA - Instrumental Neutron Activation Analysis

ICP - Inductively Coupled Plasma Spectroscopy

FA/AA - Fire Assay/Atomic Absorption

APPENDIX B  
Mine Descriptions\*

<u>Mine</u>	<u>County</u>	<u>7.5 minute quadrangle</u>	<u>Type of workings</u>	<u>Geologic setting and production</u>	<u>Remarks</u>
1. Balbach	McDuffie	Wrightsboro			Exact location unknown
2. Bell Vein	McDuffie	Wrightsboro	Numerous pits and caved shafts.	Near contact between metasediments of the Richtex Fm. and metagranodiorite	
3. Columbia	McDuffie	Wrightsboro	Numerous aligned pits and caved shafts.	Near contact between metasediments of the Richtex Fm. and metagranodiorite. 1899-1901: 971 oz. <sup>2</sup> .	
4. Edwards	McDuffie	Wrightsboro			Exact location unknown
5. Gallaher	McDuffie	Cadley			Exact location unknown
6. Gerald	McDuffie	Wrightsboro			Exact location unknown
7. Griffin	McDuffie	Aonia	Several aligned pits	Occurs near contact between metasediments of the Richtex Fm. and metagranodiorite.	
8. Hamilton	McDuffie	Wrightsboro	Several open cuts and numerous aligned pits	Occurs within metasediments of the Richtex Fm.	Two clusters of workings
9. Landers	McDuffie	Wrightsboro	Numerous aligned pits	Occurs near contact between metasediments of the Richtex Fm. and metagranodiorite.	
10. Motes/Henrich	McDuffie	Aonia	A few scattered pits	Occurs within metasediments of the Richtex Fm.	
11. Parks	McDuffie	Wrightsboro	Numerous aligned pits and caved shafts.	Occurs near contact between metasediments of the Richtex Fm. and metagranodiorite. 1891-1896: 2908 oz. <sup>1</sup> . 1908-1909: 749 oz. and some silver <sup>1</sup> .	Three clusters of workings

APPENDIX B Continued

<u>Mine</u>	<u>County</u>	<u>7.5 minute quadrangle</u>	<u>Type of workings</u>	<u>Geologic setting and production</u>	<u>Remarks</u>
12. Porter	McDuffie	Aonia	Several clusters of aligned and scattered pits.	Occurs within the largest metagranodiorite body.	Some workings associated with a shear zone.
13. Sellers	McDuffie	Cadley			Exact location unknown.
14. Tatham	McDuffie	Aonia	Numerous aligned pits and caved shafts.	Occurs near contact between metasediments of the Richtex Fm. and metagranodiorite.	
15. Woodall	McDuffie	Aonia	Numerous aligned pits and caved shafts.	Workings straddle contact between metasediments of the Richtex Fm. and metagranodiorite.	
16. Warren	Warren	Cadley	Several scattered pits and at least two filled shafts.	Occurs within interlayered metasediments and metavolcanics of the Richtex Fm.	Main workings have been filled.
17. Watson	Warren?	Cadley			Exact location unknown.
18. Edmunds	Wilkes and Lincoln	Woodlawn	Several trenches, aligned pits and caved shafts.	Occurs near contact between metasediments and metavolcanics of the Richtex Fm. and metagranodiorite.	
19. Green	Wilkes	Woodlawn	Three aligned pits	Occurs near contact between metasediments and metavolcanics of the Richtex Fm. and metagranodiorite.	
20. Hilly	Wilkes	Aonia			Exact location unknown.
21. Rivers	Wilkes	Woodlawn			On island in Clark Hill Lake (?).
22. Bussey	Lincoln	Leah	Seven small pits, one large pit and one trench.	Occurs within metaquartz monzonite.	

APPENDIX B Continued

<u>Mine</u>	<u>County</u>	<u>7.5 minute quadrangle</u>	<u>Type of workings</u>	<u>Geologic setting and production</u>	<u>Remarks</u>
23. Dill	Lincoln	Woodlawn			Exact location unknown.
24. Julia/Phelps	Lincoln	Woodlawn			Exact location unknown.
25. Paschal	Lincoln	Woodlawn			Exact location unknown.
26. Phillips	Lincoln	Woodlawn	Seven aligned pits and one caved shaft.	Occurs within metasediments of the Richtex Fm.	
27. Ramsey	Lincoln	Woodlawn	Three pits and two trenches.	Occurs within metasediments and metavolcanics of the Richtex Fm.	Some workings under Clark Hill lake.

\*Mine locations and corresponding numbers are shown on Plate 1. Mine locations and names from Fluker (1902, 1903); Jones (1902, 1909); Yeates (1902); Hurst and others (1966) and this study.

<sup>1</sup>Fluker, 1910

<sup>2</sup>Yeates, 1902

## APPENDIX C

BASE AND PRECIOUS METAL ASSAYS OF REPRESENTATIVE  
ROCK TYPES WITHIN THE STUDY AREA<sup>1</sup>

Sample Number	<sup>2</sup> Au	Ag	Cu	Pb	Zn	Mo	Ni	Co	Bi	As	Sb	Hg	<sup>3</sup> Fe	Mn	Cr	W	Ba
<u>Metagranodiorites</u>																	
*AO-1	<5	<0.2	22	5	73	2	6	9	<5	9	<5	<0.010	2.89	632	169	<20	1200
AO-9	<5	<0.2	5	6	47	1	5	8	<5	<5	<5	<0.010	2.53	605	205	<20	780
AO-25	<5	<0.2	18	7	101	3	4	10	<5	<5	<5	<0.010	3.19	802	172	<20	760
AO-34	<5	<0.2	6	7	120	2	4	4	<5	<5	<5	<0.010	2.78	869	186	<20	790
C-86	<5	<0.2	4	9	25	6	5	3	<5	<5	<5	<0.010	1.72	440	326	<20	960
C-87	<5	<0.2	3	13	36	2	6	3	<5	<5	<5	<0.010	1.64	423	233	<20	860
C-146	14	<0.2	24	9	87	5	6	7	<5	<5	<5	<0.010	3.48	841	230	<20	840
C-147	<5	<0.2	16	6	75	1	5	7	<5	<5	<5	<0.010	3.23	917	142	<20	900
C-153	<5	<0.2	6	4	67	2	6	7	<5	<5	<5	<0.010	2.66	795	206	<20	730
C-162	20	<0.2	11	5	11	2	7	4	<5	<5	<5	<0.010	1.09	310	236	<20	320
C-164	<5	<0.2	8	9	37	1	6	4	<5	<5	<5	<0.010	1.73	362	213	<20	1100
C-165	<5	<0.2	6	3	60	1	4	<1	<5	<5	<5	<0.010	2.30	475	176	<20	920
C-157	<5	<0.2	9	6	86	<1	3	3	<5	<5	<5	<0.010	3.05	664	140	<20	920
<u>Metaquartz monzonites</u>																	
AO-183	<5	<0.2	6	13	63	5	4	2	<5	<5	<5	<0.010	1.56	450	234	<20	960
L-63	<5	<0.2	6	8	60	1	4	1	<5	<5	<5	<0.010	2.10	773	282	<20	940
AO-183A	<5	<0.2	6	14	38	2	5	1	<5	<5	<5	<0.010	1.93	365	235	<20	930
L-207C	<5	<0.2	4	6	56	1	5	1	<5	<5	<5	<0.010	1.77	449	169	<20	970
L-207A	<5	<0.2	6	8	60	1	4	1	<5	<5	<5	<0.010	1.77	875	196	<20	1100
<u>Felsic metavolcanic rocks</u>																	
AO-176C	<5	<0.2	19	6	55	<1	4	5	<5	<5	<5	<0.010	1.90	448	146	<20	730
AO-177	12	<0.2	9	9	31	2	8	3	<5	<5	<5	<0.010	1.29	303	437	<20	710
AO-178	<5	<0.2	24	4	87	1	8	12	<5	<5	<5	<0.010	3.30	548	99	<20	800
AO-197	7	<0.2	11	13	37	<1	4	4	<5	<5	<5	<0.010	1.39	292	108	<20	740
C-135	<5	<0.2	11	7	58	3	4	4	<5	<5	<5	<0.010	1.77	590	174	<20	620
<u>Mafic meta-intrusions (dikes, sills, small stocks)</u>																	
AO-180	<5	<0.2	102	3	25	<1	46	15	<5	<5	<5	<0.010	1.89	263	105	<20	100
C-76	<5	<0.2	62	7	44	<1	46	19	<5	8	<5	<0.010	2.92	416	143	<20	200
C-138	<5	<0.2	53	5	47	1	18	18	<5	<5	<5	<0.010	3.22	535	110	<20	170
C-150A	7	<0.2	101	10	96	<1	24	28	<5	11	<5	<0.010	3.44	610	115	<20	210
C-152	41	<0.2	53	8	85	2	16	11	<5	<5	<5	<0.010	3.27	532	101	<20	260
C-158	<5	<0.2	33	5	35	1	62	23	<5	<5	<5	<0.010	2.34	526	195	<20	170
C-161A	<5	<0.2	37	3	42	2	31	15	<5	<5	<5	<0.010	3.54	551	159	<20	180
C-163	57	<0.2	76	5	39	<1	37	17	<5	<5	<5	<0.010	3.13	473	138	<20	360
L-53	40	<0.2	43	<2	55	<1	39	17	<5	<5	<5	<0.010	3.40	456	126	<20	100
L-228	<5	<0.2	113	5	48	<1	40	29	6	<5	<5	<0.010	5.33	967	123	<20	<20

APPENDIX C Continued

Sample Number	<sup>2</sup> Au	Ag	Cu	Pb	Zn	Mo	Ni	Co	Bi	As	Sb	Hg	<sup>3</sup> Fe	Mn	Cr	W	Ba
<u>Mafic phyllites</u>																	
A0-193A	<5	<0.2	11	8	227	<1	62	40	<5	<5	<5	<0.010	7.32	2228	127	<20	530
A0-182	26	<0.2	32	8	80	<1	23	17	<5	<5	<5	<0.010	4.38	687	87	<20	680
C-159	6	<0.2	99	5	57	1	14	15	<5	<5	<5	<0.010	4.49	663	148	<20	120
A0-176B	<5	<0.2	58	10	107	1	45	36	<5	<5	<5	<0.010	5.25	995	233	<20	320
<u>Metasediments</u>																	
C-139B	<5	<0.2	66	8	127	<1	33	23	<5	<5	<5	<0.010	5.35	794	70	<20	650
C-132A	<5	<0.2	70	6	72	1	34	21	<5	12	<5	<0.010	5.83	533	133	<20	640
C-134	<5	<0.2	33	6	67	1	16	12	<5	5	<5	<0.010	3.81	565	205	<20	700
C-144	<5	<0.2	37	6	91	2	29	22	<5	<5	<5	<0.010	5.36	310	114	<20	700
C-151	<5	<0.2	115	20	90	1	27	19	<5	16	<5	<0.010	5.10	1603	225	<20	680
WB-100	<5	<0.2	52	4	53	<1	30	20	<5	10	<5	<0.010	5.30	466	175	<20	690
WB-102	<5	<0.2	39	7	50	1	26	18	<5	<5	<5	<0.010	4.66	1000	156	<20	460
WL-200	<5	<0.2	30	9	54	3	22	19	<5	9	<5	<0.010	4.65	1083	142	<20	730
<u>Diabase dikes</u>																	
A0-41	15	<0.2	39	7	45	2	8	13	<5	<5	<5	<0.010	4.12	506	206	<20	160
A0-172	<5	<0.2	51	6	95	2	53	37	<5	<5	<5	0.022	6.20	820	166	<20	180
C-142B	<5	<0.2	70	9	96	<1	63	44	<5	<5	<5	<0.010	6.63	1091	80	<20	220
C-160	18	0.5	6	<2	29	<1	26	16	<5	<5	<5	0.029	3.41	500	278	<20	110
WL-47W	<5	<0.2	84	6	40	1	108	28	5	<5	<5	0.015	4.77	349	174	<20	800
<u>Lamprophyre dikes</u>																	
A0-35	24	0.3	36	5	103	2	85	31	5	<5	<5	<0.010	6.89	400	208	<20	950
A0-38	8	0.2	51	19	58	2	51	22	<5	<5	<5	0.057	4.66	500	124	<20	1100
A0-173	39	0.4	41	7	110	<1	131	32	<5	<5	<5	<0.010	6.71	900	251	<20	960
A0-184	10	0.4	38	9	93	<1	79	27	<5	<5	<5	0.022	6.79	300	253	<20	1100
A0-196	9	0.3	32	7	99	1	64	26	<5	<5	<5	0.023	6.80	600	161	<20	1100
WB-95B	<5	<0.2	25	43	73	<1	47	19	<5	<5	<5	0.021	3.45	500	146	<20	1800
WL-202A	<5	<0.2	50	12	53	2	60	24	<5	<5	<5	0.048	4.66	341	167	<20	1200

Mafic meta-intrusions (cont'd)

	<sup>2</sup> Pt	<sup>2</sup> Pd
A0-180	48	41
C-76	<5	9
C-138	11	11
C-150A	<5	7
C-152	9	8
C-158	22	12
C-161A	9	5
C-163	10	7
L-53	<5	1

<sup>1</sup>Unweathered samples; Values are in ppm unless otherwise noted.

<sup>2</sup>Values in ppb

<sup>3</sup>Values in %

\*Refer to Plate 3 for sample locations.

For convenience in selecting our reports from your bookshelves, they are color-keyed across the spine by subject as follows:

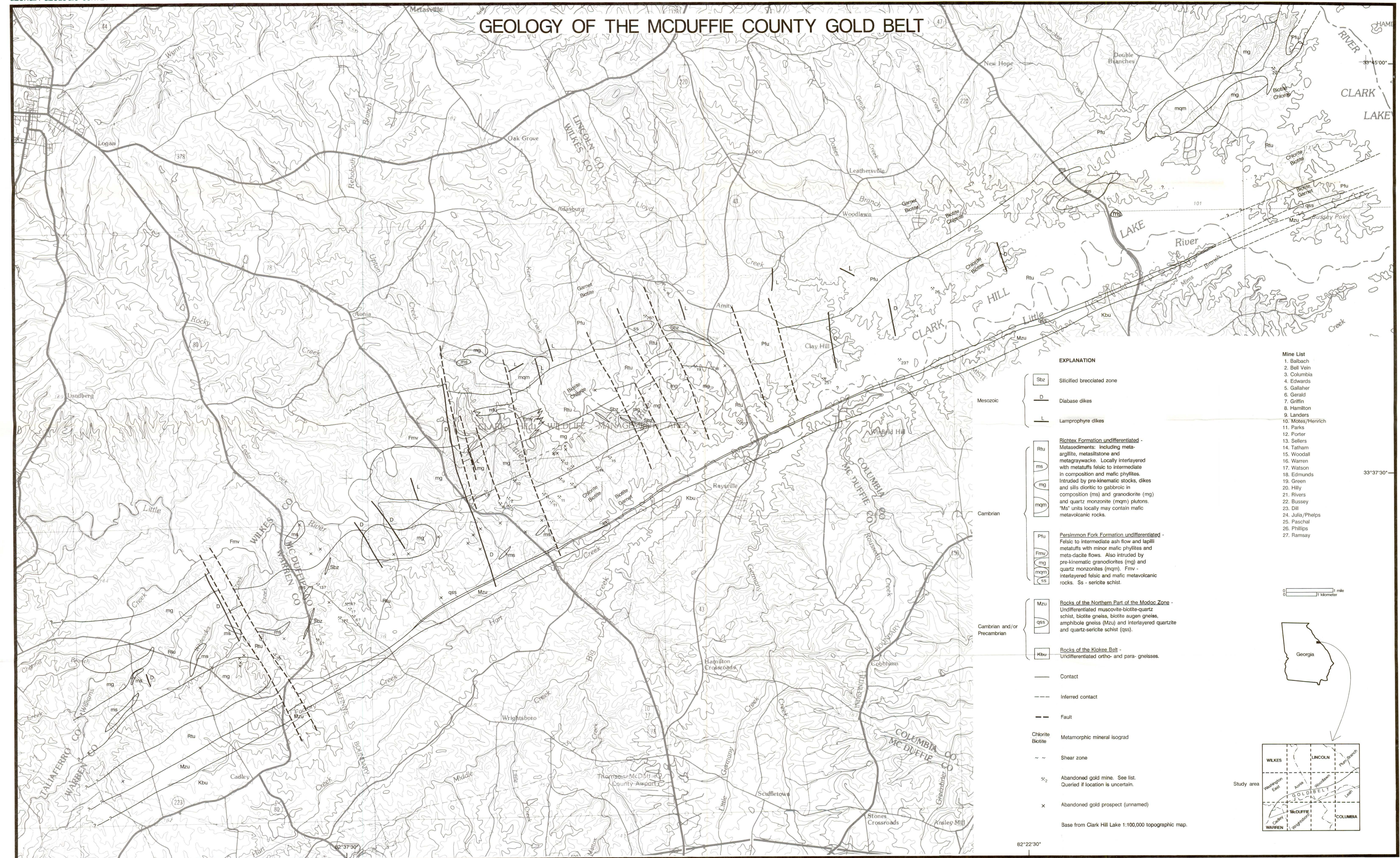
Red	Valley and Ridge mapping and structural geology
Dk. Purple	Piedmont and Blue Ridge mapping and structural geology
Maroon	Coastal Plain mapping and stratigraphy
Lt. Green	Paleontology
Lt. Blue	Coastal Zone studies
Dk. Green	Geochemical and geophysical studies
Dk. Blue	Hydrology
Olive	Economic geology
	Mining directory
Yellow	Environmental studies
	Engineering studies
Dk. Orange	Bibliographies and lists of publications
Brown	Petroleum and natural gas
Black	Field trip guidebooks
Dk. Brown	Collections of papers

Colors have been selected at random, and will be augmented as new subjects are published.

Publications Consultant: Patricia Allgood  
Cartographer: Melynda D. Lewis

The Department of Natural Resources is an equal opportunity employer and offers all persons the opportunity to compete and participate in each area of DNR employment regardless of race, color, religion, sex, national origin, age, handicap, or other non-merit factors.

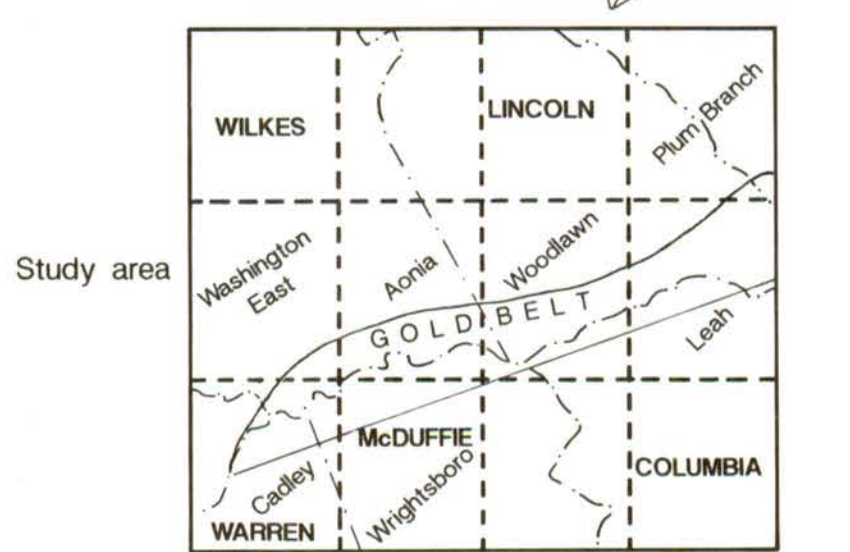
# GEOLOGY OF THE MCDUFFIE COUNTY GOLD BELT



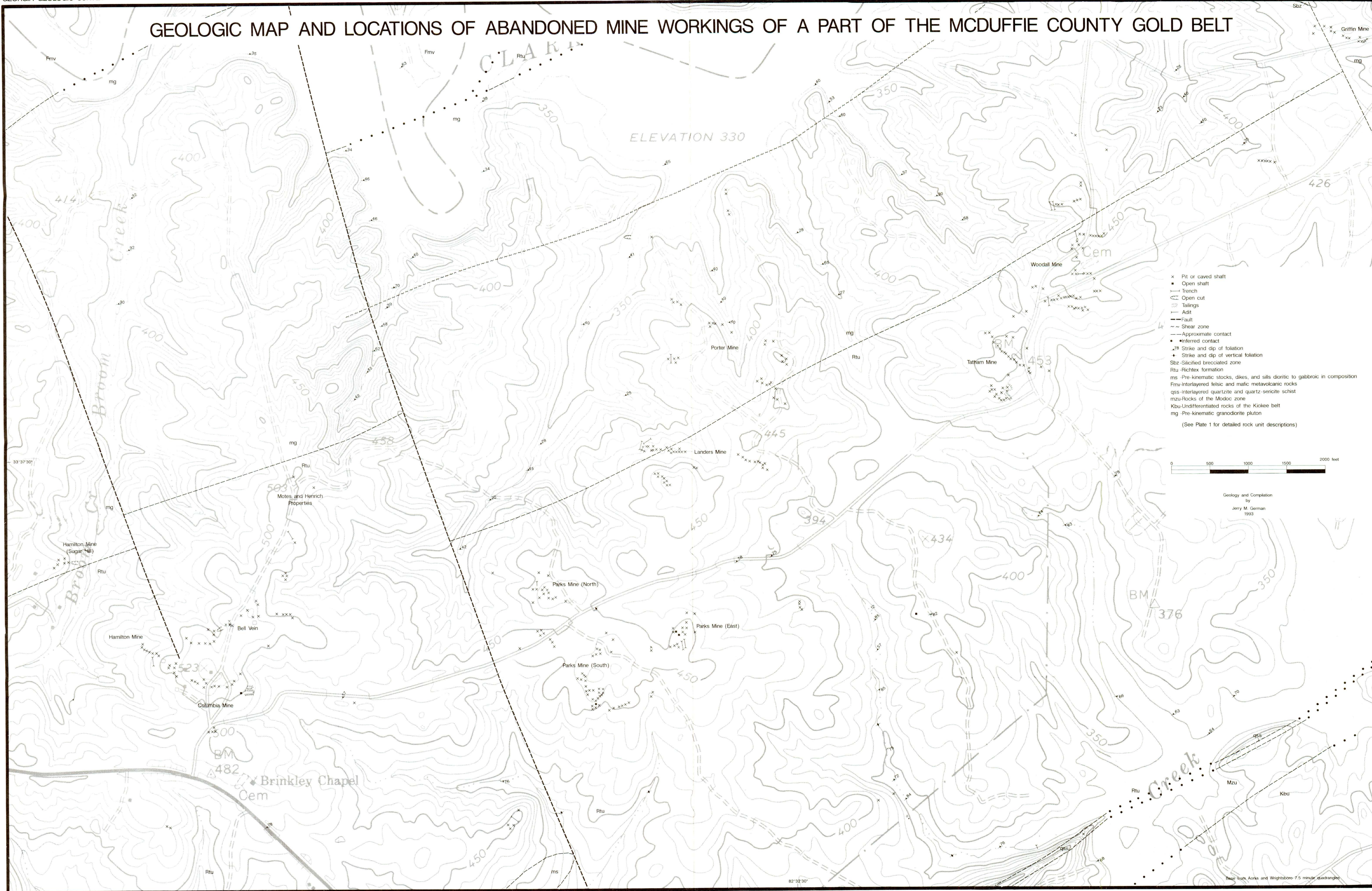
**EXPLANATION**

- Sbz Silicified brecciated zone
- Mesozoic**
  - Diabase dikes
  - Lamprophyre dikes
- Cambrian**
  - Rtu **Richtex Formation undifferentiated** - Metasediments including meta-argillite, metasiltstone and metagraywacke. Locally interlayered with metatuffs felsic to intermediate in composition and mafic phyllites. Intruded by pre-kinematic stocks, dikes and sills dioritic to gabbroic in composition (ms) and granodiorite (mg) and quartz monzonite (mqm) plutons. "Ms" units locally may contain mafic metavolcanic rocks.
  - ms
  - mg
  - mqm
  - Pfu **Persimmon Fork Formation undifferentiated** - Felsic to intermediate ash flow and lapilli metatuffs with minor mafic phyllites and meta-clastic flows. Also intruded by pre-kinematic granodiorites (mg) and quartz monzonites (mqm). Fmv - interlayered felsic and mafic metavolcanic rocks. Ss - sericite schist.
  - Fmv
  - mg
  - mqm
  - ss
- Cambrian and/or Precambrian**
  - Mzu **Rocks of the Northern Part of the Modoc Zone** - Undifferentiated muscovite-biotite-quartz schist, biotite gneiss, biotite augen gneiss, amphibole gneiss (Mzu) and interlayered quartzite and quartz-sericite schist (qss).
  - qss
  - Kbu **Rocks of the Kiokee Belt** - Undifferentiated ortho- and para- gneisses.
- Contact
- Inferred contact
- Fault
- Chlorite Biotite Metamorphic mineral isograd
- ~ ~ Shear zone
- ⊗<sub>2</sub> Abandoned gold mine. See list. Queried if location is uncertain.
- ⊗ Abandoned gold prospect (unnamed)

- Mine List**
1. Balbach
  2. Bell Vein
  3. Columbia
  4. Edwards
  5. Gallaher
  6. Gerald
  7. Griffin
  8. Hamilton
  9. Landers
  10. Motes/Henrich
  11. Parks
  12. Porter
  13. Sellers
  14. Tatham
  15. Woodall
  16. Warren
  17. Watson
  18. Edmunds
  19. Green
  20. Hilly
  21. Rivers
  22. Bussey
  23. Dill
  24. Julia/Phelps
  25. Paschal
  26. Phillips
  27. Ramsay



# GEOLOGIC MAP AND LOCATIONS OF ABANDONED MINE WORKINGS OF A PART OF THE MCDUFFIE COUNTY GOLD BELT



- x Pit or caved shaft
  - Open shaft
  - trench
  - Open cut
  - Tailings
  - Adit
  - Fault
  - Shear zone
  - Approximate contact
  - Inferred contact
  - ↗ Strike and dip of foliation
  - ⊕ Strike and dip of vertical foliation
  - Sbz-Silicified brecciated zone
  - Rtu-Richtex formation
  - ms-Pre-kinematic stocks, dikes, and sills dioritic to gabbroic in composition
  - Fmv-interlayered felsic and mafic metavolcanic rocks
  - qss-interlayered quartzite and quartz-sericite schist
  - mzu-Rocks of the Modoc zone
  - Kbu-Undifferentiated rocks of the Kiokee belt
  - mg-Pre-kinematic granodiorite pluton
- (See Plate 1 for detailed rock unit descriptions)



Geology and Completion  
by  
Jerry M. German  
1993

Based from Aonia and Wrightsboro 7.5 minute quadrangles

